PB86-181708

HYDRAULIC DESIGN SERIES
NO. 1

HYDRAULICS OF BRIDGE WATERWAYS

HYDRAULICS BRANCH
BRIDGE DIVISION
OFFICE OF ENGINEERING

by Joseph N. Bradley

U.S. DEPARTMENT OF TRANSPORTATION/Federal Highway Administration

SECOND EDITION REVISED MARCH 1978, WASHINGTON, D.C.

REPRODUCED BY
U.S. DEPARTMENT OF COMMERCE
NATIONAL TECHNICAL
INFORMATION SERVICE
SPRINGFIELD, VA 22161

Technical Report Documentation Page

1. Report No.	2. Government Accession No.	3. Recipient's Catalog No.
FHWA-EPD-86-101		

4. Title and Subtitle	5. Report Date
Hydraulics of Bridge Waterways, Hydraulic Design Series (HDS) No. 1	Revised March 1978
	6. Performing Organization Code
7. Author(s) Joseph N. Bradley	8. Performing Organization Report No.
9. Performing Organization Name and Address Office of Engineering, HNG-31 Federal Highway Administration 400 7th Street, SW. Washington, D.C. 20590	10. Work Unit No. (TRAIS)
	11. Contract or Grant No.
12. Sponsoring Agency Name and Address	13. Type of Report and Period Covered
	14. Sponsoring Agency Code

15. Supplementary Notes

16. Abstract

This publication presents design procedures for the hydraulic analysis of bridge waterway openings. The text describes the general nature of the constriction created by constructing a highway/bridge crossing in a floodplain and provides detailed step-by-step design procedures for analyzing the flow through a bridge to calculate flow velocities and bridge backwater. The method of analysis is based on the results of hydraulic model studies conducted at the Colorado State Universty and on later measurements and field data collected by U.S. Geological Survey. This is the second edition of this publication as revised in March 1978.

Sketches and design charts are included to provide a practical method of analysis, and many example problems are used to illustrate application of the design method for varying site conditions. Special design problems include dual bridges, skewed and eccentric crossings, abnormal stage, backwater with scour, superstructure and/or roadway inundated, spur dikes and bridge backwater with supercritical flow.

17. Key Words	18. Distribution Statement
Bridge Backwater; Conveyance; Critical Depth; Inundation; Normal Stage; Scour; Spur Dikes; Stage-Discharge; Type of Flow; Type I Flow; Type II Flow; Water Surface Elevations	No restrictions. This document is available to the public through the National Technical Information Service, Springfield, Virginia 22161.

19. Security Classif. (of this report)	20. Security Classif. (of this page)	21. No. of Pages	22. Price
Unclassified	Unclassified	124	

Form DOT F 1700.7 (8-72) Reproduction of completed page authorized

ERRATA - HYDRAULIC DESIGN SERIES NO. 1, SECOND EDITION, 1970, "HYDRAULICS OF BRIDGE WATERWAYS"

Pages v-x: Change to pages iii-viii, respectively.

Page v, References to the "Bureau of Public Roads" should be changed to "Federal Highway Administration."

Page v, Last Paragraph: Carl S. Izzard to Carl F. Izzard.

Page 9, Column 1, 9th line from the bottom: Change "w_p" to "W_p".

Page 11, Column 2, 4th line from bottom of page: Change "advise" to "advice."

Page 13, Column 1, line 19: Change "solutions," to "solutions;".

Page 13, Column 2, line 8: Insert "for flow at normal stage" between "constriction*" and "or".

Page 15, Figure 7: Change ordinate title "ΔK" to "ΔK_p".

Page 21, Column 2, 3rd line from bottom: Change "$h_b^*/h_b + h_3^*$" to "$h_b^*/(h_b^*+h_3^*)$".

Page 39, Paragraph 7.4 Enlarged Waterways. Add: Any proposal to reduce backwater by excavation to enlarge a bridge waterway area should be carefully studied. If there is reason to believe that the enlarged area cannot be maintained or that the stability of the stream will be disturbed, alternate solutions such as additional spans should be considered.

Page 41 through 44: Beginning with Equation (20), Change all upper case symbols "Yu", "$\overline{Y}$" and "Y_3" to lower case.

Page 41, Column 2, Lines 7 and 10: Change "c_d" to "C_d".

Page 51, Column 1, Line 7: Change "normal to" to "at an angle with".

Page 51, Column 1, Line 18: Change "bridge embankment" to "bridge approach embankment".

For sale by the Superintendent of Documents, U.S. Government Printing Office
Washington, D.C. 20402

Stock No. 050-001-00133-1

Page 51, Column 2, Lines 9 and 10: Change "below the river bed" to "deep".

Page 52, Figure 28: In upper right of figure, change contour 105 to 185. In upper left, 180 contour should not join 185 contour.

Page 53, Column 2: Equation 24 should read:

$$\frac{X^2}{L_s^2} + \frac{Y^2}{(0.4L_s)^2} = 1$$

Page 53, Column 2, Lines 33 and 34: Change "30 feet" to "50 feet".

Page 54, Figure 30: Delete the insert figure showing a 45° skew bridge and the accompanying note.

Page 54, Column 2 and continuing on page 55, Column 1: Delete two sentences beginning: "For bridges skewed at an angle of 45°, it is recommended---" Substitute: "From meager testing done to date, there is not sufficient evidence to warrant using longer dikes at either abutment on skewed bridges. Lengths obtained from Figure 30 should generally be adequate for either normal or skewed crossings."

Page 56, Figure 33: Change dimension "B" to "$0.4L_s$".

Page 56, Figure 33: On Section A-A, show Design Water Surface 2' minimum below top of dike and change "2:1" to "2:1 or Flatter".

Page 56, Column 2, Last Line: Change "20591" to "20590".

Page 57, Figure 34: Change upper case symbols "$\bar{Y}$" and "Y_{2c}" to lower case.

Page 58, Equation 26: Make symbol changes indicated for page 57.

Page 58, Column 2, Line 10: Change Example 13 to Example 11.

Page 60, Figure 35: Delete Figure 35.

Page 60, Column 2, Line 9: Delete the sentence," The second series of reports contain ...", and substitute the sentence, "Subsequent reports contain up-to-date compilation of data."

Pages 60 and 61: Delete the paragraph "Recently a nationwide series of water supply papers was completed..." and substitute the paragraph:

"The Geological Survey is preparing a report for each State decribing hydrologic procedures for estimating flows at ungaged sites in that State. The engineer making the hydrologic analysis should contact the State District Office of the U.S. Geological Survey to obtain the latest information available."

Page 61, Column 1: Delete the paragraph "The Bureau of Public Roads has made...".

Page 61, Column 1: Delete the footnote at the bottom of the column.

Page 66, Figure 36: In elevation, change "$\overline{Y}$ = 12.35" to "$\overline{y}$ = 12.35".

Page 67, Table 2: Change "Q_a" and "Q_c" to "Q_c" and "Q_a", respectively.

Page 67, Column 2, 1st line: Change "6384" to "5494".

Page 67, Column 2, Lines 4 and 5: Change to,

"$1.62\left[\left(\frac{2,434}{5,664}\right)^2 - \left(\frac{2,534}{6,494}\right)^2\right] 0.92 = 1.62 \times 0.048 \times 0.92 = 0.07$ft."

Page 67, Column 2, Line 7: Change to "$h_1^* = 1.07 + 0.07 = 1.14$ ft."

Page 67, Column 2, Third line from bottom: Change "12.36 ft." to "12.35 ft.".

Page 68, Column 1, Lines 2 and 3: Change "12.36" to "12.35".

Page 68, Column 2, Example 2, Lines 24 and 39: Change "12.36" to "12.35".

Page 79 through 82: Change all upper case symbols "Y" to lower case.

Page 80, Column 2, Line 11: Change "W_p" to "ΣW_p".

Page 81, Figure 46 A and B: Add note, "River bottom shown is bottom of equivalent trapezoid."

Page 84, Table 6: Add note, "Spillthrough abutment above water surface treated as vertical abutment." In BRIDGE INFORMATION INPUT, reverse numbers for Left abutment position, to read XAB(1)...0, XAB(2)...354.7 and YAB(1)...0, YAB(2)...93.5 Do likewise for the Right abutment position and make it read XAB(3)...427, XAB(4)...0 and YAB(3)...92.5, YAB(4)...0.

Page 85, Figure 47: Change symbol "y" to "$\bar{y}$".

Page 85, Column 1, Line 13: Change "92,50" to "92.50".

Page 87, Column 2, 8th line from bottom: Change "Messers" to "Messrs".

Page 88, Column 1, Second line from bottom: Change "V_2^2" to "V_1^2".

Page 89, Column 2, Line 8: Change "$\bar{Y}$" to lower case.

Page 89, Column 2, Next to last line: Change "proposals" to "proposal".

Page 91: Delete references 12 and 15.

Page 95, Column 1, Line 6: Change "Y_{2c}" to lower case.

Page 98, Page 99, Table A-1, and Page 102, Table B-2: Change all upper case symbols "Y" to lower case.

Page 104, Column 1, Line 4: Change "less" to "larger".

Page 107, Table B-3, Column (4): Change symbol Y_n to lower case.

PREFACE

The design information in the first edition of "Hydraulics of Bridge Waterways," published in 1960, was based principally on the results of hydraulic model studies and was definitely limited in its range of application. Over the intervening 10 years the U.S. Geological Survey has taken measurements and collected field data on the hydraulics of bridges during floods. Upon examination of the field data it was deemed advisable to reevaluate the model results to determine the actual limits of application and then utilize the field data to complete the design curves.

This edition thus contains revisions to some of the design curves. A considerable amount of new material has been added such as chapters on partially inundated superstructures, the proportioning of spur dikes at bridge abutments, and supercritical flow under a bridge, together with examples. An appendix has also been included to show how the general expressions for bridge backwater were derived and to explain how and why changes were made to some of the former design curves. The field results have added considerably to the reliability of the information contained herein.

Mr. Lester A. Herr, Chief of the Hydraulics Branch, Bridge Division, requested and supervised the preparation of this revised edition of the "Hydraulics of Bridge Waterways." Many thanks go to Mr. Herr and Mr. J. K. Searcy of his staff for their time and helpful suggestions in the technical editing of the present edition. The research program on bridge waterways, which was the basis of the first edition, was directed by Carl S. Izzard, then Chief of the Hydraulics Research Division of the Bureau of Public Roads. The writer, who served as project supervisor, is greatly indebted to Mr. Izzard for his gifted guidance and timely suggestions.

CONTENTS

FIGURES

TABLES

Chapter I.—INTRODUCTION

1.1 General. There was a time, now past, when backwater caused by the presence of bridges during flood periods was considered a necessary nuisance—first, because the public clamored for bridges to replace ferries and fords; and second, because there was no accurate means of determining the amount of backwater a bridge would produce after it was in place. With the spread of urbanization; with indefinite, unenforceable restrictions on the construction of housing and business establishments on flood plains of rivers and streams throughout the country; with new highway bridges being constructed at an ever-increasing rate; and with property values increasing at an unprecedented rate in the past two decades, it is now imperative that the backwater produced by new bridges be kept within very knowledgeable and reasonable limits. This places demands on the hydraulic engineer, who has not been consulted too often in the past, to promote and develop a more scientific approach to the bridge waterway problem. Progress in structural design has kept pace with the times. Structural engineers are well aware of the economies which can be attained in the proper type, selection and design of a bridge of a given overall length and height. The role of the hydraulic engineer in establishing what the length and vertical clearance should be and where the bridge should be placed is less well understood due principally to the lack of hydrological and hydraulic information on the waterways.

In fact, until recently, bridge lengths and clearances have been proportioned principally on rough calculations, individual judgment, and intuition. This may still be true in some cases. Today traffic volumes have become so great on primary roads that bridge failures or bridges out of service for any length of time can cause severe economic loss and inconvenience; even closing one lane of an arterial highway for repairs creates pandemonium.

Confining flood waters unduly by bridges can cause excessive backwater resulting in flooding of upstream property, backwater damage suits, overtopping of roadways, excessive scour under the bridge, costly maintenance, or even loss of a bridge. On the other hand, overdesign or making bridges longer than necessary for the sake of safety, can add materially to the initial cost, especially when dual or multiple lane bridges are involved. Both extremes in design have been experienced. Somewhere between the two extremes is the bridge which will prove not only safe but the most economical to the public over a long period of time. Finding that design is of great concern to the Bureau of Public Roads, which has sponsored and financed research on related projects for the past decade and a half.

Recent improvements in methods of dealing with the magnitude and frequency of floods, experimental information on scour, and the determination of expected backwater all are providing stepping stones to a more scientific approach to the bridge waterway problem. This publication is intended to provide, within the limitations discussed in chapter XIII, a means of determining the effect of a given bridge upon the flow in a stream. It does not prescribe criteria as to the allowable amount of backwater or frequency of the design flood; these are policy matters that must take into account class of highway, density of traffic, seriousness of flood damage, foundation conditions and other factors.

1.2 Waterway studies. In recognition of the need for dependable hydraulic information, the Bureau of Public Roads initiated a cooperative research project with Colorado State University in 1954 which culminated in the investigation of several features of the waterway problem. These included a study of bridge backwater (*18*),* scour at abutments and piers, and the effect of scour on backwater. Concurrently with this work, the Iowa State Highway Commission and the Bureau of Public Roads sponsored studies of scour at bridge piers (*23*) and scour at abutments (*24*) at the Iowa Institute of Hydraulic Research at Iowa City. In 1957 the State Highway Departments of Mississippi and Alabama, in cooperation with the Bureau of

* Italic numbers in parentheses refer to publications listed in the selected bibliography.

Public Roads, sponsored a project at Colorado State University to study means of reducing scour under a bridge by the use of spur dikes (*19*, *25*) (elliptical shaped earth embankments placed at the upstream end of a bridge abutment).

The above laboratory studies, in which hydraulic models served as the principal research tool, have been completed. Since then considerable progress has been made in the collection of field data by the U.S. Geological Survey to substantiate the model results and extend the range of application. There is still much to be learned from field observations and it is recommended that this phase of investigation be continued for sometime to come.

1.3 Bridge backwater. An account of the testing procedure, a record of basic data, and an analysis of results on the bridge backwater studies are contained in the comprehensive report (*18*) issued by Colorado State University. Results of research described in that report were drawn upon for this publication, which deals with that part of the waterway problem that pertains to the nature and magnitude of backwater produced by bridges constricting streams. This publication is prepared specifically for the designer and contains practical design charts, procedures, examples, and a text limited principally to describing the proper use of the information.

1.4 Nature of bridge backwater. It is seldom economically feasible or necessary to bridge the entire width of a stream as it occurs at flood flow. Where conditions permit, approach embankments are extended out onto the flood plain to reduce costs, recognizing that, in so doing, the embankments will constrict the flow of the stream during flood stages. This is acceptable practice so long as it is done within reason.

The manner in which flow is contracted in passing through a channel constriction is illustrated in figure 1. The flow bounded by each adjacent pair of streamlines is the same (1,000 c.f.s.). Note that the channel constriction appears to produce practically no alteration in the shape of the streamlines near the center of the channel. A very marked change is evidenced near the abutments, however, since the momentum of the flow from both sides (or flood plains) must force the advancing central portion of the stream over to gain entry to the constriction. Upon leaving the constriction the flow gradually expands (5 to 6 degrees per side) until normal conditions in the stream are again reestablished.

Constriction of the flow causes a loss of energy, the greater portion occurring in the reexpansion downstream. This loss of energy is reflected in a rise in the water surface and in the energy line upstream from the bridge. This is best illustrated by a profile along the center of the stream, as shown in figures 2A and 3A. The normal stage of the stream for a given discharge, before constricting the channel, is represented by the dash line labeled "normal water surface." (Water surface is abbreviated as "W.S." in the figures.) The nature of the water surface after constriction of the channel is represented by the solid line, "actual water surface." Note that the water surface starts out above normal stage at section 1, passes through normal stage close to section 2, reaches minimum depth in the vicinity of section 3, and then returns to normal stage a considerable distance downstream, at section 4. Determination of the rise in water surface at section 1, denoted by the symbol h_1* and referred to as the bridge backwater, is the primary objective of this publication. Attention is called to a common misunderstanding that the drop in water surface across the embankment, Δh, is the backwater caused by a bridge. This is not correct as an inspection of figure 2A or 3A will show. The backwater is represented by the symbol h_1* on both figures and is always less than Δh.

The Colorado laboratory model represented the ideal case since the testing was done principally in a rectangular, fixed bed, adjustable sloping flume, 8 feet wide by 75 feet long. Roughness of the bed was changed periodically but for any particular set of tests, it was uniform throughout the flume. Except for roughness of the bed, the flow was in no way restrained from contracting and expanding. The model data would apply to relatively straight reaches of a stream having approximately uniform slope and no restraint to lateral movement of the flow. Field measurements indicate that a stream cross section can vary considerably without causing serious error in the computation of backwater. The very real problem of scour was avoided in the initial tests by the use of rigid boundaries. Ignoring scour in computations will give generous backwater values but scour must be considered in assessing the safety of abutments and piers. The increase in water area in the constriction caused by scour will in turn produce a reduction in backwater over that for a rigid bed. On the other hand, unusually heavy vegetation on the flood plain downstream can interfere with the natural reexpansion process to such an extent as to increase the bridge backwater over normal conditions.

1.5 Types of flow encountered. There are

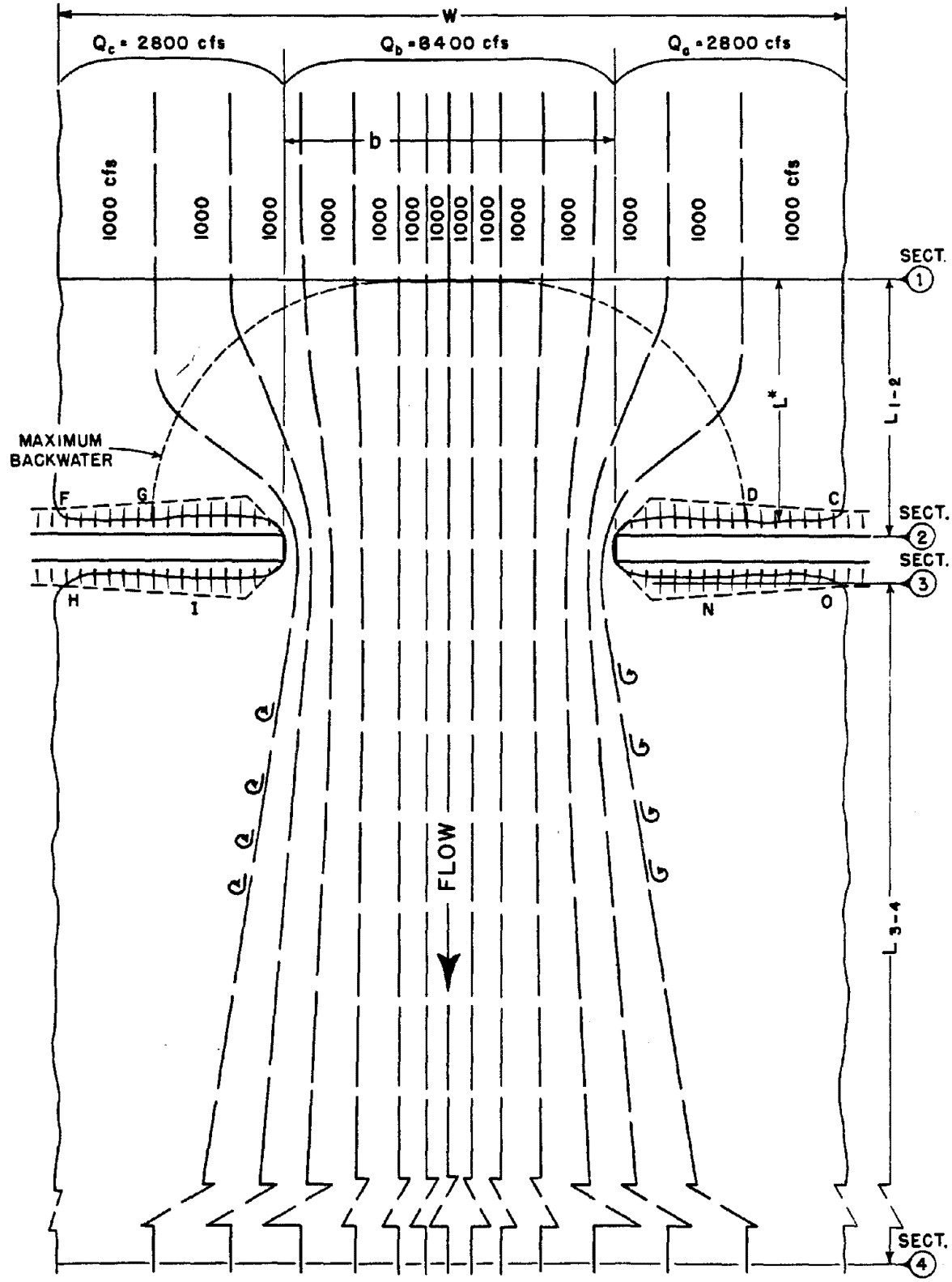

Figure 1.—Flow lines for typical normal crossing.

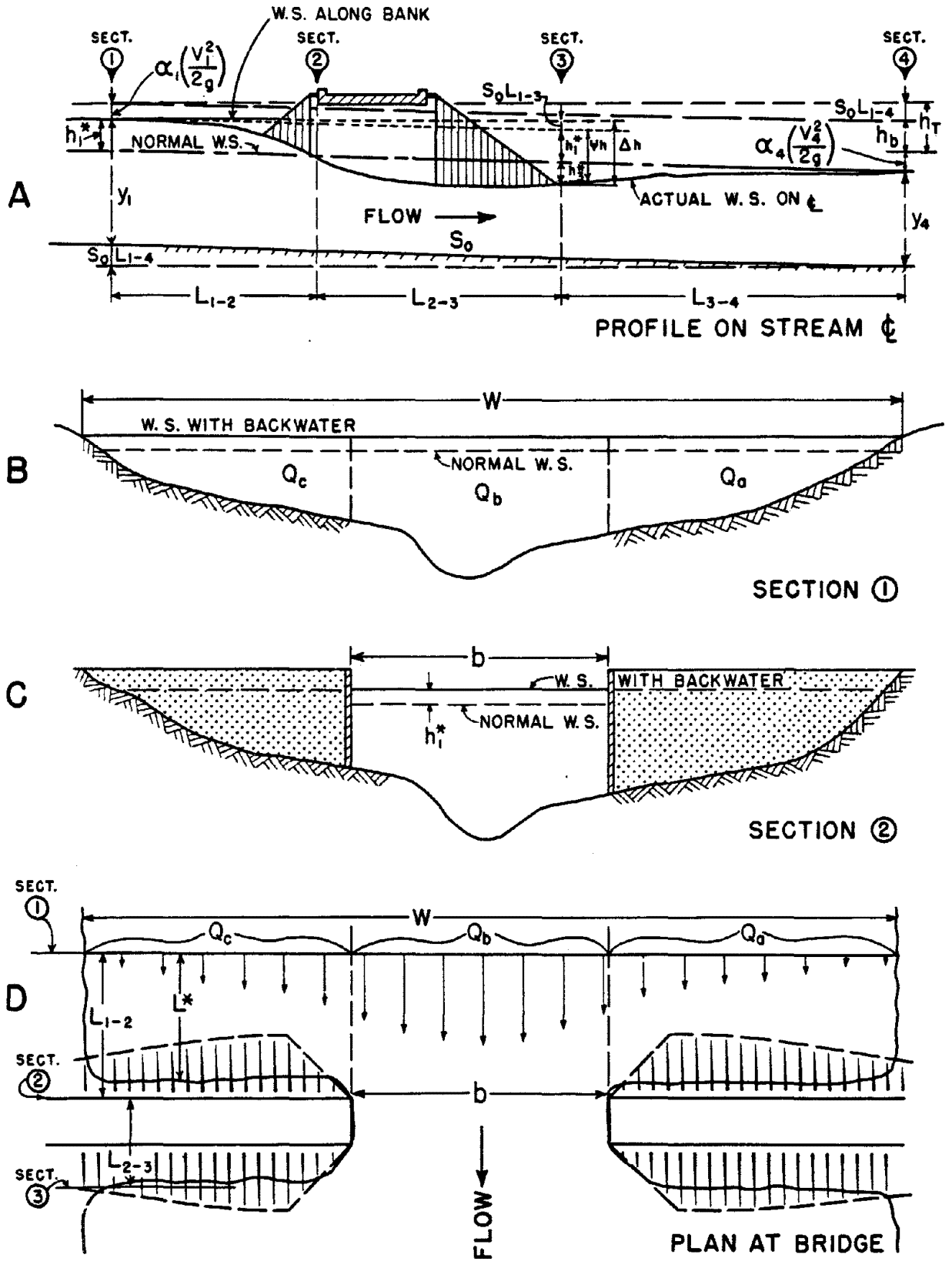

Figure 2.—Normal crossing: Wingwall abutments.

three types of flow which may be encountered in bridge waterway design. These are labeled types I through III on figure 4. The long dash lines shown on each profile represent normal water surface, or the stage the design flow would assume prior to placing a constriction in the channel. The solid lines represent the configuration of the water surface, on centerline of channel in each case, after the bridge is in place. The short dash lines represent critical depth, or critical stage in the main channel (Y_{1c} and Y_{4c}) and critical depth within the constriction, Y_{2c}, for the design discharge in each case. Since normal depth is shown essentially the same in the four profiles, the discharge, boundary roughness and slope of channel must all increase in passing from type I to type IIA, to type IIB, to type III flow.

Type I Flow

Referring to figure 4A, it can be observed that normal water surface is everywhere above critical depth. This has been labeled type I or subcritical flow, the type usually encountered in practice. With the exception of chapter X, and example 11, all design information in this publication is limited to type I (subcritical flow). The backwater expression for type I flow is obtained by applying the conservation of energy principle between sections 1 and 4. The method of analysis is presented in section A.1, appendix A.

Type IIA Flow

There are at least two variations of type II flow which will be described here under types IIA and IIB. For type IIA flow, figure 4B, normal water surface in the unconstricted channel again remains above critical depth throughout but the water surface passes through critical depth in the constriction. Once critical depth is penetrated, the water surface upstream from the constriction, and thus the backwater, becomes independent of conditions downstream (even though the water surface returns to normal stage at section 4). Thus the backwater expression for type I flow is not valid for type II flow.

Type IIB Flow

The water surface for type IIB flow, figure 4C, starts out above both normal water surface and critical depth upstream, passes through critical depth in the constriction, next dips below critical depth downstream from the constriction and then returns to normal. The return to normal depth can be rather abrupt as in figure 4C, taking place in the form of a poor hydraulic jump, since normal water surface in the stream is above critical depth. A backwater expression applicable to both types IIA and IIB flow has been developed by equating the total energy between section 1 and the point at which the water surface passes through critical stage in the constriction. (See section A.2, appendix A.)

Type III Flow

In type III flow, figure 4D, the normal water surface is everywhere below critical depth and the flow throughout is supercritical. This is an unusual case requiring a steep gradient but such conditions do exist, particularly in mountainous regions. Theoretically backwater should not occur for this type, since the flow throughout is supercritical. It is more than likely that an undulation of the water surface will occur in the vicinity of the constriction, however, as indicated on figure 4D.

1.6 Field verification. The first edition of this bulletin was prepared principally from the results of model studies verified by several backwater measurements taken by the U.S. Geological Survey during floods on medium size bridges. The field structures measured up to 220 feet in length with flood plains as wide as 0.5 mile. A summary of this information is contained in the comprehensive model study report (*18*). It was presumed that the design information could be used in the range prescribed with confidence. The applicability of the information to structures with larger width to depth ratios remained to be proven.

Since publication of the first edition, the U.S. Geological Survey has made additional field measurements during floods at an assortment of bridges. These measurements were sponsored by the Mississippi Highway Department and the Bureau of Public Roads and were made at bridges up to 2,100 feet in length in the State of Mississippi. Flood plains were generally heavily vegetated and extremely wide which boosted the width to depth ratios, formerly limited to 112, to over 700. A summary of the field data to date is included in tables B–1, B–2, and C–1.

The recently acquired field data have indicated that the model studies are only partially valid for type I flow. This was principally due to the width to depth limitation. For bridge opening ratios (sec. 1.10) less than $M=0.55$, the flow in the model could change from type I to type II, but regardless

of the value of the contraction ratio M, all field structures investigated in the State of Mississippi operated well within the subcritical range. It was thus necessary to revise the former backwater base curve, figure 6, and some others. Where changes in the former design curves have been made, mention is made of this fact in the appropriate chapter and explanations and data supporting these changes are included in appendix B. To maintain continuity and brevity in the design procedure, extraneous material has been reserved for the appendixes.

The changes incorporated in this edition are in the backwater coefficient curve (fig. 6), the distance to maximum backwater curve (fig. 13), and dual bridges (figs. 14 and 15). Figure 10 for skewed crossings and figure 12 for differential level across embankments have been changed only in format to facilitate their use. New sections have been added on partially inundated bridges and flow over roadway (ch. VIII), spur dikes (ch. IX), and backwater coefficients for type II flow (ch. X).

1.7 Definition of symbols. Most of the symbols used in this publication are recorded here for reference. Symbols not found here are defined where first mentioned.

A_1 = Area of flow including backwater at section 1 (figs. 2B and 3B) (sq. ft.).

A_{n1} = Area of flow below normal water surface at section 1 (figs. 2B and 3B) (sq. ft.).

A_{n2} Gross area of flow in constriction below normal water surface at section 2 (figs. 2C and 3C) (sq. ft.).

A_4 Area of flow at section 4 at which normal water surface is reestablished (fig. 2A) (sq. ft.).

A_p = Projected area of piers normal to flow (between normal water surface and streambed) (sq. ft.).

A_s = Area of scour measured on downstream side of bridge (sq. ft.).

a = Area of flow in a subsection of approach channel (sq. ft.).

B = Width of test flume or $A_1/\bar{y}$ for field structures.

b = Width of constriction (figs. 2C, 3C, and sec. 1.8) (ft.).

b_s = Width of constriction of a skew crossing measured along centerline of roadway (fig. 9) (ft.).

C = h_{1s}^*/h_1^* = Correction factor for backwater with scour.

C_b = Backwater coefficient for flow type II.

C_f = Freeflow coefficient for flow over roadway embankment.

C_s = Submergence factor for flow over roadway.

$D_b = \dfrac{h_b^*}{h_b^*+h_3^*}$ = Differential level ratio.

e = Eccentricity = $(1-Q_c/Q_a)$ where

$$Q_c < Q_a,$$

or $(1-Q_a/Q_c)$ where

$$Q_c > Q_a.$$

g = Acceleration of gravity = 32.2 (ft./sec.^{2}).

h_T = Total energy loss between sections 1 and 4 (figs. 2A and 3A) (ft.).

h_b = $h_T-S_0L_{1-4}$ = Energy loss caused by constriction (figs. 2A and 3A) (ft.).

h_1^* = Total backwater or rise above normal stage at section 1 (figs. 2A and 3A) (ft.).

h_{1s}^* = Backwater with scour (ft.).

h_b^* = Backwater computed from base curve (fig. 6) (ft.).

h_d^* = Backwater produced by dual bridges, measured at section 1 (fig. 14).

h_3^* = Vertical distance from water surface on downstream side of embankment to normal water surface at section 3 (figs. 2A and 3A) (ft.).

Δh = $h_1^*+h_3^*+S_0L_{1-3}$ = Difference in water surface elevation across roadway embankment (figs. 2A and 3A) (ft.).

J = A_p/A_{n2} = Ratio of area obstructed by piers to gross area of bridge waterway below normal water surface at section 2 (fig. 7).

K_b = Backwater coefficient from base curve (fig. 6).

ΔK_p = Incremental backwater coefficient for piers (fig. 7).

ΔK_e = Incremental backwater coefficient for eccentricity (fig. 8).

ΔK_s = Incremental backwater coefficient for skew (fig. 10).

K^* = $K_b+\Delta K_p+\Delta K_e+\Delta K_s$ = Total backwater coefficient for subcritical flow.

k = Conveyance in subsection of approach channel.

k_b = Conveyance of portion of channel within projected length of bridge at section 1 (figs. 2B and 3B and sec. 1.9).

k_a, k_c = Conveyance of that portion of the natural flood plain obstructed by the roadway embankments (subscripts refer to left and

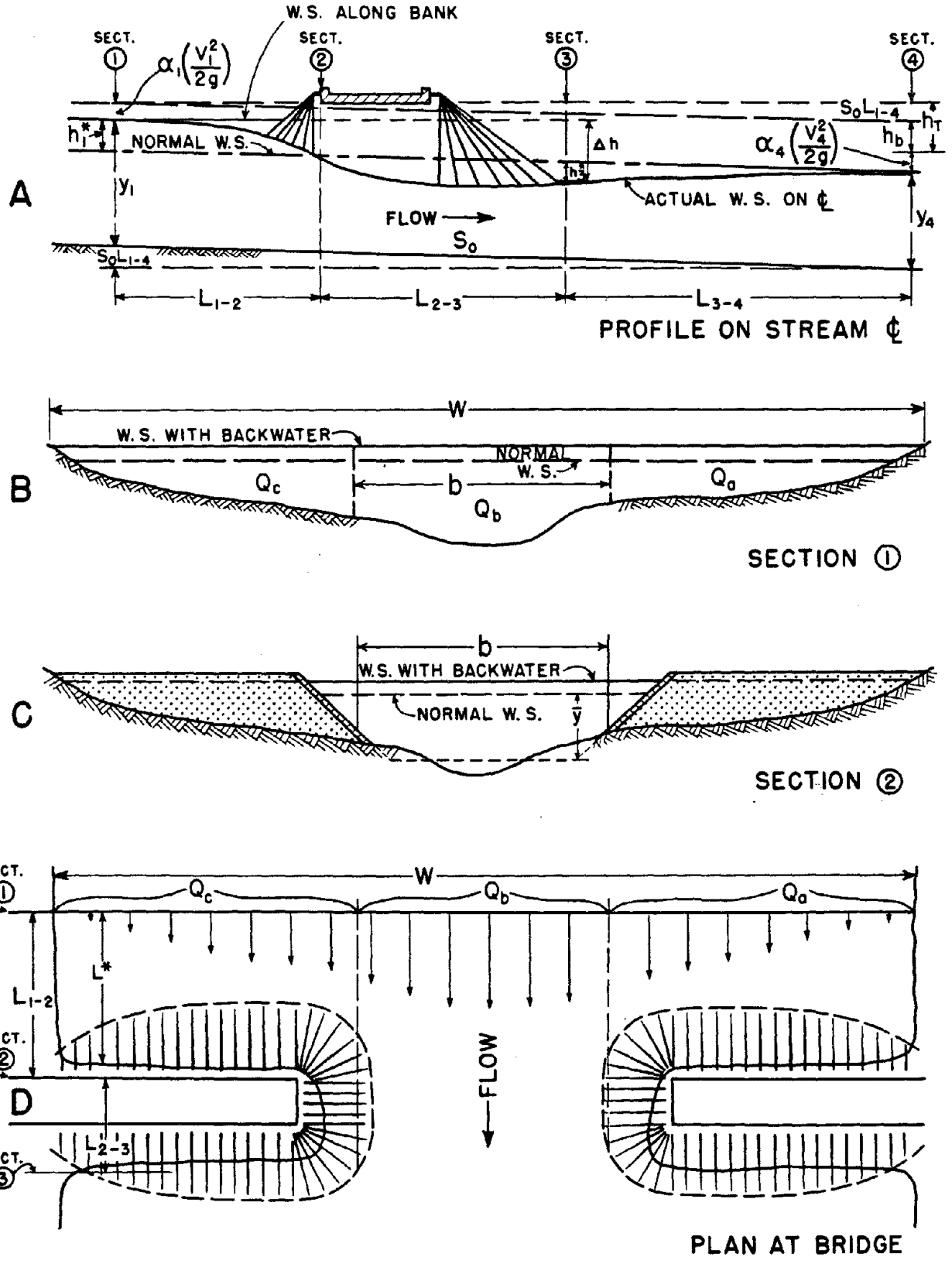

Figure 3.—Normal crossings: Spillthrough abutments.

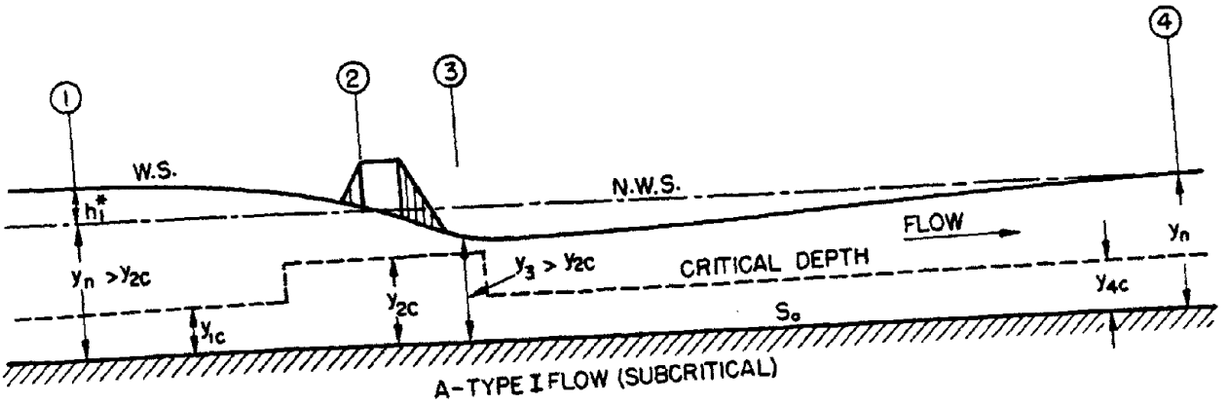

A-TYPE I FLOW (SUBCRITICAL)

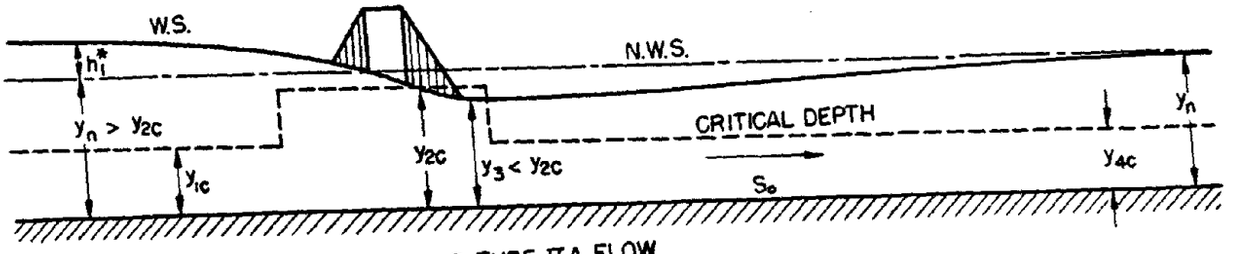

B-TYPE IIA FLOW
(PASSES THROUGH CRITICAL)

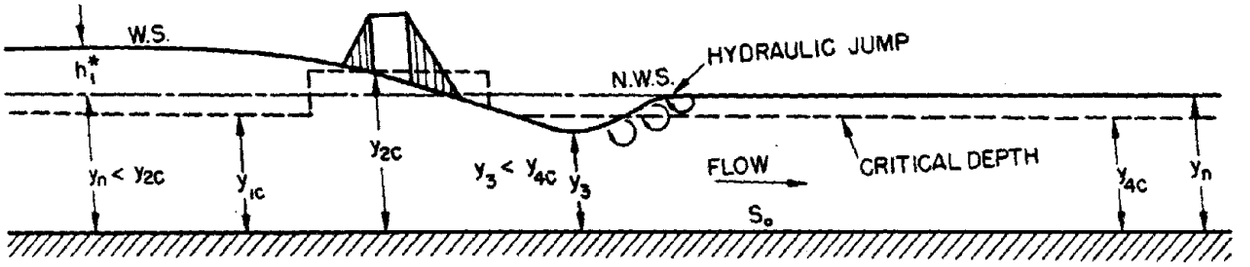

C-TYPE IIB FLOW
(PASSES THROUGH CRITICAL)

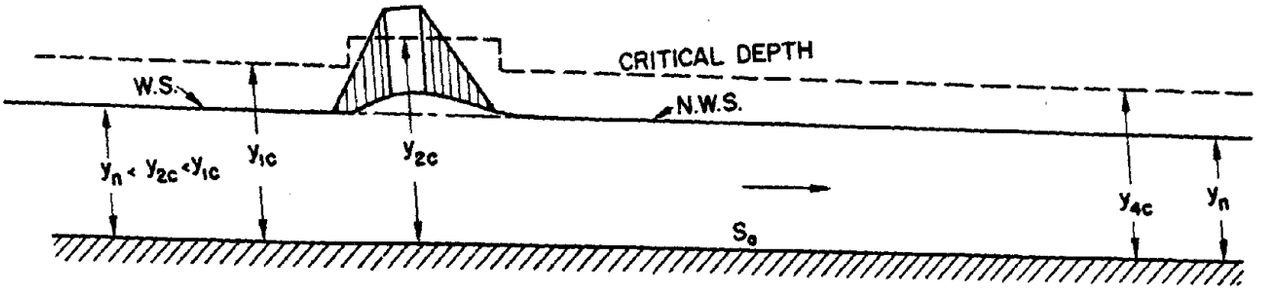

D-TYPE III FLOW
(SUPERCRITICAL)

Figure 4.—Types of flow encountered.

right side, facing downstream) (figs. 2B and 3B and sec. 1.9).

K_1 = Total conveyance at section 1 (sec. 1.9).

L_{1-4} = Distance from point of maximum back water to reestablishment of normal water surface downstream, measured along centerline of stream (figs. 2A and 3A) (ft.).

L_{1-3} = Distance from point of maximum backwater to water surface on downstream side of roadway embankment (figs. 2A and 3A) (ft.).

L_{1-2} = Distance from point of maximum backwater to upstream face of bridge deck (figs. 2A and 3A) (ft.).

L^* = Distance from point of maximum backwater to water surface on upstream side of roadway embankment, measured parallel to centerline of stream (fig. 13) (ft.).

L_d = Distance between upstream face of first bridge and downstream face of second bridge (dual bridges) (ft.).

l = Overall width of roadway or bridge (ft.).

M = Bridge opening ratio (sec. 1.10).

n = Manning roughness coefficient (table 1).

p = Wetted perimeter of a subsection of a channel (ft.).

Q_b = Flow in portion of channel within projected length of bridge at section 1 (fig. 1) (c.f.s.).

Q_a, Q_c = Flow over that portion of the natural flood plain obstructed by the roadway embankments (fig. 1) (c.f.s.).

Q = $Q_a+Q_b+Q_c$ = Total discharge (c.f.s.).

r = a/p = Hydraulic radius of a subsection of flood plain or main channel (ft.).

S_0 = Slope of channel bottom or normal water surface.

V_1 = Q/A_1 = Average velocity at section 1 (ft./sec.).

V_4 = Q/A_4 = Average velocity at section 4 (ft./sec.).

V_{n2} = Q/A_{n2} = Average velocity in constriction for flow at normal stage (ft./sec.).

V_{2c} = Critical velocity in constriction (ft./sec.).

w_p = Width of pier normal to direction of flow (fig. 7) (ft.).

W = Surface width of stream including flood plains (fig. 1) (ft.).

y_1 = Depth of flow at section 1 (ft.).

y_4 = Depth of flow at section 4 (ft.).

y_n = Normal depth of flow in model (ft.).

$\bar{y}$ = A_{n2}/b = Mean depth of flow under bridge, referenced to normal stage, (fig. 3C) (ft.).

y_{1c} = Critical depth at section 1 (ft.).

y_{2c} = Critical depth in constriction (ft.).

y_{4c} = Critical depth at section 4 (ft.).

α_1 = Velocity head coefficient at section 1 (sec. 1.11) (Greek letter alpha).

α_2 = Velocity head coefficient for constriction (Greek letter alpha.).

η = h_d^*/h_1^* = Backwater multiplication factor for dual bridges (Greek letter eta).

σ = Multiplication factor for influence of M on incremental backwater coefficient for piers (fig. 7B) (Greek letter sigma.).

ψh = $h_1^*+h_3^*$ = for single bridge (Greek letter psi.).

ψh_{3B} = $h_d^*+h_{3B}^*$ = Term used in computing difference in water surface elevation across two embankments (dual crossings) (fig. 14).

ξ = $\psi h_{3B}/\psi h$ = Differential level multiplication factor for dual bridges (sec. 5.3) (Greek letter xi.).

ω = Correction factor for eccentricity (fig. 13) (Greek letter omega.).

ϕ = Angle of skew—degrees (fig. 9) (Greek letter phi.).

SPUR DIKES

L_s = Length of spur dike (ft.) (fig. 30).

Q_f = Lateral or flood plain flow (c.f.s.).

Q_{100} = Discharge confined to 100 feet of stream width adjacent to bridge abutment (c.f.s.).

$\bar{y}_{100}$ = Average depth of flow in 100 feet of stream adjacent to bridge abutment.

Q_f/Q_{100} = Spur dike discharge ratio.

1.8 Definition of terms. Specific explanation is given below with respect to the concept of several of the terms and expressions frequently used throughout the discussion:

Normal stage.—Normal stage is the normal water surface elevation of a stream at a bridge site, for a particular discharge, prior to constricting the stream (see figs. 2A and 3A). The profile of the water surface is essentially parallel to the bed of the stream.

Abnormal stage.—Where a bridge site is located upstream from, but relatively close to, the confluence of two streams, high water in one stream can produce a backwater effect extending for some distance up the other stream. This can cause the stage at a bridge site to be abnormal, meaning higher than would exist for the tributary alone. An abnormal

stage may also be caused by a dam, another bridge, or some other constriction downstream. The water surface with abnormal stage is not parallel to the bed (fig. 16).

Normal crossings.—A normal crossing is one with alignment at approximately 90° to the general direction of flow during high water (as shown in fig. 1).

Eccentric crossing.—An eccentric crossing is one where the main channel and the bridge are not in the middle of the flood plain (fig. 8).

Skewed crossing.—A skewed crossing is one that is other than 90° to the general direction of flow during flood stage (fig. 9).

Dual crossing.—A dual crossing refers to a pair of parallel bridges, such as for a divided highway (fig. 14).

Multiple bridges.—Usually consisting of a main channel bridge and one or more relief bridges.

Width of constriction, b.—No difficulty will be experienced in interpreting this dimension for abutments with vertical faces since b is simply the horizontal distance between abutment faces. In the more usual case involving spillthrough abutments, where the cross section of the constriction is irregular, it is suggested that the irregular cross section be converted to a regular trapezoid of equivalent area, as shown in figure 3C. Then the length of bridge opening can be interpreted as:

$$b = \frac{A_{n2}}{\bar{y}}$$

Width to depth ratio.—Defined as width of flood plain to mean depth in constriction

$$\frac{B}{y_n} \text{ (model) or } \frac{A_1}{\bar{y}^2} \text{ for irregular cross section}$$

1.9 Conveyance. Conveyance is a measure of the ability of a channel to transport flow. In streams of irregular cross section, it is necessary to divide the water area into smaller but more or less regular subsections, assigning an appropriate roughness coefficient to each and computing the discharge for each subsection separately. According to the Manning formula for open channel flow, the discharge in a subsection of a channel is:

$$q = \frac{1.49}{n} a r^{2/3} S_0^{1/2}$$

By rearranging:

$$\frac{q}{S_0^{1/2}} = \frac{1.49}{n} a r^{2/3} = k$$

where k is the conveyance of the subsection. Conveyance can, therefore, be expressed either in terms of flow factors or strictly geometric factors. In bridge waterway computations, conveyance is used as a means of approximating the distribution of flow in the natural river channel upstream from a bridge. The method will be demonstrated in the examples of chapter XII. Total conveyance K_1 is the summation of the individual conveyances comprising section 1.

1.10 Bridge opening ratio. The bridge opening ratio, M, defines the degree of stream constriction involved, expressed as the ratio of the flow which can pass unimpeded through the bridge constriction to the total flow of the river. Referring to figure 1,

$$M = \frac{Q_b}{Q_a + Q_b + Q_c} = \frac{Q_b}{Q} \qquad (1)$$

or,

$$M = \frac{8{,}400}{14{,}000} = 0.60.$$

The irregular cross section common in natural streams and the variation in boundary roughness within any cross section result in a variation in velocity across a river as indicated by the stream tubes in figure 1. The bridge opening ratio, M, is most easily explained in terms of discharges, but it is usually determined from conveyance relations. Since conveyance is proportional to discharge, assuming all subsections to have the same slope, M can be expressed also as:

$$M = \frac{K_b}{K_a + K_b + K_c} = \frac{K_b}{K_1} \qquad (2)$$

1.11 Kinetic energy coefficient. As the velocity distribution in a river varies from a maximum at the deeper portion of the channel to essentially zero along the banks, the average velocity head, computed as $(Q/A_1)^2/2g$ for the stream at section 1, does not give a true measure of the kinetic energy of the flow. A weighted average value of the kinetic energy is obtained by multiplying the average velocity head, above, by a kinetic energy coefficient, α_1, defined as:

$$\alpha_1 = \frac{\Sigma(qv^2)}{QV_1^2} \qquad (3a)$$

Where

v = average velocity in a subsection.
q = discharge in same subsection.
Q = total discharge in river.
V_1 = average velocity in river at section 1 or Q/A_1.

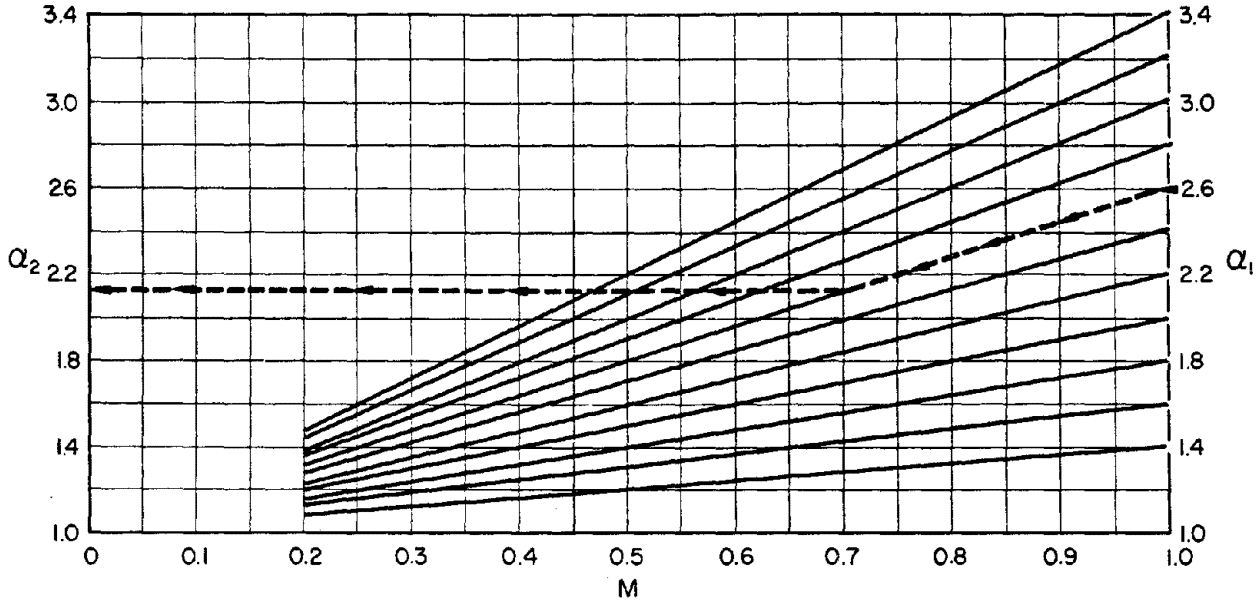

Figure 5.—Aid for estimating α_2.

The method of computation will be further illustrated in the examples in chapter XII.

A second coefficient, α_2, is required to correct the velocity head for nonuniform velocity distribution under the bridge,

$$\alpha_2 = \frac{\Sigma(qv^2)}{QV_2^2} \qquad (3b)$$

where v, q and Q are defined as above but apply here to the constricted cross section and

V_2 = average velocity in constriction = Q/A_2.

The value of α_1 can be computed but α_2 is not readily available for a proposed bridge. The best that can be done in the case of the latter is to collect, tabulate and compare values of α_2 from existing bridges. This has been done and values of both α_1 and α_2 are tabulated in columns 13 and 14 of table *B*–2. The information for determining α_2 was obtained from current meter traverses and soundings taken from the downstream side of bridges by the USGS. Figure 5, relating α_2 to α_1 and the contraction ratio, M, is supplied for estimating purposes only. The value of α_2 is usually less than α_1 for a given crossing but this is not always the case. Actually there should be no definite relation between the two but there is a trend. Local factors at the bridge should also be considered such as asymmetry of flow, variation in cross section and extent of vegetation in the bridge opening. Perhaps the best advise for estimating α_2 is to lean toward the generous side. The construction of the chart shown on figure 5 is described in section B.3, appendix B.

Chapter II.—COMPUTATION OF BACKWATER

2.1 Expression for backwater. Bridge backwater analysis is far from simple regardless of the method employed. Many minor as well as major variables are involved in any single waterway problem. For the model which was installed in a rectangular flume and operated with uniform roughness, minor variables such as type and geometry of abutments, width of abutments, slope of embankments, roadway widths and width to depth ratio could be evaluated in relation to the Froude Number as was done in the comprehensive model study report (*18*). In the case of bridges in the field where roughness of flood plain and main channel differ materially and channel cross sections are irregular, the Froude Number is no longer a meaningful parameter and minor variables lose their significance. This is especially true as bridge length is increased. Fortunately, reasonable accuracy is acceptable in most bridge backwater solutions, thus, a practical method, utilizing the dominant variables, is presented in this chapter for computing backwater produced by bridge constrictions.

A practical expression for backwater has been formulated by applying the principle of conservation of energy between the point of maximum backwater upstream from the bridge, section 1, and a point downstream from the bridge at which normal stage has been reestablished, section 4 (fig. 2A). The expression is reasonably valid if the channel in the vicinity of the bridge is essentially straight, the cross sectional area of the stream is fairly uniform, the gradient of the bottom is approximately constant between sections 1 and 4, the flow is free to contract and expand, there is no appreciable scour of the bed in the constriction and the flow is in the subcritical range.

The expression for computation of backwater upstream from a bridge constricting the flow, which is developed in the comprehensive report (*18*), is as follows:

$$h_1^* = K^*\alpha_2 \frac{V^2_{n2}}{2g} + \alpha_1 \left[\left(\frac{A_{n2}}{A_4} \right)^2 - \left(\frac{A_{n2}}{A_1} \right)^2 \right] \frac{V^2_{n2}}{2g} \quad (4)$$

Where

h_1^* = total backwater (ft.).
K^* = total backwater coefficient.
α_1 & α_2 = as defined in expressions 3a and 3b (sec. 1.11).
A_{n2} = gross water area in constriction measured below normal stage (sq. ft.).
V_{n2} = average velocity in constriction* or Q/A_{n2} (f.p.s.).
A_4 = water area at section 4 where normal stage is reestablished (sq. ft.).
A_1 = total water area at section 1, including that produced by the backwater (sq. ft.).

To compute backwater, it is necessary to obtain the approximate value of h_1^* by using the first part of expression (4):

$$h_1^* = K^*\alpha_2 \frac{V^2_{n2}}{2g} \quad (4a)$$

The value of A_1 in the second part of expression (4), which depends on h_1^*, can then be determined and the second term of the expression evaluated:

$$\alpha_1 \left[\left(\frac{A_{n2}}{A_4} \right)^2 - \left(\frac{A_{n2}}{A_1} \right)^2 \right] \frac{V^2_{n2}}{2g} \quad (4b)$$

This part of the expression represents the difference in kinetic energy between sections 4 and 1, expressed in terms of the velocity head, $V^2_{n2}/2g$. Expression (4) may appear cumbersome, but this is not the case.

Since the comprehensive report (*18*) is generally not available, a concise explanation regarding the development of the above backwater expression and the losses involved is included in appendix A of this bulletin under type I flow.

2.2 Backwater coefficient. Two symbols are interchangeably used throughout the text and both are backwater coefficients. The symbol K_b is the backwater coefficient for a bridge in which only the bridge opening ratio, M, is considered. This is known

* The velocity, V_{n2}, is not an actual measurable velocity, but represents a reference velocity readily computed for both model and field structures.

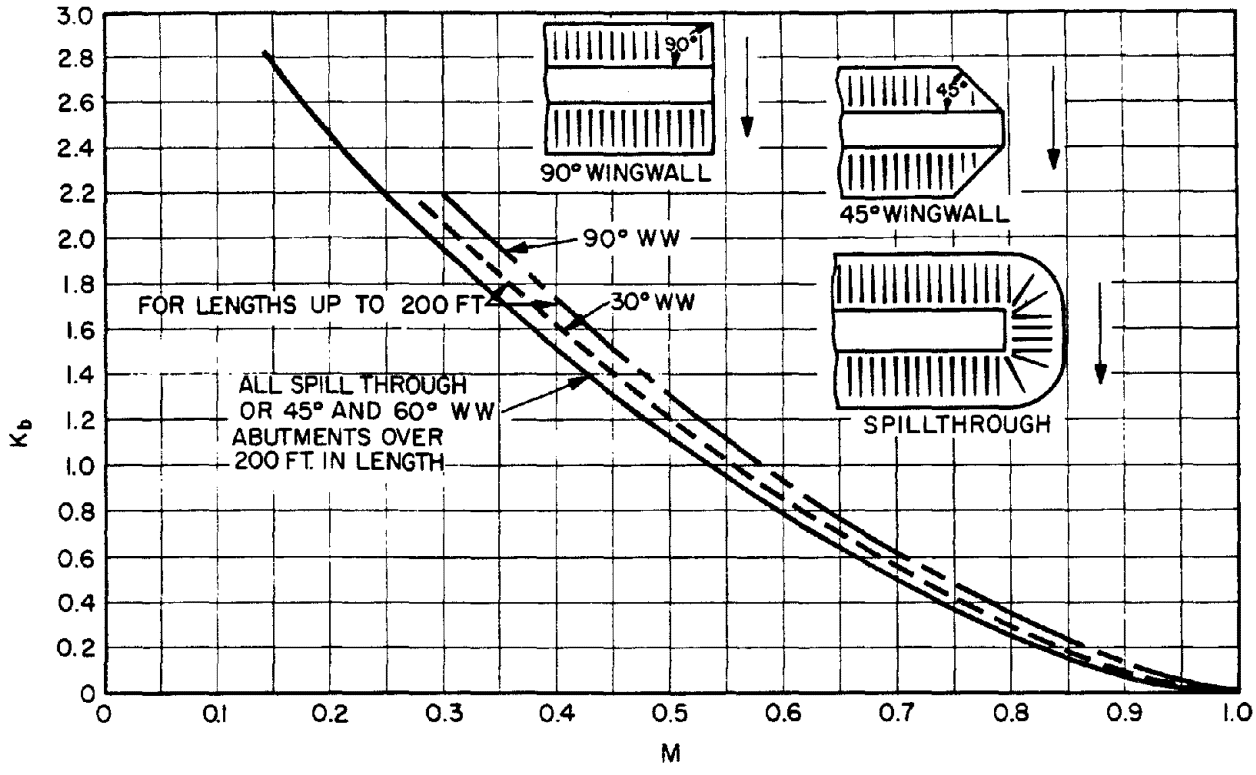

Figure 6.—Backwater coefficient base curves (subcritical flow).

as a base coefficient and the curves on figure 6 are called base curves. The value of the overall backwater coefficient, K^*, is likewise dependent on the value of M but also affected by:

1. Number, size, shape, and orientation of piers in the constriction,
2. Eccentricity or asymmetric position of bridge with respect to the valley cross section, and
3. Skew (bridge crosses stream at other than 90° angle).

It will be demonstrated that K^* consists of a base curve coefficient, K_b, to which is added incremental coefficients to account for the effect of piers, eccentricity and skew. The value of K^* is nevertheless primarily dependent on the degree of constriction of flow at a bridge.

2.3 Effect of M and abutment shape (base curves). Figure 6 shows the base curves for backwater coefficient, K_b, plotted with respect to the opening ratio, M, for wingwall and spillthrough abutments. Note how the coefficient, K_b, increases with channel constriction. The lower curve applies for 45° and 60° wingwall abutments and all spillthrough types. Curves are also included for 30° wingwall abutments and for 90° vertical wall abutments for bridges up to 200 feet in length. These shapes can be identified from the sketches on figure 6. Seldom are bridges with the latter type abutments more than 200 feet long. For bridges exceeding 200 feet in length, regardless of abutment type, the lower curve is recommended. This is because abutment geometry becomes less important to backwater as a bridge is lengthened. The base curve coefficients of figure 6 apply to crossings normal to flood flow and do not include the effect produced by piers, eccentricity and skew. Since the backwater coefficient base curve, figure 6, has been modified in this book, the reasoning and the supporting data for making this change have been placed in section B.1, appendix B.

2.4 Effect of piers (normal crossings). Backwater caused by introduction of piers in a bridge constriction has been treated as an incremental backwater coefficient designated ΔK_p, which is added to the base curve coefficient K_b when piers are present in the waterway. The value of the incremental backwater coefficient, ΔK_p, is dependent on the ratio that the area of the piers bears to the gross area of the bridge opening, the type of piers (or piling in the case of pile bents), the value of the bridge opening ratio, M, and the angularity of the

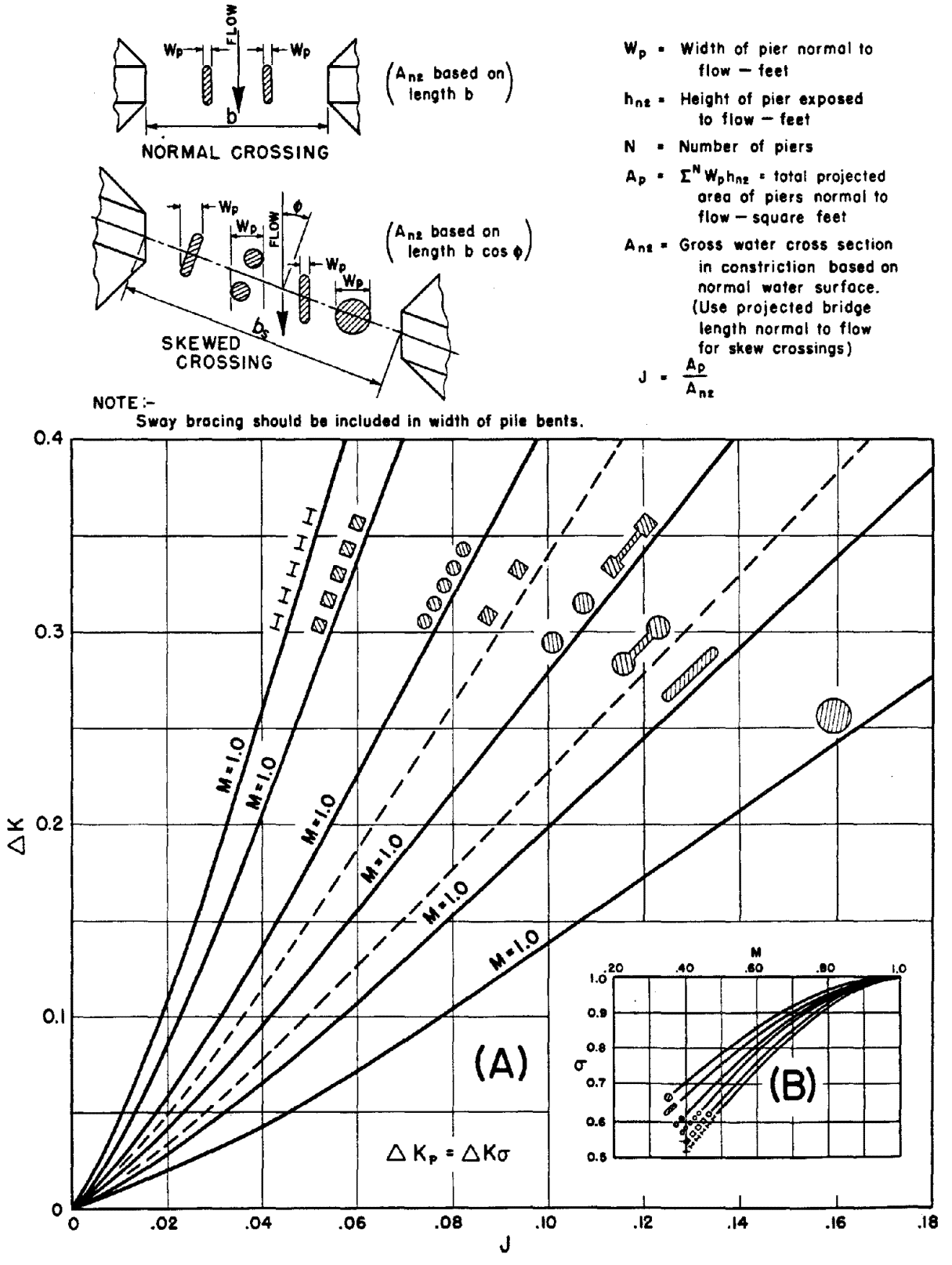

Figure 7.—Incremental backwater coefficient for piers.

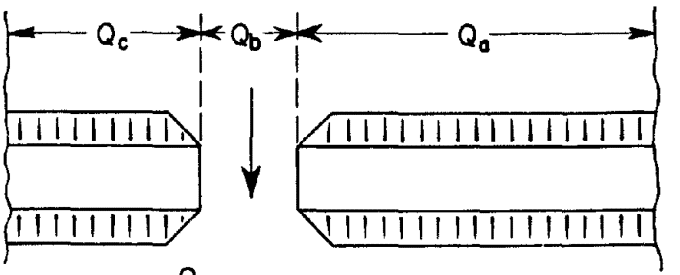

$$e = (1 - \frac{Q_c}{Q_a}) \quad \text{where} \quad Q_c < Q_a \quad \text{or}$$

$$e = (1 - \frac{Q_a}{Q_c}) \quad \text{where} \quad Q_a < Q_c$$

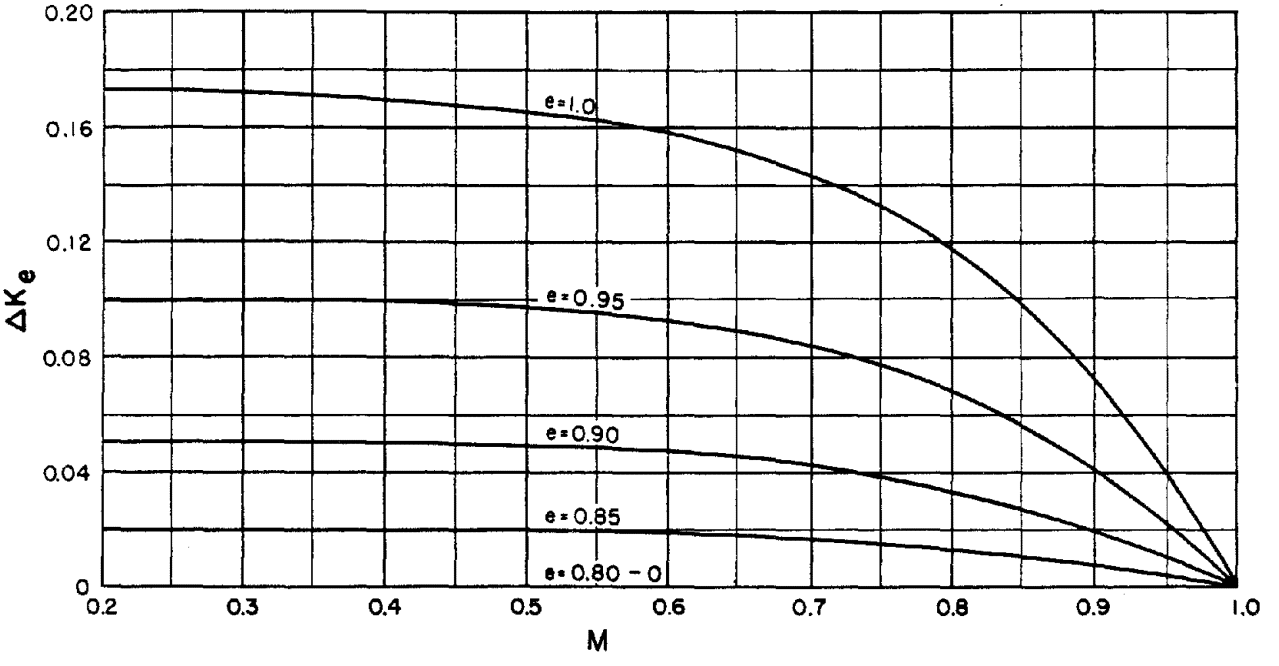

Figure 8.—Incremental backwater coefficient for eccentricity.

piers with the direction of flood flow. The ratio of the water area occupied by piers, A_p, to the gross water area of the constriction, A_{n2}, both based on the normal water surface, has been assigned the letter J. In computing the gross water area, A_{n2}, the presence of piers in the constriction is ignored. The incremental backwater coefficient for the more common types of piers and pile bents can be obtained from figure 7. By entering chart A with the proper value of J and reading upward to the proper pier type, ΔK is read from the ordinate. Obtain the correction factor, σ, from chart B for opening ratios other than unity. The incremental backwater coefficient is then:

$$\Delta K_p = \sigma \Delta K$$

The incremental backwater coefficients for pile bents can, for all practical purposes, be considered independent of diameter, width, or spacing of piles but should be increased if there are more than 5 piles in a bent. A bent with 10 piles should be given a value of ΔK_p about 20 percent higher than that shown for bents with 5 piles. If there is a possibility of trash collecting on the piers, or piles, it is ad-

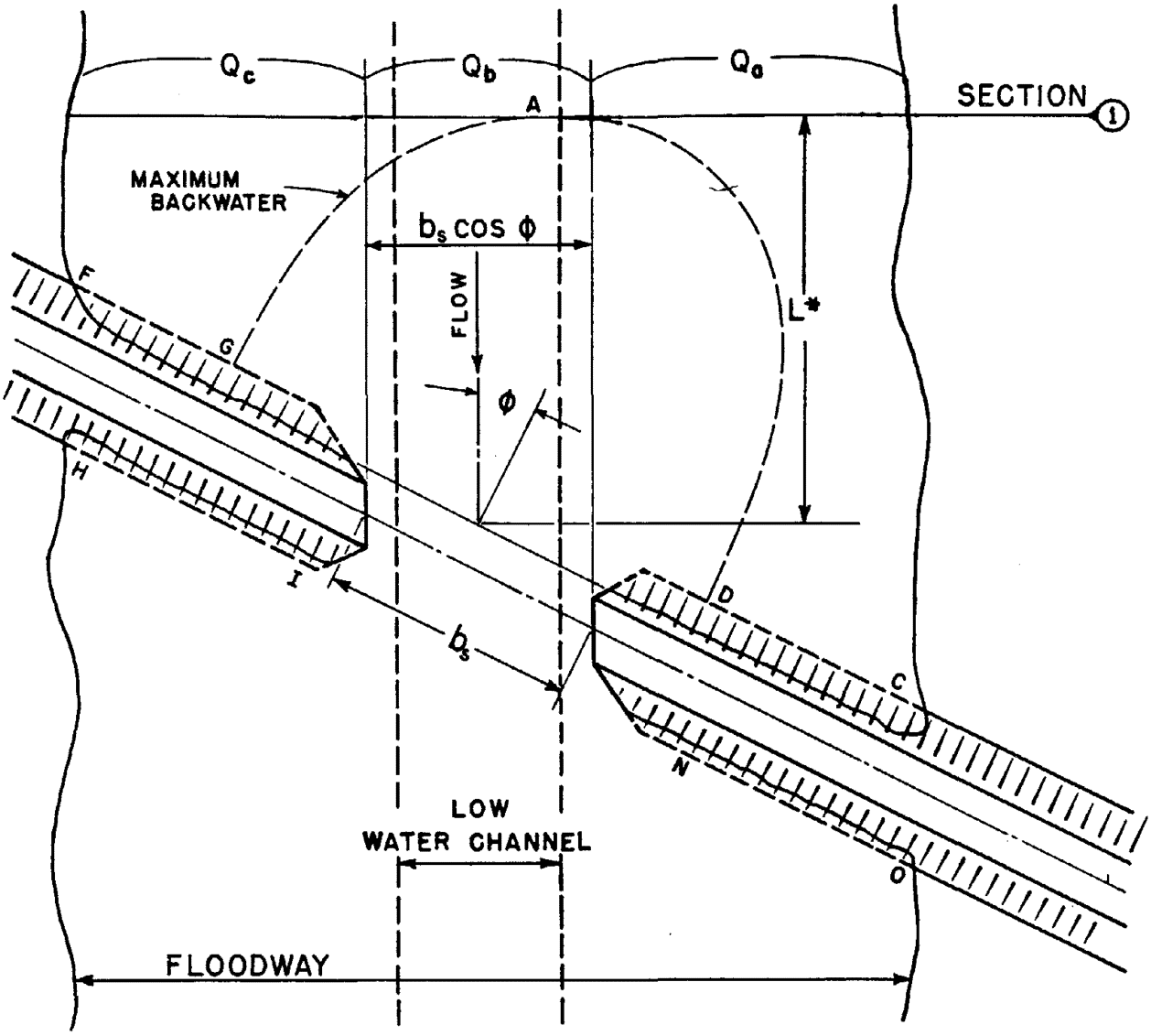

Figure 9.—Skewed crossings.

visable to use a larger value of J to compensate for the added obstruction. For a normal crossing with piers, the total backwater coefficient becomes:

$$K^* = K_b \text{ (fig. 6)} + \Delta K_p \text{ (fig. 7)}$$

2.5 Effect of piers (skewed crossings). In the case of skewed crossings, the effect of piers is treated as explained for normal crossings (sec. 2.4) except for the computation of J, A_{n2} and M. The pier area for a skewed crossing, A_p, is the sum of the individual pier areas normal to the general direction of flow, as illustrated by the sketch in figure 7. Note how the width of pier W_p is measured when the pier is not parallel to the general direction of flow. The area of the constriction, A_{n2}, for skewed crossings, is based on the projected length of bridge, $b_s \cos \phi$ (fig. 9). Again, A_{n2} is a gross value and includes the area occupied by piers. The value of J is the pier area, A_p, divided by the projected gross area of the bridge constriction, both measured normal to the general direction of flow. The computation of M for skewed crossings is also based on the projected length of bridge, which will be further explained in section 2.7.

2.6 Effect of eccentricity. Referring to the sketch in figure 8, it can be noted that the symbols Q_a and Q_c at section 1 were used to represent the portion of the discharge obstructed by the approach embankments. If the cross section is extremely asymmetrical so that Q_a is less than 20 percent of Q_c

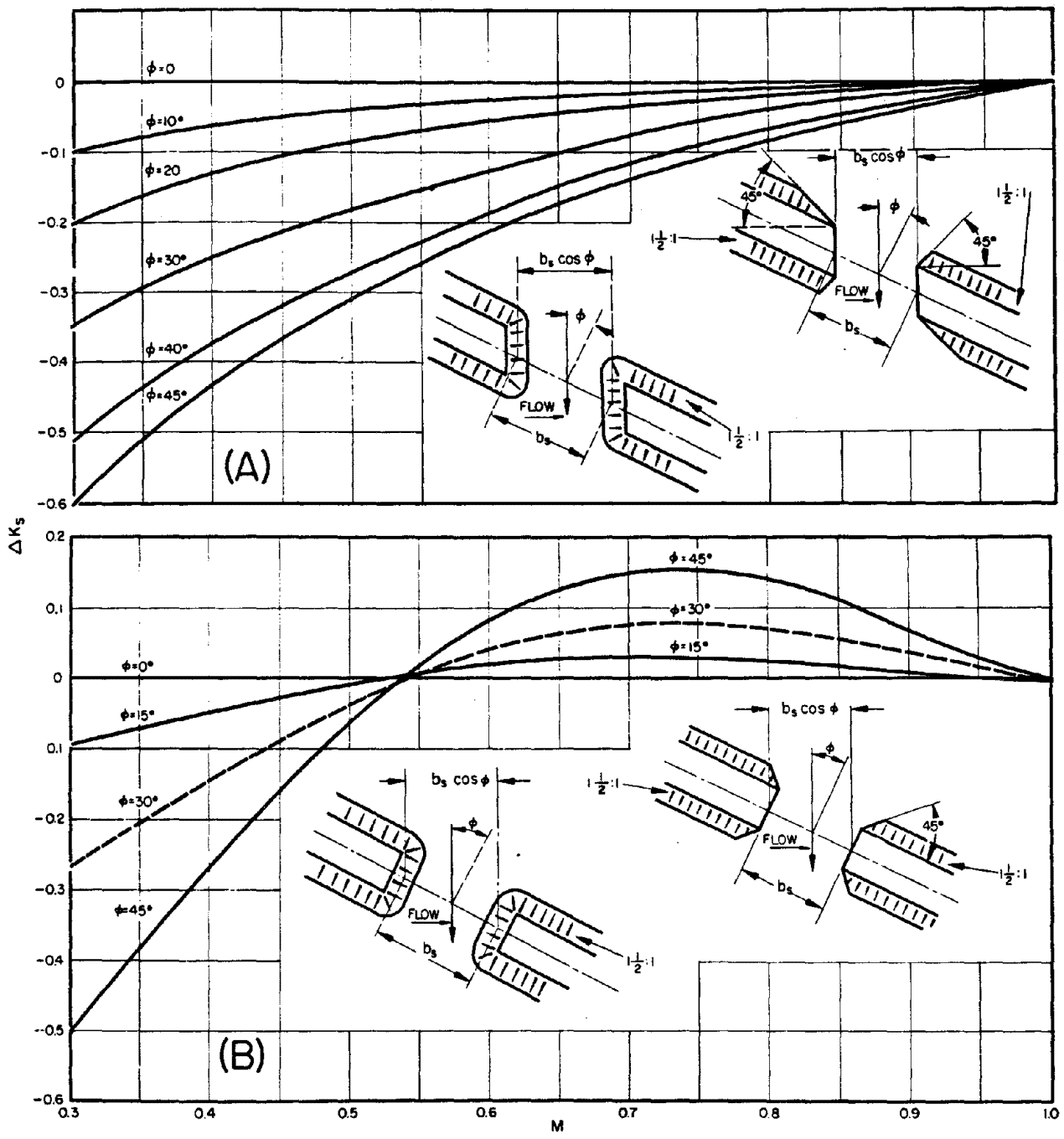

Figure 10.—Incremental backwater coefficient for skew.

or vice versa, the backwater coefficient will be somewhat larger than for comparable values of M shown on the base curve. The magnitude of the incremental backwater coefficient, ΔK_s, accounting for the effect of eccentricity, is shown in figure 8. Eccentricity, e, is defined as 1 minus the ratio of the lesser to the greater discharge outside the projected length of the bridge, or:

$$e = 1 - \frac{Q_c}{Q_a} \quad \text{where} \quad Q_c < Q_a$$

or: (5)

$$e = 1 - \frac{Q_a}{Q_c} \quad \text{where} \quad Q_c > Q_a.$$

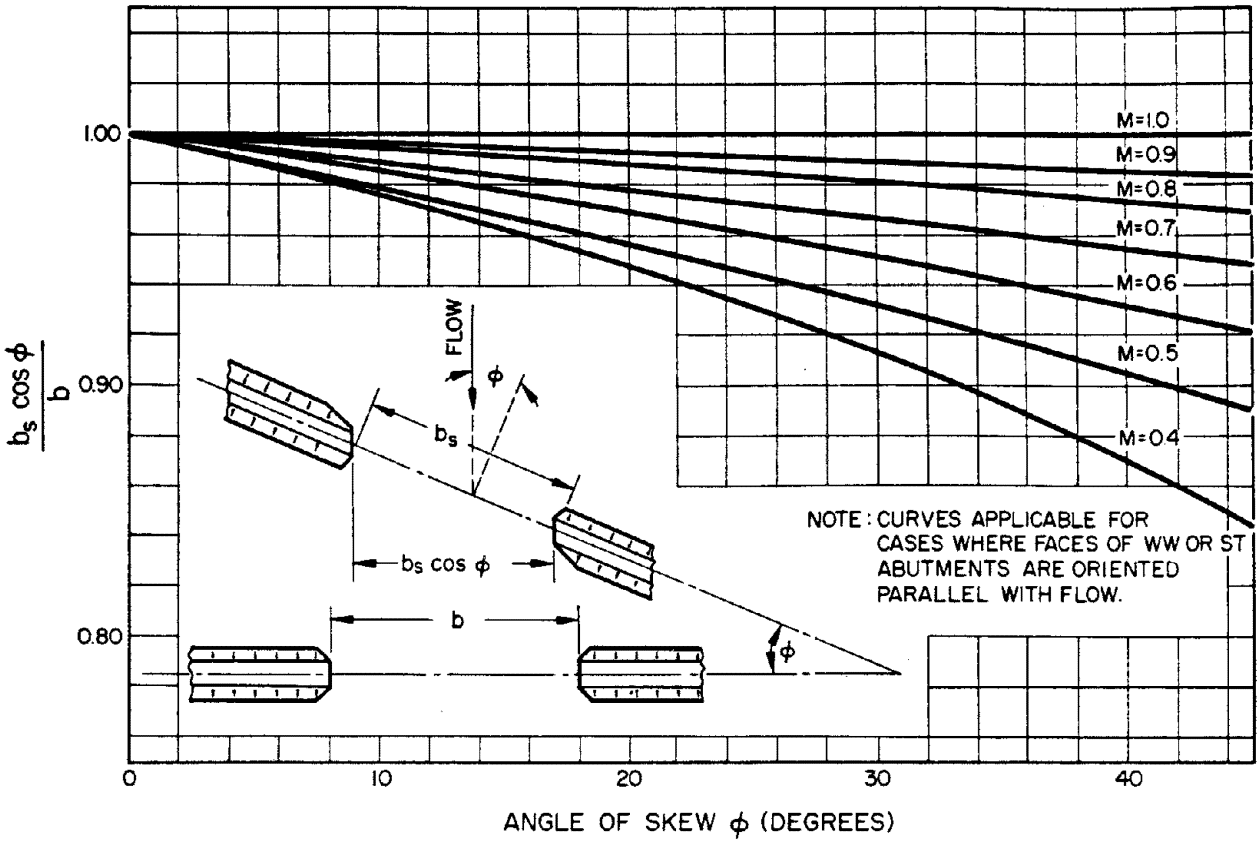

Figure 11.—Ratio of projected to normal length of bridge for equivalent backwater (skewed crossings).

Reference to the sketch in figure 8 will aid in clarifying the terminology. For instance, if $Q_c/Q_a = 0.05$, the eccentricity $e = (1 - 0.05)$ or 0.95 and the curve for $e = 0.95$ in figure 8 would be used for obtaining ΔK_e. The largest influence on the backwater coefficient due to eccentricity will occur when a bridge is located adjacent to a bluff where a flood plain exists on only one side and the eccentricity is 1.0. The overall backwater coefficient for an extremely eccentric crossing with wingwall or spillthrough abutments and piers will be:

$K^* = K_b$ (fig. 6) $+ \Delta K_p$ (fig. 7) $+ \Delta K_e$ (fig. 8).

2.7 Effect of skew. The method of computation for skewed crossings differs from that of normal crossings in the following respects: The bridge opening ratio, M, is computed on the projected length of bridge rather than on the length along the centerline. The length is obtained by projecting the bridge opening upstream parallel to the general direction of flood flow as illustrated in figure 9. The general direction of flow means the direction of flood flow as it existed previous to the placement of embankments in the stream. The length of the constricted opening is $b_s \cos \phi$, and the area A_{n2} is based on this length. The velocity head, $\frac{V^2_{n2}}{2g}$, to be substituted in expression (4) (sec. 2.1) is based on the projected area A_{n2}. The method will be further illustrated in example 3, chapter XII.

Figure 10 shows the incremental backwater coefficient, ΔK_s, for the effect of skew, for wingwall and spillthrough type abutments. The incremental coefficient varies with the opening ratio, M, the angle of skew of the bridge ϕ, with the general direction of flood flow, and the alignment of the abutment faces, as indicated by the sketches in figure 10. Note that the incremental backwater coefficient, ΔK_s, can be negative as well as positive. The negative values result from the method of computation and do not necessarily indicate that the backwater will be reduced by employing a skewed crossing. These incremental values are to be added algebraically to K_b obtained from the base curve. The total backwater coefficient for a skewed crossing with abutment faces aligned with the flow

and piers would be:

$K^* = K_b$ (fig. 6) + ΔK_p (fig. 7) + ΔK_s (fig. 10A).

It was observed during the model testing that skewed crossings with angles up to 20° produced no particularly objectionable results for any of the abutment shapes investigated. As the angle increased above 20°, however, the flow picture deteriorated; flow concentrations at abutments produced large eddies, reducing the efficiency of the waterway and increasing the possibilities for scour. The above statement does not apply to cases where a bridge spans most of the stream with little constriction.

Figure 11 was prepared from the same model information as figure 10A. By entering figure 11 with the angle of skew and the projected value of M, the ratio $b_s \cos \phi / b$ can be read from the ordinate. Knowing b and h_1^* for a comparable normal crossing, one can solve for b_s, the length of opening needed for a skewed bridge to produce the same amount of backwater for the design discharge. The chart is especially helpful for estimating and checking and its use will be demonstrated in example 3, chapter XII.

Chapter III.—DIFFERENCE IN WATER LEVEL ACROSS APPROACH EMBANKMENTS

3.1 Significance. The difference in water surface elevation between the upstream and downstream side of bridge approach embankments, Δh, has been interpreted erroneously as the backwater produced by a bridge. This is not the backwater as the sketch on figure 12 will attest. The water surface at section 3, measured along the downstream side of the embankment, is lower than normal stage by the amount h_3^*. There is an occasional exception to this, however, when flow is obstructed from returning to the flood plain by dense vegetation or high water from a downstream tributary produces ponding and an abnormal stage at the bridge site.

The difference in level across embankments, Δh, is always larger than the backwater, h_1^*, by the sum $h_3^* + S_0 L_{1-3}$, where S_0 is the natural slope of the stream (fig. 12). The method of determining L_{1-3}, which is the distance from section 1 to section 3, needs specific explanation but this will be deferred until chapter IV. The differential level is significant in the determination of backwater at bridges in the field since Δh is the most reliable head measurement that can be made. Fortunately, the backwater and Δh bear a definite relationship to each other for any particular structure. Thus, if one is known the other can be determined.

3.2 Base curves. A base curve for determining downstream levels was constructed entirely from model data which was found especially consistent when presented by the parameters shown. No satisfactory way has been found to experimentally isolate the backwater from Δh when making field measurements, so in this case the model curves must suffice. The differential level ratio, $h_b^*/h_b^* + h_3^*$, is plotted with respect to the opening ratio, M, on figure 12.

The numerator, h_b^*, represents the backwater at a

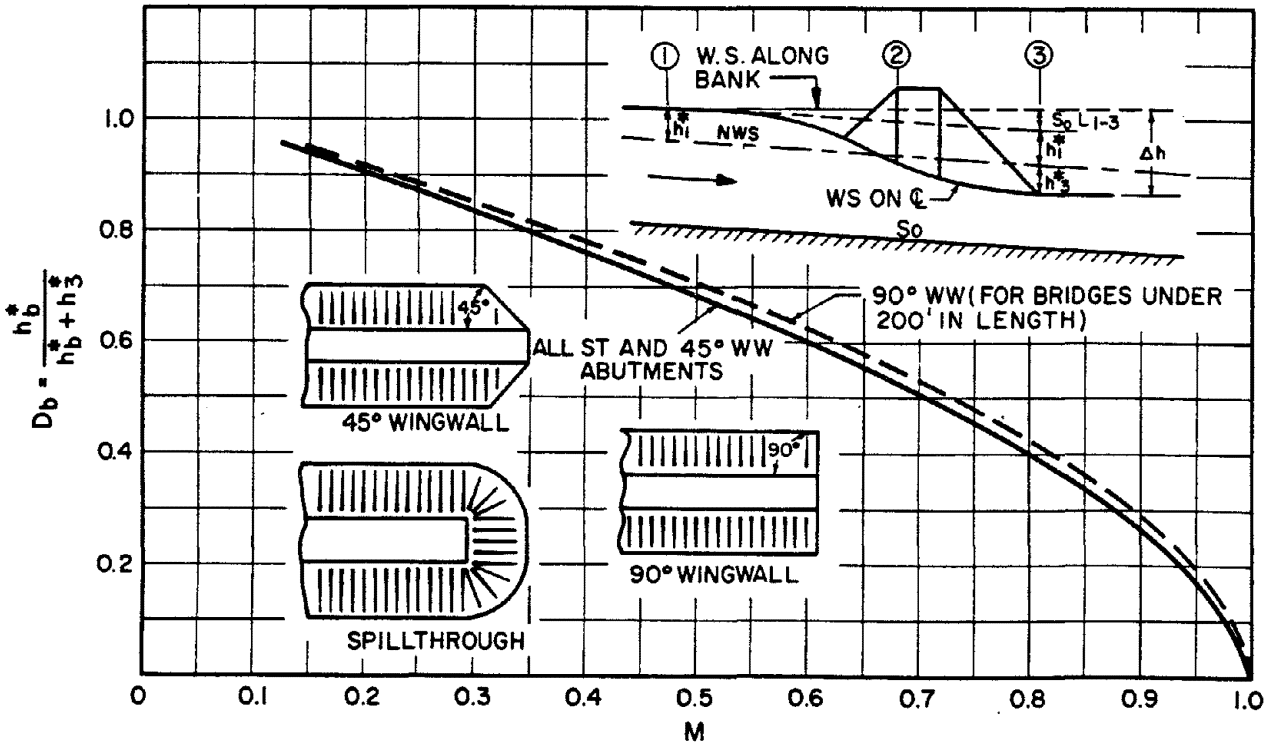

Figure 12.—Differential water level ratio base curves.

bridge, exclusive of pier effect, and h_3^* is the difference in level between normal stage and the water surface on the downstream side of the embankment at section 3. The ordinate of figure 12 will be referred to as the differential level ratio to which the symbol D_b has been assigned. The water surface depicted at section 3 represents the average level along the downstream side of the embankment from H to I and N to O in figure 1. For crossings involving wide flood plains and long embankments, the distances H to I and N to O each have been arbitrarily limited to not more than two bridge lengths. The solid curve on figure 12 is to be used for 45° and 60° wingwall abutments and all spillthrough abutments regardless of bridge length. The upper curve, denoted by the broken line, is for bridges with lengths up to 200 feet having 90° vertical wall and other abutment shapes which severely constrict the flow.

Assuming the backwater, h_b^*, has already been computed for a normal crossing, without piers, eccentricity or skew, the water surface on the downstream side of the embankment is obtained by entering the curve on figure 12 with the contraction ratio, M, and reading off the differential level ratio

$$D_b = \frac{h_b^*}{h_b^* + h_3^*}$$

or

$$h_3^* = h_b^* \left(\frac{1}{D_b} - 1\right) \qquad (6)$$

The elevation on the downstream side of the embankment is simply normal stage at section 3, less h_3^* (fig. 12), except for the special case where the entire water surface profile is shifted upward by ponding from downstream or restricted flood plains.

3.3 Effect of piers. As piers were introduced in the bridge constrictions in the model, it was found that the backwater increased while the value of h_3^* showed no measurable change regardless of the value of J (sec. 2.4). Therefore, the procedure for determining h_3^* with piers is exactly as explained in section 3.2 without piers.

3.4 Effect of eccentricity. In the case of severely eccentric crossings, the difference in level across the embankment considered here applies only to the side of the river having the greater flood plain discharge. In plotting the experimental differential level ratios with respect to M for eccentric crossings, without piers, it was found that the points fell directly on the base curve (fig. 12). The individual values of h_b^* and h_3^* for eccentric conditions are different than for symmetrical crossings, but the ratio of one to the other, for any given value of M, remains unchanged. Thus, figure 12 can also be considered applicable to eccentric crossings if used correctly. To obtain h_3^* for an eccentric crossing, with or without piers, enter the proper curve in figure 12 with the value of M and read D_b as before. In this case:

$$D_b = \frac{h_b^* + \Delta h_e^*}{h_b^* + \Delta h_e^* + h_3^*}$$

or

$$h_3^* = (h_b^* + \Delta h_e^*) \left(\frac{1}{D_b} - 1\right). \qquad (7)$$

3.5 Drop in water surface across embankment (normal crossing). Having computed h_3^* as described in the preceding paragraphs and knowing the total backwater h_1^* (computed according to the procedure in ch. II), the difference in water surface elevation across the embankment (fig. 12) is:

$$\Delta h = h_3^* + h_1^* + S_0 L_{1-3} \qquad (8)$$

where h_1^* is total backwater, including the effect of piers and eccentricity, and $S_0 L_{1-3}$ is the normal fall in streambed from section 1 to section 3.

3.6 Water surface on downstream side of embankment (skewed crossing). The differential level across roadway embankments for skewed crossings is naturally different for opposite sides of the river, the amount depending on the configuration of the stream, bends in the vicinity of the crossing, the degree of skew, etc. These factors can be so variable that a generalized model study can shed little light on the subject.

Individual values of h_1^* and h_3^* for skewed crossings again differ from those for symmetrical crossings, but the differential level ratio across the embankments at either end of the bridge can be considered the same as for normal crossings for any given value of M. The value of M is, of course, based on the projected length of bridge as explained in section 2.7. Thus, it is again possible to use figure 12 for skewed crossings. The differential level ratio, D_b, with or without piers, is obtained by entering the chart with the proper opening ratio, M. Then:

$$h_3^* = (h_b^* + \Delta h_e^*) \left(\frac{1}{D_b} - 1\right). \qquad (9)$$

The results for the left embankment in the model or side farthest downstream (fig. 9) were more reliable than those for the right embankment,

farthest upstream, due to the limited width of the test flume. The results were fairly consistent, however, and the experimental points fell slightly to both sides of the base curve (fig. 12) for both wingwall and spillthrough abutments. The water surface elevations along the upstream side of the embankments (fig. 9) from *D* to *C* were consistently higher than for the opposite upstream side *F* to *G*. Likewise, the water surface elevations along the downstream side of the embankments were higher from *N* to *O* than for the right bank *H* to *I*. The difference in level across embankments, however, was essentially the same for both sides of the river. Data for the above can be found in the comprehensive report (*18*).

Chapter IV.—CONFIGURATION OF BACKWATER

4.1 Distance to point of maximum backwater. In backwater computations, it will be found necessary in some cases to locate the point or points of maximum backwater with respect to the bridge. The maximum backwater in line with the midpoint of the bridge occurs at point *A* (fig. 13B), this point being a distance, L^*, from the waterline on the upstream side of the embankment. Where flood plains are inundated and embankments constrict the flow, the elevation of the water surface throughout the areas *ABCD* and *AEFG* will be essentially the same as at point *A*, where the backwater measurement was made on the models. This characteristic has been verified from field measurements made by the U.S. Geological Survey on bridges where the flood plains on each side of the main channel were no wider than twice the bridge length and hydraulic roughness was relatively low. The comprehensive report (*18*) contains further discussion of this feature.

For crossings with exceptionally wide, rough flood plains, this essentially level ponding may not occur.

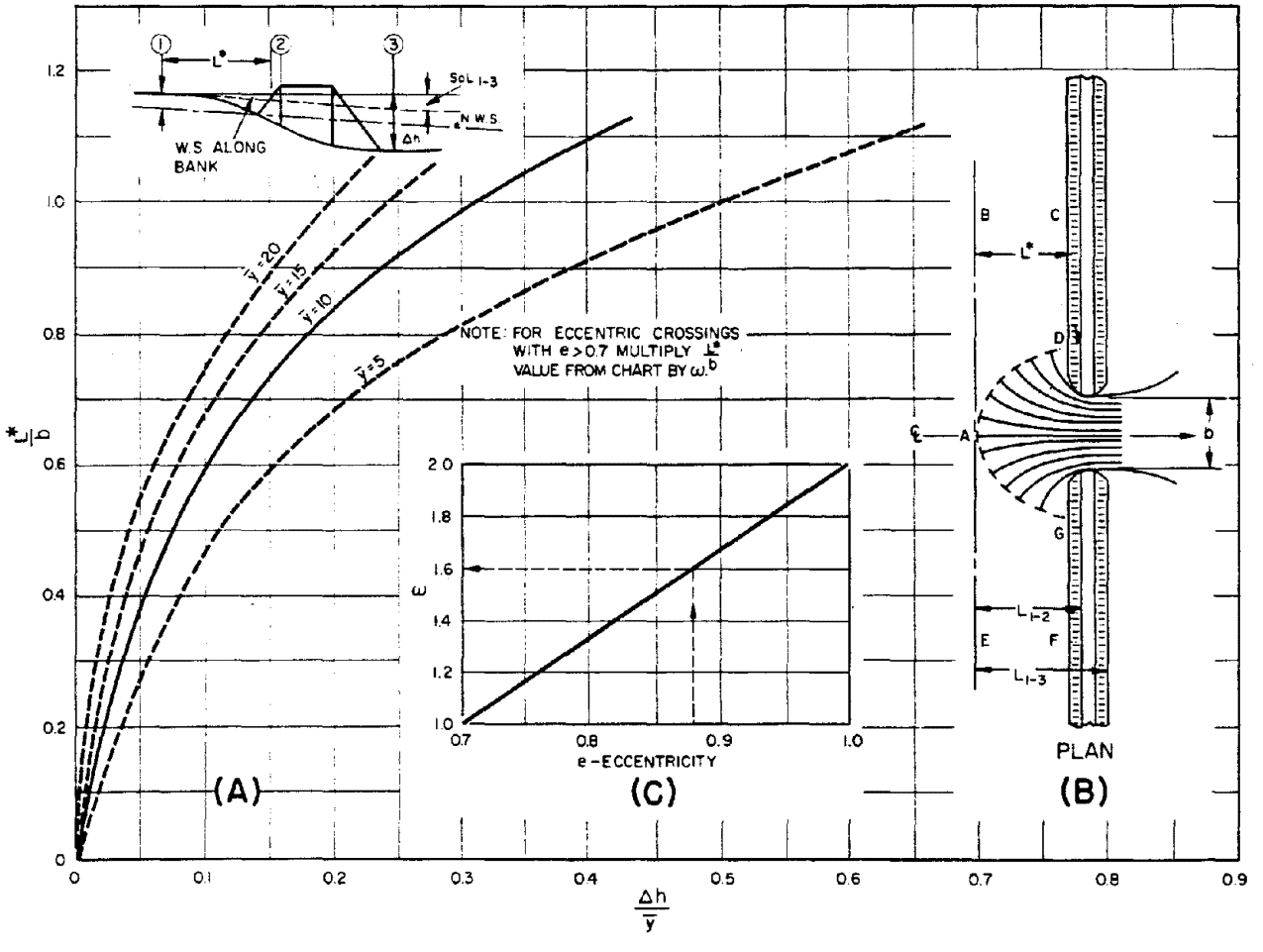

Figure 13.—Distance to maximum backwater.

Flow gradients may exist along the upstream side of the embankments due to borrow pits, ditches and cleared areas along the right-of-way. These flow gradients along embankments are likely to be more pronounced on the falling than on the rising stage of a flood. A correlation is needed between the water level along the upstream side of embankments and point A since it is difficult to obtain water surface elevations at point A in the field during floods. For the purpose of design and field verification, it has been assumed that the average water surface elevation along the upstream side of embankments, for as much as two bridge lengths adjacent to each abutment (F to G and D to C), is the same as at point A (fig. 13B).

4.2 Normal crossings. Figure 13 has been prepared for determining distance to point of maximum backwater, measured normal to centerline of bridge. The chart differs from the one presented in the first edition, which was based entirely on model data applicable to only a very limited portion of the problem. The curves on figure 13 of this book were developed from information supplied by the U.S. Geological Survey on a number of field structures during floods. The resulting chart is considered superior to the former one although there still remains room for improvement as additional field data become available. The method of revision is explained in section B.2, appendix B.

Referring to figure 13, the normal depth of flow under a bridge is defined here as $\bar{y} = A_{n2}/b$, where A_{n2} is the cross sectional area under the bridge, referred to normal water surface, and b is the width of waterway. A trial solution is required for determining the differential level across embankments, Δh, but from the result of the backwater computation it is possible to make a fair estimate of Δh. To obtain distance to maximum backwater for a normal channel constriction, enter figure 13A with appropriate value of $\Delta h/\bar{y}$ and $\bar{y}$ and obtain the corresponding value of L^*/b. Solving for L^*, which is the distance from point of maximum backwater (point A) to the water surface on the upstream side of embankment (fig. 13B), and adding to this the additional distance to section 3, which is known, gives the distance L_{1-3}. Then the computed difference in level across embankments is

$$\Delta h = h_1^* + h_3^* + S_0 L_{1-3}. \tag{8}$$

Should the computed value of Δh differ materially from the one chosen, the above procedure is repeated until assumed and computed values agree. Generally speaking, the larger the backwater at a given bridge the further will point A move upstream. Of course, the value of L^* also increases with length of bridge.

4.3 Eccentric crossings. Eccentric crossings with extreme asymmetry perform much like one half of a normal symmetrical crossing with a marked contraction of the jet on one side and very little contraction on the other. For cases where the value of e (sec. 2.6) is greater than 0.70, enter the abscissa on figure 13A with $\Delta h/\bar{y}$ and $\bar{y}$ and read off the corresponding value of L^*/b as usual. Next multiply this value of L^*/b by a correction factor, ω, which is obtained from figure 13C. For example, suppose $\Delta h/\bar{y} = 0.20$, $\bar{y} = 10$ and $e = 0.88$, the corrected value would be $L^*/b = 0.84 \times 1.60$. Distance to maximum backwater is then $L^* = 1.34b$ with eccentricity.

4.4 Skewed crossings. In the case of skewed crossings, the water surface elevations along opposite banks of a stream are usually different than at point A; one may be higher and the other lower depending on the angle of skew, the configuration of the approach channel, and other factors. To obtain the approximate distance to maximum backwater L^* for skewed crossings (fig. 9), the same procedure is recommended as for normal crossings except the ordinate of figure 13 is read as L^*/b_s, where b_s is the full length of skewed bridge (fig. 9).

Chapter V.—DUAL BRIDGES

5.1 Arrangement. With the advent of divided highways, dual bridges of essentially identical design, placed parallel and only a short distance apart, are now common. The backwater produced by dual bridges is naturally larger than that for a single bridge, yet less than the value which would result by considering the two bridges separately. As the combinations of dual bridges encountered in the field are legion, it was necessary to restrict model tests to the simplest arrangement; namely, identical

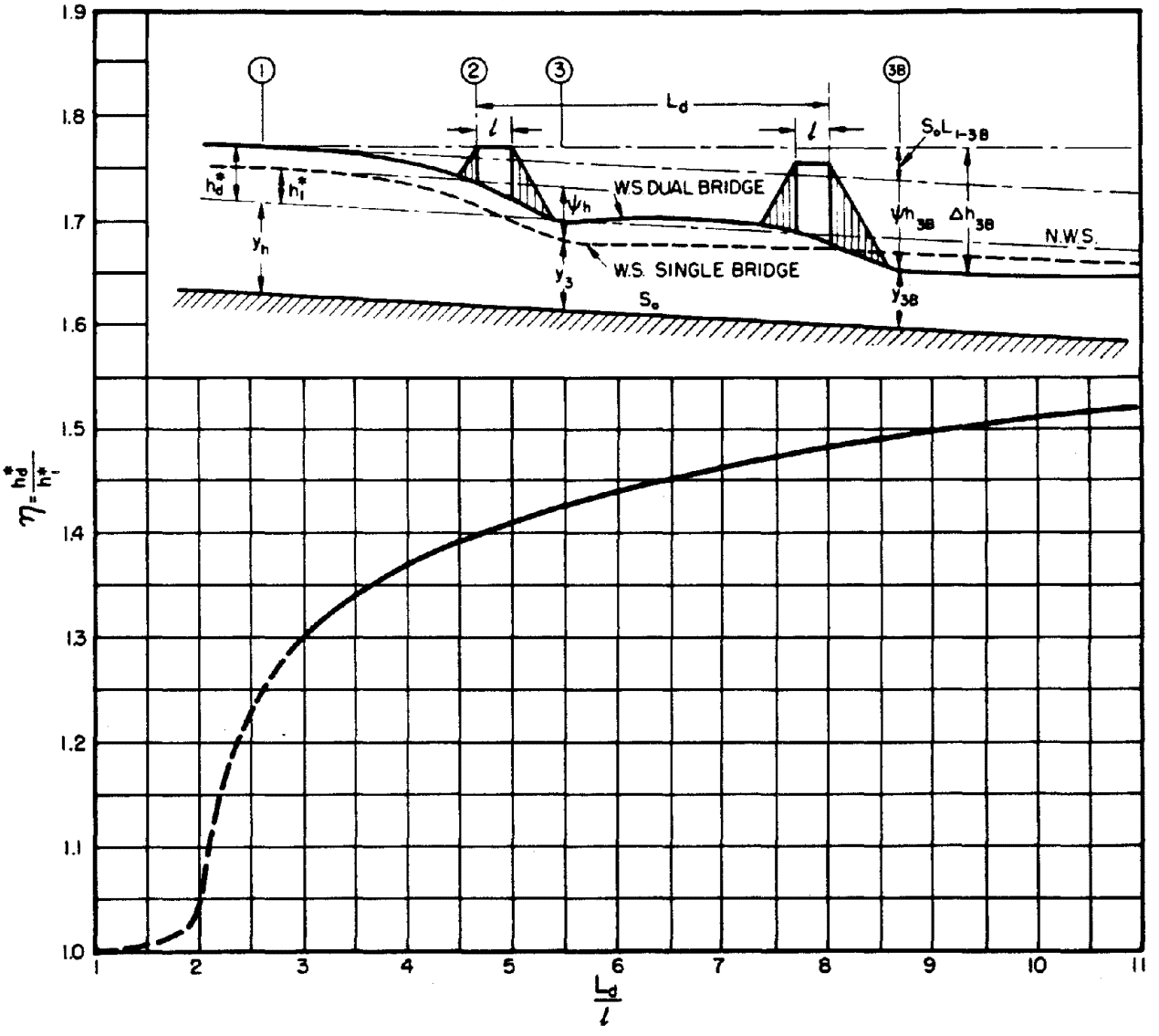

Figure 14.—Backwater multiplication factor for dual bridges.

parallel bridges crossing a stream normal to the flow (see sketch in fig. 14). The tests were made principally with 45° wingwall abutments, but also included a limited number of the spillthrough type, both having embankment slopes of 1½:1. The distance between bridges was limited by the range permissible in the model which was 10 feet or $L_d/l = 11$ (fig. 14).

5.2 Backwater determination. The method of testing consisted of establishing normal flow conditions, then placing one bridge constriction in the flume and measuring the backwater, h_1^*. A second bridge constriction, identical to the first, was next placed downstream and the backwater for the combination, h_d^*, was measured upstream from the first bridge. The ratio, h_d^*/h_1^*, thus obtained, is plotted with respect to the parameter, L_d/l, on figure 14, where l is the width of bridge and L_d is the distance from the upstream face of the first bridge to the downstream face of the second bridge. The curve was established from tests made with and without piers. The ratio, h_d^*/h_1^*, which is assigned the symbol η, increases as the bridges are moved apart, apparently reaching a limit and then decreases as the distance between the bridges is further increased. The range of the model was sufficient to explore only the rising portion of the curve but most cases in practice will fall within this range. With bridges in close proximity to one another, the flow pattern is elongated but little different from that of a single bridge. As the bridges are spaced farther apart, the embankment of the second bridge interferes with the expanding jet from the first, which must again contract and reexpand downstream from the second bridge, producing additional turbulence and loss of energy.

To determine backwater for dual bridges meeting the above requirements, it is necessary first to compute the backwater, h_1^*, for a single bridge, as previously outlined in chapter II. The backwater for the dual combination, measured upstream from the first bridge (fig. 14), is then:

$$h_d^* = h_1^* \eta \qquad (10)$$

5.3 Drop in water surface across embankments. In the case of dual bridges, the designer may wish to know the water surface elevation on the downstream side of the roadway embankment of the first bridge, or the water surface elevation on the downstream side of the embankment of the second bridge. Fluctuations in the water surface between bridges, due to turbulence and surging, caused the measurements to be so erratic that it was thought inadvisable to include the results here. These data are available in the comprehensive report (*18*). A characteristic to be noted in this connection, however, is that the water surface between bridges usually stands above normal stage. (See sketch in fig. 14.)

The water surface downstream from the second bridge, on the other hand, was quite stable permitting accurate measurements. The procedure for determining the water surface level immediately downstream from the second bridge embankment at section 3B (see sketch in fig. 14) consists of first computing h^*_1 and h^*_3 for the upstream bridge as was outlined in chapters II and III, respectively. For convenience, the sum $h^*_1+h^*_3$ for the single bridge is assigned the symbol ψh. Likewise the sum $h^*_d + h^*_{3B}$ for the two-bridge combination is represented by the symbol ψh_{3B}. The ratio of the second head differential to the first carries the symbol ξ, or

$$\xi = \frac{h^*_d + h^*_{3B}}{h^*_1 + h^*_3} = \frac{\psi h_{3B}}{\psi h}. \qquad (11)$$

The ratio ξ has been plotted with respect to L_d/l on figure 15. To obtain the drop in level ψh_{3B} for the dual bridge combination, it is only necessary to multiply ψh for the single bridge by the factor ξ from figure 15. The difference in water surface elevation between the upstream side of the first bridge embankment and the downstream side of the second should then be:

$$\Delta h_{3B} = \psi h_{3B} + S_0 L_{1-3B} \text{ or } \Delta h_{3B} = \psi h \xi + S_0 L_{1-3B}. \qquad (12)$$

Should the water surface level on the downstream

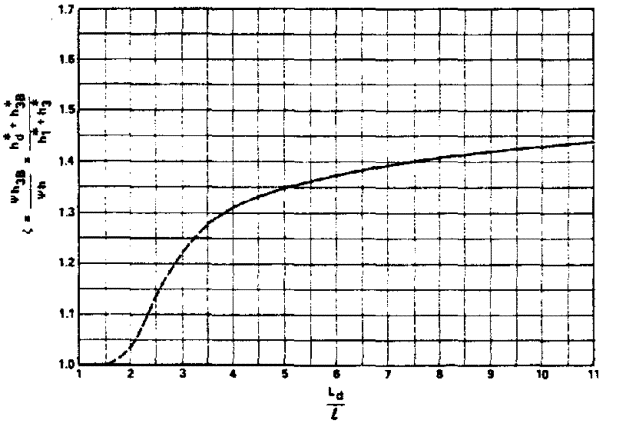

Figure 15.—Differential level multiplication factor for dual parallel bridges.

side of the second bridge embankment at section $3B$ be desired relative to normal stage:

$$h^*_{3B} = \psi h_{3B} - h^*_d.$$

The left end of the curves on figures 14 and 15 are shown as broken lines since no data were taken to definitely establish their positions in this region. The computation of backwater for dual bridges is further explained in example 2 of chapter XII. The charts for dual bridges in this publication differ from those in the first edition for reasons discussed in section B.4, appendix B.

Chapter VI.—ABNORMAL STAGE-DISCHARGE CONDITION

6.1 Definition. Up to this point the discussion has concerned streams flowing at normal stage; i.e., the natural flow of the stream has been influenced only by the slope of the bed and the boundary resistance along channel bottom and flood plains. Sometimes the stage at a bridge site is not normal but is increased by unnatural backwater conditions from downstream. A general backwater curve may be produced, beginning at the confluence of tributary and main stream or at a dam, and may extend a considerable distance upstream if the stream gradient is flat. Where bridges are placed close to the confluence of two streams, abnormally high stage-discharge conditions can be of importance in design. For example, if a stream can always be counted on to flow at abnormally high stage during floods at a particular bridge site, the increased waterway area may permit a shorter bridge than would be possible under normal-stage conditions. To take advantage of the situation, the length of bridge would be determined on the basis of (1) the minimum abnormal stage expected which would produce the largest backwater increment, or (2) the maximum expected abnormal stage which may produce the highest stage upstream. Since estimating the design stage at a bridge site under abnormal conditions can be a complicated process, requiring much individual judgment, the approach to the computation of backwater in this case has been treated strictly as an approximate solution or a case where it is more important to understand the problem than to attempt precise computations. (See ref. 17 for general backwater types.)

6.2 Backwater determination. Tests were made by first establishing normal flow in the test flume as usual, without a constriction. The tailgate was then adjusted to increase the depth of flow by, say, 10 percent for the same discharge, after which a centerline profile was obtained. The resulting water surface is labeled "abnormal stage" in figure 16. Abutments were then placed in the flume and a second centerline profile was made of the water surface. The difference between the second water surface measurement and the previous one at abnormal stage, both made at section 1, is defined as the backwater h^*_{1A}. Similar backwater measurements were made for other degrees of bridge constriction and for depths of flow up to 40 percent greater than normal stage by regulating the tailgate. Since the backwater analysis as developed is based on flow at normal stage, expression (4) (sec. 2.1) is, strictly speaking, not valid for abnormal stage-discharge conditions. The results described in this chapter apply specifically to a model on approximately a 1:40 scale with channel slope of 0.0012 and a Manning roughness factor of 0.024. The results do shed some light on this phase of the backwater problem, and an approximate solution may, in many cases, be preferable to none.

6.3 Backwater expression. The experimental backwater coefficients for abnormal stage discharge (without piers, eccentricity, and skew) were computed according to the expression:

$$K_{bA} = \frac{h^*_{1A}}{\alpha_2 V^2_{2A}/2g} \tag{13}$$

where h^*_{1A} is backwater measured above abnormal stage at section 1 and $V_{2A} = Q/A_{2A}$, where A_{2A} is gross area of constriction based on abnormal stage (see fig. 16). The subscript A has been added throughout to signify that this is a special case, not to be confused with other expressions which precede or follow. Actually, expression (13) is a modification of expression (4a). Model backwater coefficients computed according to expression (13) were found to plot on both sides of the base curve (fig. 6). The test results, which appear in the comprehensive report (*18*), plot in no particular order with regard to the degree of abnormality or difference in stage.

As the method of computation chosen results in backwater coefficients approximating those of the base curves, it is further assumed that the curves for incremental backwater coefficients, previously established for piers, eccentricity, and skew, may be reasonably applicable to abnormal stage-dis-

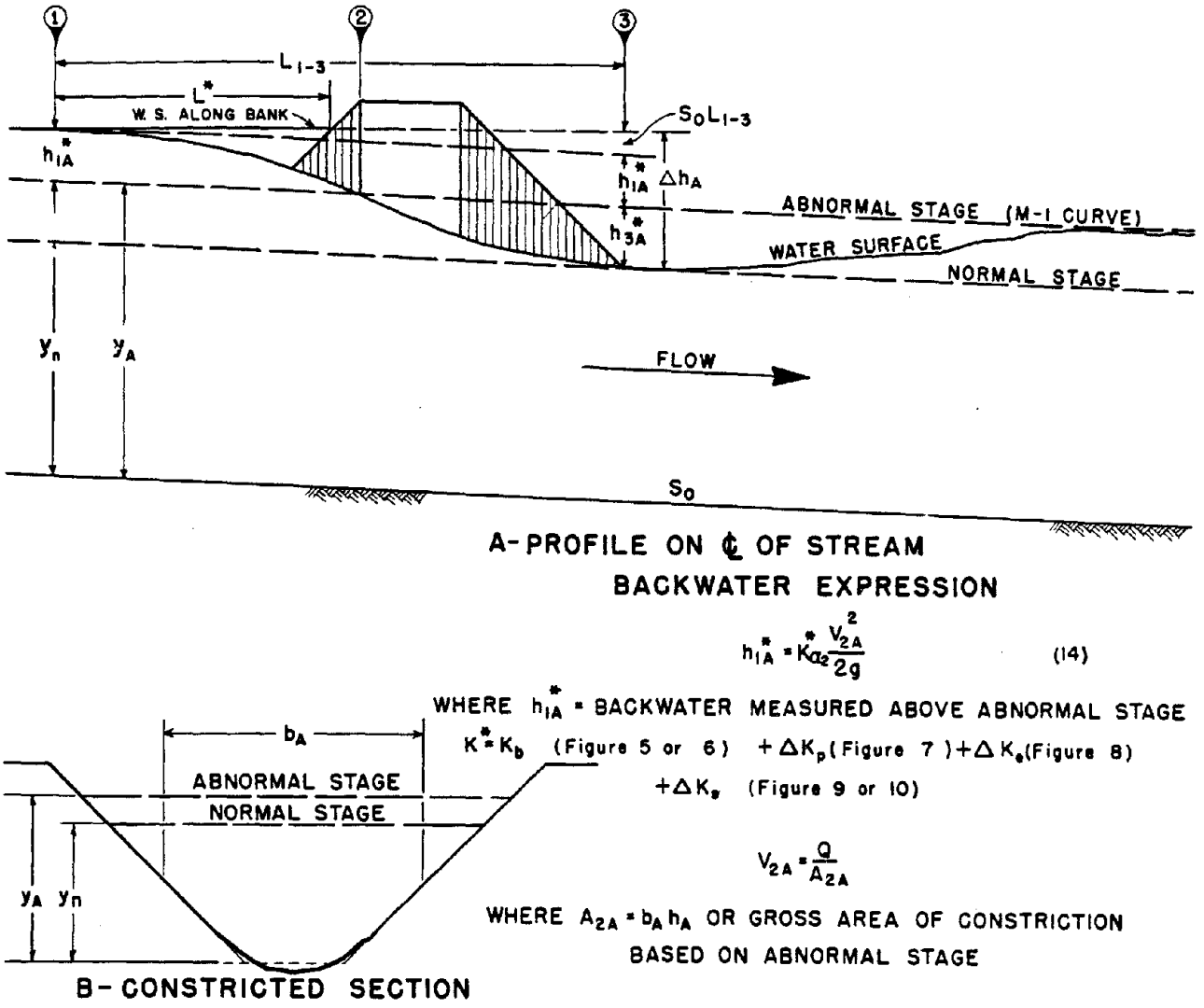

Figure 16.—Backwater with abnormal stage-discharge condition.

charge conditions. If this is permissible, the expression for the computation of backwater for abnormal stage discharge would then read:

$$h^*_{1A} = K^*\alpha_2 \frac{V^2_{2A}}{2g} \qquad (14)$$

where $K^* = K_b$ (fig. 6) $+\Delta K_p$ (fig. 7) $+\Delta K_s$ (fig. 8) $+\Delta K_s$ (fig. 10). Thus, the method and sources used to obtain the overall backwater coefficient remain unchanged. The one and important difference in expressions (13) and (14) is insertion of the velocity head for *abnormal stage* rather than normal stage.

6.4 Drop in water surface across embankments. The experimental points for the differential level ratio for abnormal stage discharge (without piers) were also found to agree fairly well with the base curve (fig. 12). The information is included in the comprehensive report (*18*). To obtain the water surface along the downstream side of the roadway embankment for abnormal stage discharge, figure 12 is considered applicable but approximate. The method of computation is similar to that explained in chapter III; the principal differences lie in the manner in which the backwater is computed for abnormal stage conditions. Other symbols involved in the abnormal stage-discharge computation also bear the subscript *A*, so the differential level ratio:

$$D_b = \frac{h^*_{bA}}{h_{bA}{}^* + h^*_{3A}} \qquad (15)$$

or

$$h^*_{3A} = h^*_{bA}\left(\frac{1}{D_b} - 1\right) \tag{16}$$

where:

D_b = differential level ratio from base curve, figure 12 (no adjustment is needed for eccentricity or skew);

h^*_{bA} = backwater above abnormal stage (without piers);

h^*_{3A} = vertical distance from water surface to abnormal stage at section 3 (this dimension will be the same with or without piers).

Except for minor revisions, the reporting of this chapter on abnormal stage discharge is the same as that which appeared in the original publication. The above procedures for bridge backwater computations with abnormal stage will be demonstrated in example 5 of chapter XII.

Chapter VII.—EFFECT OF SCOUR ON BACKWATER

7.1 General. Thus far the discussion of backwater has been limited to the case where the bed of a stream in the vicinity of a bridge is considered rigid or immovable and, thus, does not degrade with introduction of embankments, abutments, and piers. It was necessary to obtain the initial experimental data under more or less ideal conditions before introducing the further complication of a movable bed. In actuality the bed is usually composed of much loose material, some of which will move out of the constriction during flood flows. Nature wastes little time in attempting to restore the former regime, or the stage-discharge relation which existed prior to constriction of the stream. For within-bank flow little changes, but for flood flows there exists an altered regime, with a potential to enlarge the waterway area under the bridge.

Bearing in mind that during floods a stream is usually transporting sediment at its capacity, the process might be described as follows, with the aid of figure 17. Constriction of a stream produces backwater at flood flows; backwater is indicative of an increase in potential energy upstream. This makes possible higher velocities in the constriction, thus, increasing the transport capacity of the flow to above normal in this reach. The greater capacity for transport results in scouring of the bed in the vicinity of the constriction; the removed material is usually carried a short distance downstream and dropped as the stream again returns to full width. As the scouring action proceeds, the waterway area under the bridge enlarges, the velocity and resistance to flow decreases, and a reduction in the amount of backwater results. If the bed is composed of alluvial material, free to move, and a flood persists for a sufficient period of time, degradation under the bridge may approach a state of equilibrium; e.g., the scour hole can reach such proportions that the rate of transport out of the hole is matched by the rate of transport into the hole from upstream. Upon reaching this state of equilibrium, it will be found that the stream has been practically restored to its former regime so far as stage discharge is concerned and the backwater has all but disappeared. This state could be fully realized in the model operating under controlled conditions.

Seldom is it possible to reach this extreme state in the field where backwater becomes negligible as cohesive, compacted, and cemented soils are encountered together with boulders and vegetation which materially retard the scouring process. Also the stage of most rivers in flood does not remain constant for any appreciable length of time. Nevertheless, now that information is available for the extreme case of equilibrium scour, this should be of value in predicting the lesser scour at field structures. In cases where abutments and piers can be keyed into bedrock, it may be advisable to encourage scour in the interest of utilizing a shorter bridge. This same objective is sometimes attained in another way by enlarging the waterway area under a bridge by excavation during construction. In such cases, it is desirable to be able to determine the amount of backwater to be expected after localized enlargement of the waterway. There is always the possibility, however, that deposition may refill the excavated channel to essentially its original condition. Maintaining a channel as constructed is not easily accomplished.

7.2 Nature of scour. It is advisable to mention a few of the characteristics of scour, as observed during the model experiments, prior to considering the effect of scour on backwater. Where the depth of flow is essentially uniform and the bed is composed of a narrow gradation of clean sand, as was the case in the model, scour was greatest in the vicinity of the abutments, as shown in figure 17B, and little scour was evidenced in the center of the constriction unless the scour holes overlapped. This is better illustrated by a photograph of the model in figure 18 which shows the nature of scour around a 45° wingwall abutment and at two circular piers after a test run. The zero contour line represents normal elevation of the sandbed before placing the embankment in the flume. The remainder of the contour lines, which are at 0.2-foot intervals, define

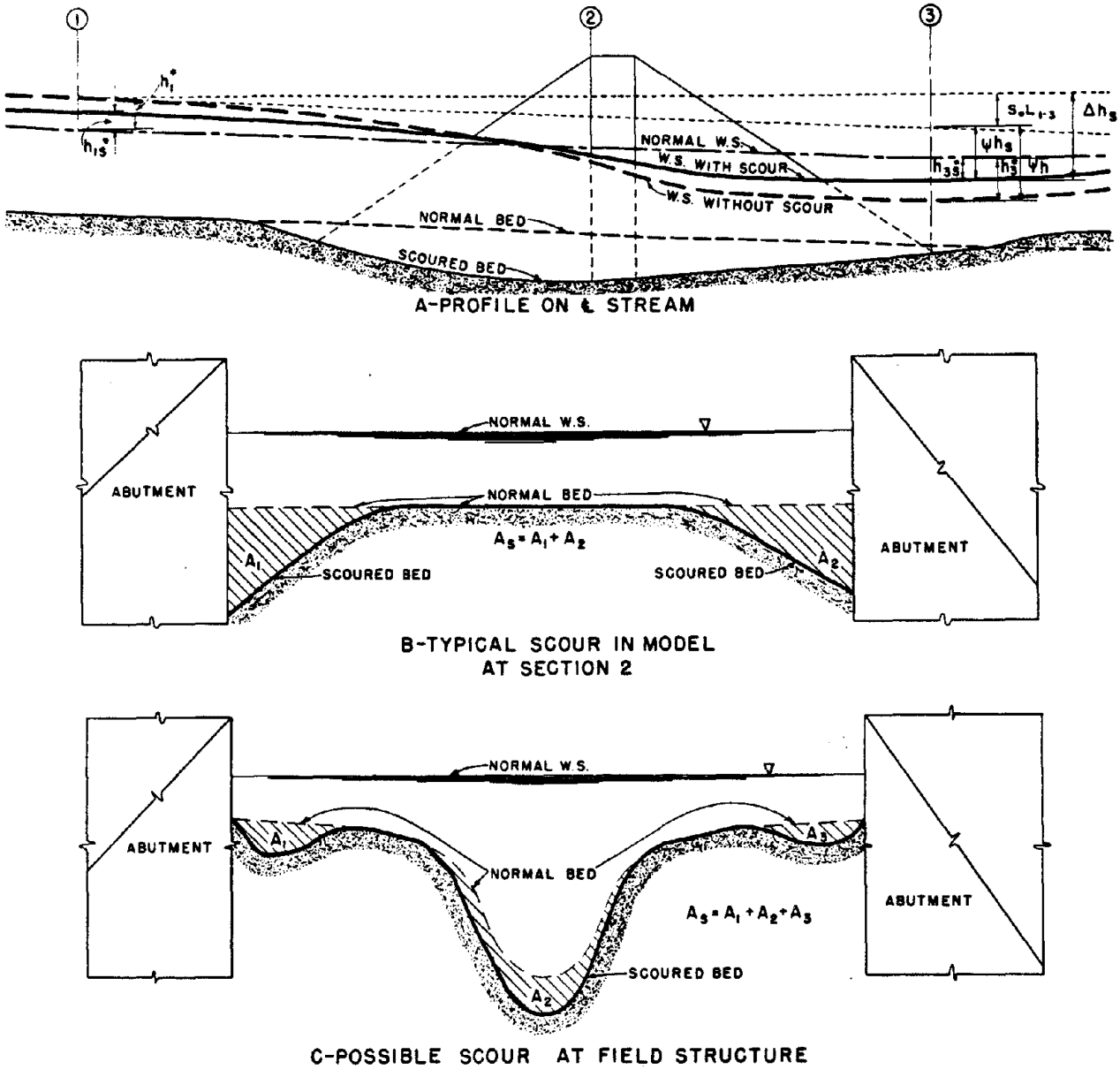

Figure 17.—Effect of scour on bridge backwater.

the resulting scour hole produced by initially constricting the channel 38 percent with the embankment. This photograph is included to demonstrate that scour in the model did not occur uniformly across the constriction, but was greatest at points where concentration of flow occurs. It can be noted that scour around the two circular piers is minor compared to scour at the abutment.

Figure 19 is a cross section of the same scour hole, measured along the upstream side of the bridge. The normal flow depth was 0.52-foot in this case, while the maximum equilibrium scour at the abutment amounted to twice this value. The pattern of scour experienced in the model is not necessarily indicative of that which will occur in a stream.

It is not only difficult to predict the magnitude of scour, but it is equally difficult to predict the location of scour at field structures since the depth of flow from flood plain to main channel can differ widely as well as the direction and concentration of flow. In the model the greatest concentration occured at the abutments, while in the field the deeper scour may occur in the main channel as indicated in figure 17C. Should the main flow or a secondary current be directed toward an abutment during flood, or should a concentration of flow exist near

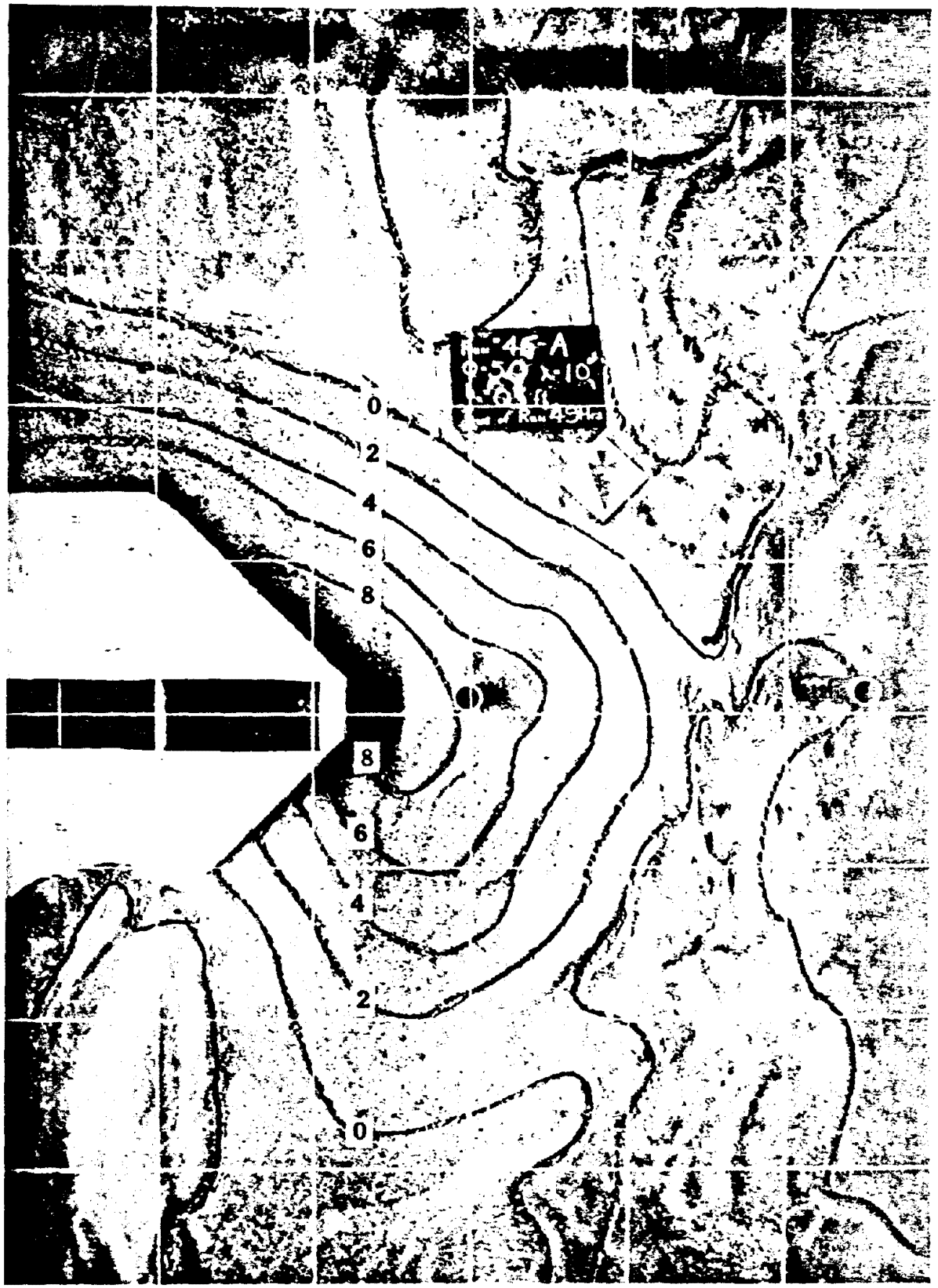

Figure 18.—Scour at wingwall abutment and single circular piers (model).

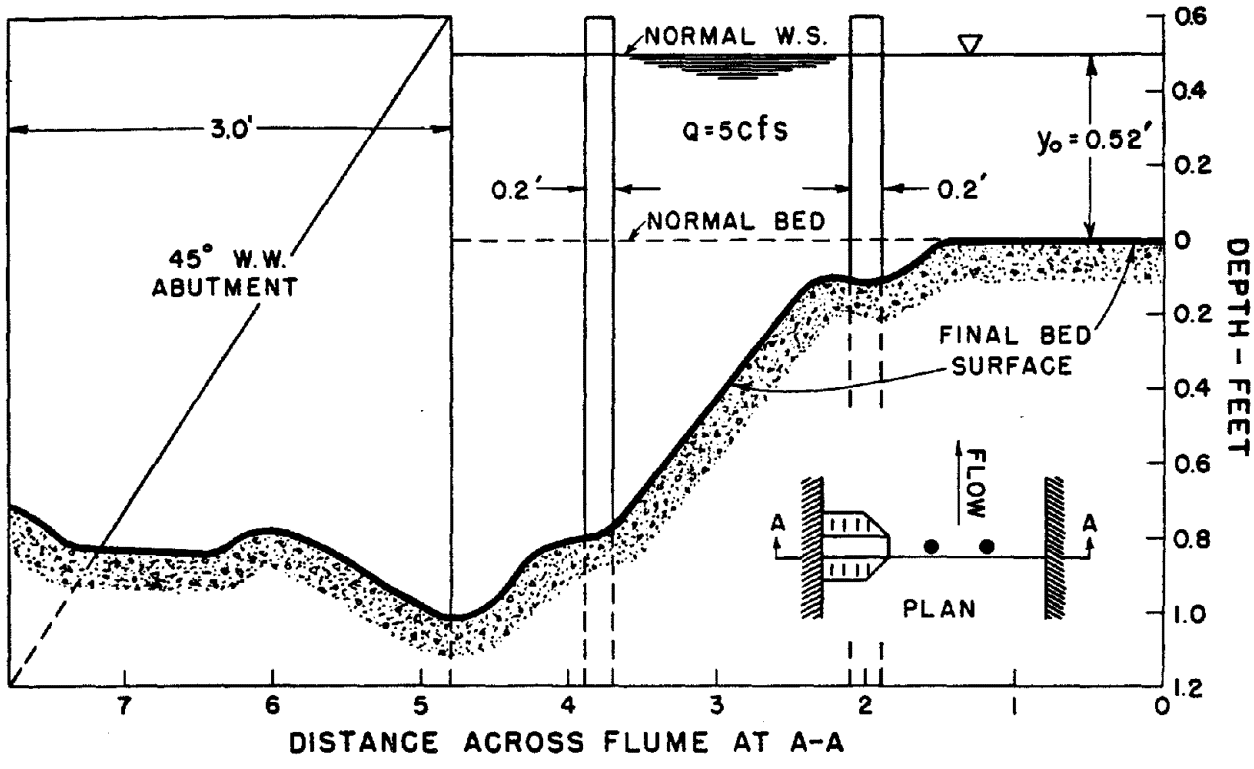

Figure 19.—Cross section of scour at upstream side of bridge (model).

an abutment, the area adjacent to the abutment is definitely vulnerable to scour. It is not the intention here to go into detail on the vagaries of scour, since this would require much illustrative matter and explanation, but merely to point out a few features fundamental to understanding the effect of scour on backwater. References 20, 21, 23, 24, and 29 are recommended for the study and prediction of scour at bridge abutments and piers.

7.3 Backwater determination. From the foregoing it can be seen that any means of increasing the waterway area under a bridge can be effective in reducing the backwater. It is by no means a simple task to measure backwater in a model with a bed that is free to produce sand dunes, which advance slowly down the channel continually altering conditions of flow. The majority of tests were made in a flume of rectangular cross section, 8 feet wide by 150 feet long, in which the former rigid bed was replaced by an 8-inch layer of sand. Normal flow was first established for a given discharge, then abutments were placed in the flume and the flow allowed to continue uninterrupted until a stable condition of scour was established. At this time final measurements were taken of the backwater, the difference in level across embankments, and the cross section of the scoured bed under the bridge. The resulting backwater and the differential in level across embankments, with scour, were then compared with the backwater and differential level, respectively, for an immovable bed operating under similar conditions of flow and geometry. The values used for the rigid bed were computed according to the methods outlined in chapters II and III. Holding the discharge and abutment geometry the same for any test, the reduction in backwater was related directly to the volume or cross sectional area of scour. Scour and velocity are usually measured from the downstream side of a bridge, since this is the most practical way of obtaining these measurements during flood flows. Also the effective area of scour, so far as the computation of backwater is concerned, will more likely correspond to the scour at the downstream side than that at the upstream side of a bridge. Thus, the area of scour measured at the downstream side, denoted as A_s, will be used for the computation of backwater. The model tests showed the scour at the downstream side to average about 75 percent of that at the upstream side of the bridge.

A design curve derived from the model experiments is included as figure 20. The correction factor for backwater with scour ($C = h^*_{1_s}/h^*_1$) is plotted with respect to A_s/A_{n2}, where the terms bearing the sub-

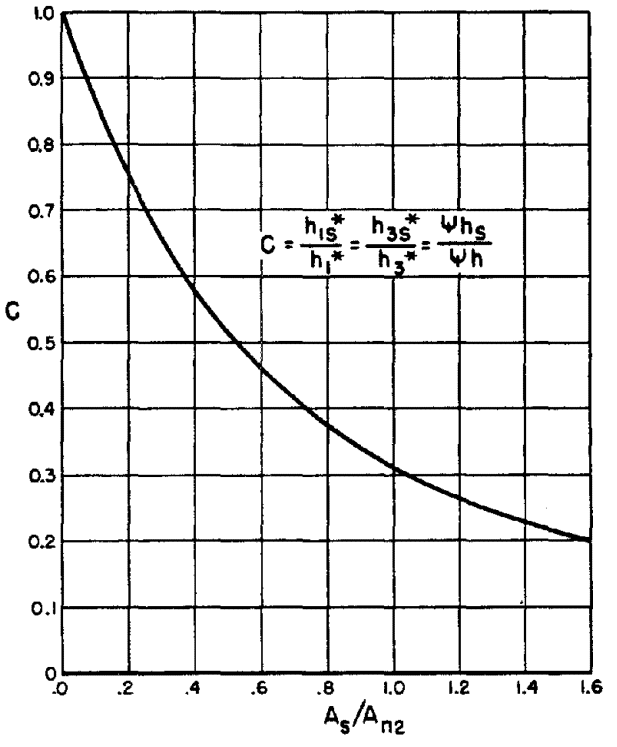

Figure 20.—Correction factor for backwater with scour.

script s, designate values with scour; those not bearing this subscript represent the same values computed with rigid bed. Supposing the backwater at a given bridge was 1 foot with no scour; it would be reduced to 0.52-foot were scour to enlarge the waterway area by 50 percent, or it would be reduced to 0.31-foot should the waterway area be doubled. The same reduction applies equally well to the ratios h^*_{3s}/h^*_3 and $\psi h_s/\psi h$ (see fig. 17A) so one curve will suffice for all three. Thus to obtain backwater and related information for bridge sites where scour is to be encouraged, where scour cannot be avoided, or where the waterway is to be enlarged during construction, it is first necessary to compute the backwater and other quantities desired according to the method outlined in chapters II and III for a rigid bed, using the original cross section of the stream at the bridge site. These values are then multiplied by a common coefficient from figure 20 as follows:

$$h_{1s}^* = Ch^*_1 \tag{17}$$

$$h^*_{3s} = Ch_3^* \tag{18}$$

$$\psi h_s = C\psi h \tag{19}$$

7.4 Enlarged waterways. The designer will probably be reluctant to depend on scour as a means of enlarging a waterway and thereby reducing backwater. If the waterway is enlarged by excavation, there is little to gain by excavating much beyond the limits (upstream or downstream) of the embankments as the downstream channel acts as the control (fig. 18). If additional volume is removed upstream or downstream, the channel may simply refill by deposition. Any enlargement of the cross section should be maintained to prevent reduction of area by the growth of willows and similar vegetation. Field surveys of existing bridges where channel enlargements have once been made should reveal worthwhile information on the question of permanence of enlarged waterways. Example 6, chapter XII, which is based on an actual occurrence involving a flash flood on a stream with a bed consisting of noncohesive material, is included to demonstrate how backwater is reduced by scour.

Attention is called to the well known fact that scour measured after flood waters have subsided does not give a true indication of the extent of scour which occurred during the peak of the flood. This is evidenced by many incidents where bridge spans and piers have fallen into a stream during a flood and have been buried deep in the bed. As flood waters recede, the transport capacity as well as the velocity of the flow drops off, with the result that material is deposited all along the streambed as well as in the constriction.

Chapter VIII.—SUPERSTRUCTURE PARTIALLY INUNDATED

8.1 The problem. Cases arise in which it is desirable to compute the backwater upstream from a bridge or the discharge under a bridge when flow is in contact with the girders. Once flow contacts the upstream girder of a bridge, orifice flow is established so the discharge then varies as the square root of the effective head. The result is a rather rapid increase in discharge for a moderate rise in upstream stage. The greater discharge, of course, increases the likelihood of scour under the bridge. Inundation of the bridge deck is a condition the designer seldom contemplates in design but it occurs frequently on older bridges.

Two cases were studied; the first where only the upstream girder was in the water as indicated by the sketch on figure 21 and the second, where the bridge constriction is flowing full, all girders in the flow, as shown in figure 22.

The procedure followed in the model tests for either case was to set a discharge and adjust the depth of flow such that it was constant throughout the flume (normal depth with rigid bed). A pair of abutments was next placed in the flow and the backwater h_1*, produced by these abutments, was measured. Next a bridge deck, with girder depth exaggerated, was placed between the abutments and gradually lowered until the upstream girder made contact with the flow. Immediately the backwater increased; the deck was then firmly secured in place to prevent further movement. The new backwater denoted as h^*_u, was then measured, as well as the vertical distance Z, between the bottom of the upstream girder and the floor of the channel. Other runs were made with the bridge deck further depressed, but in no case was flow over the bridge permitted. The above test procedure was then repeated for changes in abutment geometry using both wingwall and spillthrough abutments. The test results are on record in the comprehensive model study report (*18*).

8.2 Upstream girder in flow (case I). Several methods were attempted in analysis of the data. It was found that for practical purposes, the opening ratio, M, could be eliminated as a variable once orifice flow was established; the most logical and simple method of approach was then to treat this flow condition as a sluice gate problem (extreme case).

Using a common expression for sluice gate flow

$$Q = c_d b_N Z \left[2g \left(Y_u - \frac{Z}{2} + \alpha_1 V_1^2/2g \right) \right]^{1/2} \quad (20)$$

where

Q = total discharge—c.f.s.
c_d = Coefficient of discharge
b_N = net width of waterway (excluding piers)—ft.
Z = vertical distance—bottom of upstream girder to mean river bed under bridge—ft., and
Y_u = vertical distance—upstream water surface to mean river bed at bridge—ft.

For case I, the coefficient of discharge C_d, is plotted with respect to the parameter Y_u/Z on figure 21. The upper curve applies to the coefficient of discharge where only the upstream girder is in contact with the flow. By substituting values in expression (20), it is possible to solve for either the water surface upstream or the discharge under the bridge, depending on the quantities known. It appears that the coefficient curve (fig. 21) approaches zero as Y_u/Z becomes unity. This is not the case since the limiting value of Y_u/Z for which expression (20) applies is not much less than 1.1. There is a transition zone somewhere between $Y_u/Z = 1.0$ and 1.1 where free surface flow changes to orifice flow or vice versa. The type of flow within this range is unpredictable. For $Y_u/Z = 1.0$, the flow is dependent on the natural slope of the stream, while this factor is of little concern after orifice flow is established or $Y_u/Z > 1.1$.

In computing a general river backwater curve across the bridge shown on figure 21, it is necessary to know water surface elevation downstream as well

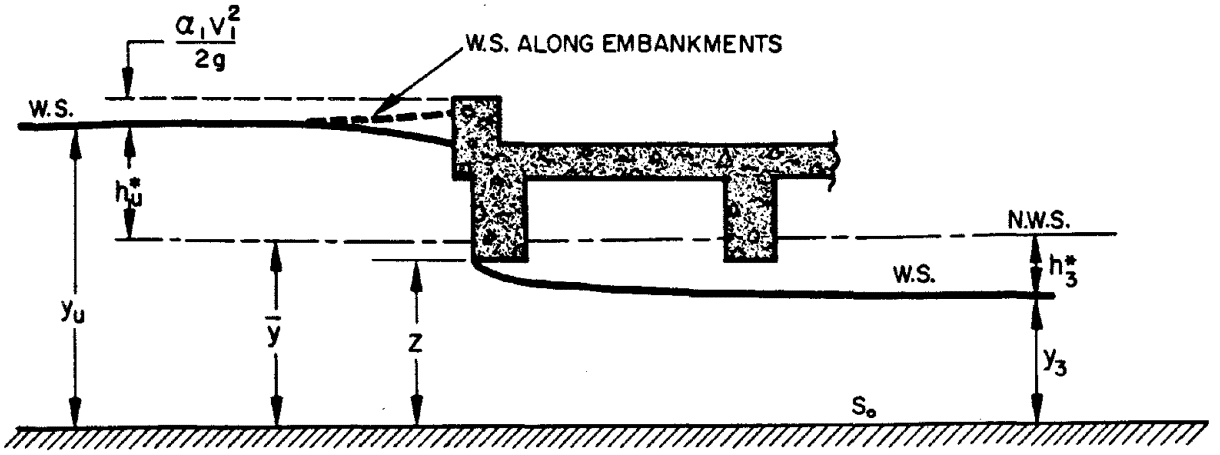

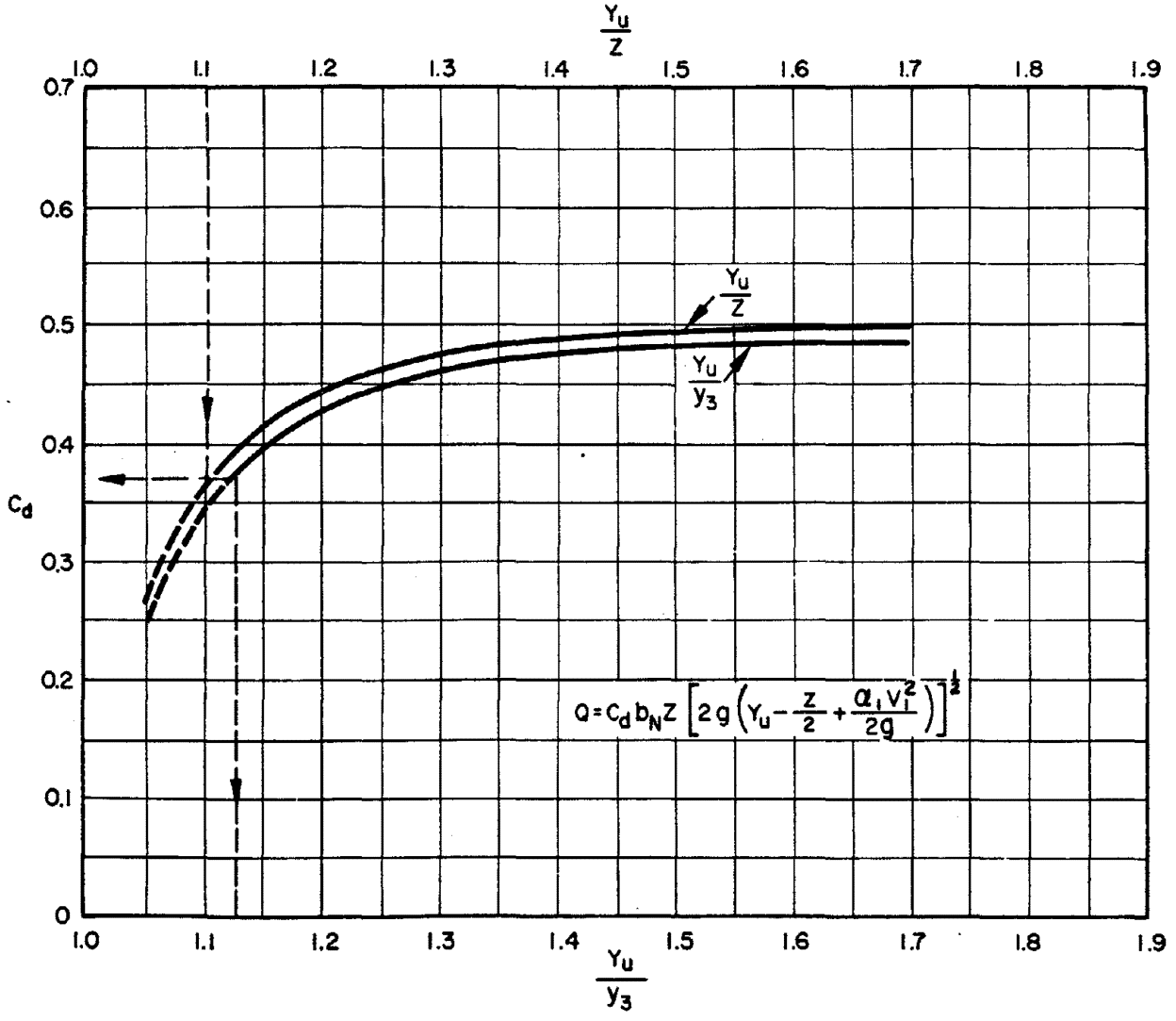

Figure 21.—Discharge coefficients for upstream girder in flow (case I).

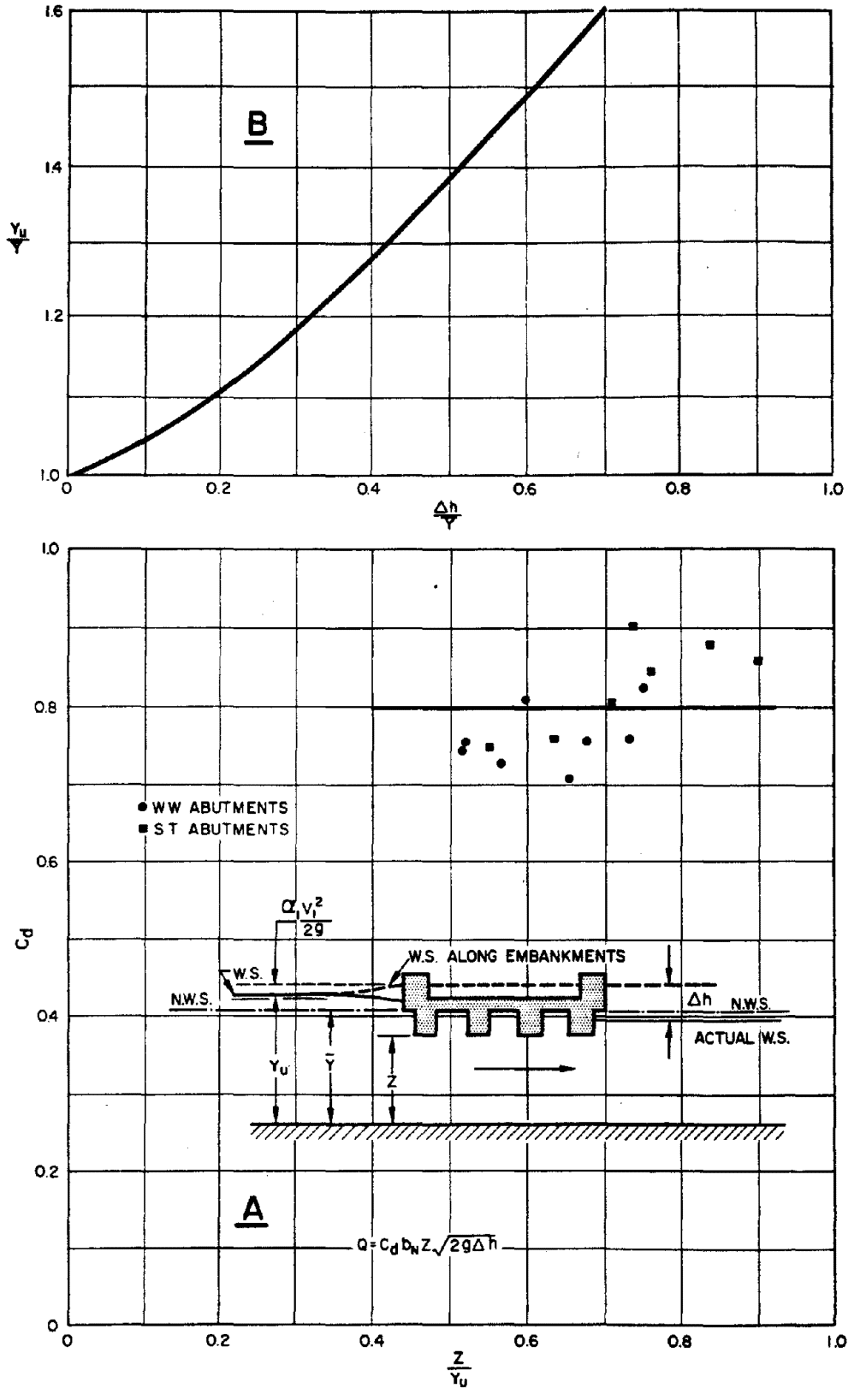

Figure 22.—Discharge coefficient for all girders in flow (case II).

as upstream from the bridge. The approximate depth of flow, y_3, can be obtained from figure 21 by entering the top scale with the proper value of Y_u/Z and reading down to the upper curve, then over horizontally to the lower curve, and finally down to the lower scale as shown by the arrows. The lower scale gives the ratio of Y_u/Y_3. The method is illustrated in example 7 of chapter XII.

8.3 All girders in contact with flow (case II). Where the entire area under the bridge is occupied by the flow, the computation is handled in a different manner. To compute the water surface upstream from the bridge, the water surface on the downstream side and the discharge must be known. Or if the discharge is desired, the drop in water surface across the roadway embankment, Δh, and the net area under the bridge is required. The experimental points on figure 22A, which are for both wingwall and spillthrough abutments, show the coefficient of discharge to be essentially constant at 0.80 for the range of conditions tested. The equation recommended for the average two to four lane concrete girder bridge for case II is

$$Q = 0.80\, b_N Z (2g\Delta h)^{1/2} \qquad (21)$$

where the symbols are defined as in expression (20). Here the net width of waterway (excluding width of piers) is used again. It is preferable to measure Δh across embankments rather than at the bridge proper. The partially inundated bridge compares favorably with that of a submerged box culvert (*14*) but on a larger scale. Submergence, of course, can increase the likelihood of scour under a bridge.

Again for working up general backwater curves for a river, such as is done by the Corps of Engineers, Bureau of Reclamation, and other agencies, it is desirable to know the drop in water level across existing bridges as well as the actual water surface elevation either upstream or downstream from the bridge. Once Δh is computed from expression (21), the depth of flow upstream, Y_u, can be obtained from chart B, figure 22, where $\bar{Y}$ is depth from normal stage to mean river bed at bridge in feet. The procedure will be further explained by example 8 of chapter XII.

8.4 Safety of bridge. A rather common source of bridge failure results from the superstructure being virtually pushed or lifted off the abutments and piers by the combination of buoyancy and dynamic forces. Inundation reduces the effective weight of a concrete bridge to about 0.6 of its weight in air. Should air be trapped under the deck between girders, the effective weight can be further reduced to a dangerous limit so that only moderate horizontal forces are required to jar or slide bridge spans off their pedestals. The horizontal forces consist of unbalanced hydrostatic pressure, or ponding, acting on the upstream face of the bridge (aggravated by the collection of trash), plus energy inherent in the moving mass of water (*32*), plus impact forces produced by buildings, barges and large floating objects striking a bridge. The impact from large floating objects can be lethal if the bridge is already under stress and the girders are not anchored to the piers. The force of impact can be calculated by equating impulse against momentum:

$$F \cdot \Delta t = \frac{W}{g}(V_1 - V_0)$$

or

$$F = \frac{W}{g}\frac{(V_1 - V_0)}{\Delta t}, \qquad (22)$$

where Δt is time required to bring the mass, W/g, floating down river at a velocity, V_1, to rest upon striking a solid object. Say a wooden structure weighing 8 tons, is carried down a swollen river at 5 ft./sec.; the force it would exert on impact would depend on the resilience of the object, the resilience of the bridge span it strikes and the manner in which it strikes. Suppose it makes a square hit so that its velocity changes from 5 ft./sec. to zero in 0.5 second. The force of impact would be

$$F = \frac{16{,}000(5 - 0)}{32.2 \times 0.5} = 4{,}970 \text{ lbs.}$$

On the other hand, assume that a mattress of trash collected on the upstream side of the bridge offers a cushioning effect so that the time interval for the velocity to change from 5 ft./sec. to zero is now 2.5 seconds. This would reduce the impact force by five times to 994 lbs. Here is a case where trash can serve a useful purpose. Figure 23 shows what the combination of buoyant and horizontal forces can do to a bridge which can break away from its supports. Air trapped under these 80-foot prestressed concrete spans and the force of the flood water against the girders carried these two spans several hundred feet downstream from the substructure and stacked them.

Section 1.7.56, entitled "Anchor Bolts" in the AASHO standard specifications for Highway Bridges, 1969, specifies that girders preferably shall be securely anchored to the substructure. This is an inexpensive and recommended precaution. Where

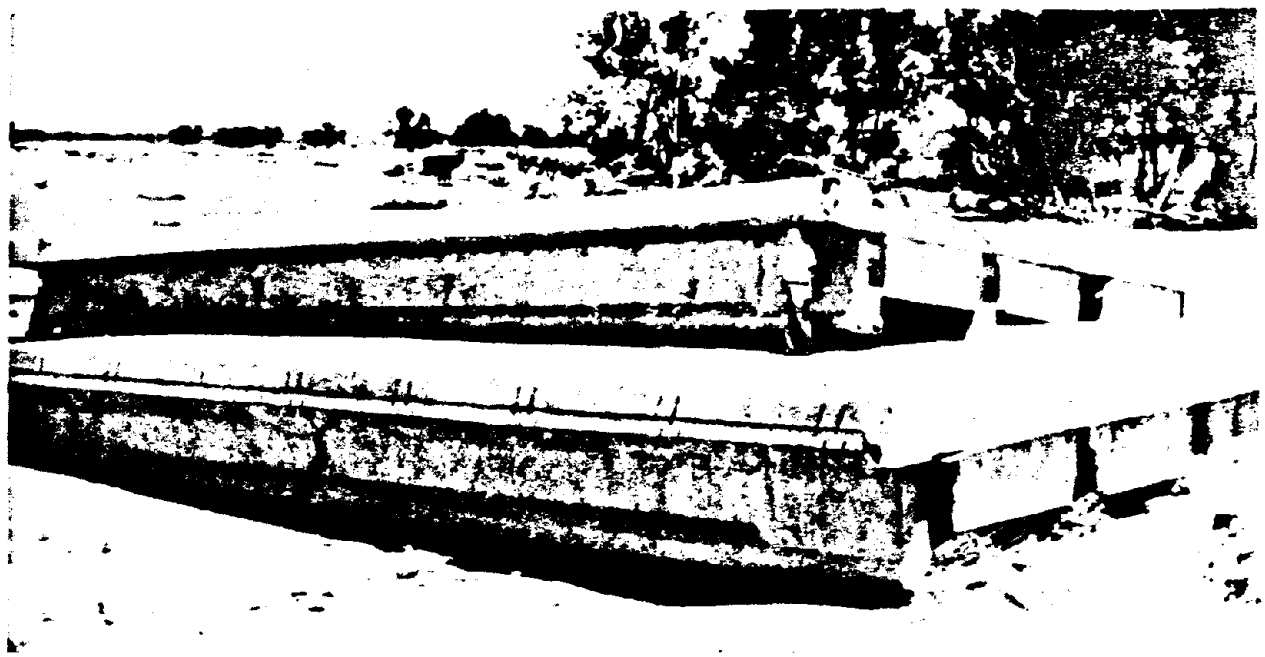

Figure 23.—Buoyant and horizontal forces moved these 80-foot spans downstream.

there is a possibility of the flow coming in contact with the deck during heavy or unusual floods, it is recommended that girders be anchored, tied or blocked in such a way that they cannot be pushed or lifted off their pedestals by hydraulic forces. Even the construction of blocks on the downstream end of pier caps, which could be provided at practically no extra cost, would help prevent failure caused by sliding. Buoyancy forces can be reduced by providing air vents near the top of girders so that entrapped air may escape. In many cases simple precautions such as these can save a bridge superstructure.

8.5 Flow over roadway. In cases where bridge clearance is such that girders become inundated during floods, there is a good possibility that flow also occurs over portions of the approach roadway. Should it be desired to determine the discharge flowing over the roadway, a chart is included as figure 24. Credit for this work should go to Kindsvater and Sigurdson (*7* and *37*).

To determine the discharge flowing over a roadway, first enter curve *B* (figure 24) with H/l and obtain the free flow coefficient of discharge C_f. Should the value of H/l be less than 0.15, it is suggested that C_f be read from curve *A* of the same figure. If submergence is present (e.g., if H/D is larger than 0.7) enter curve *C* with the proper value of submergence in percent and read off the submergence factor C_s/C_f. The resulting discharge is obtained by substituting values in the expression:

$$Q = C_f L H^{3/2} \cdot C_s/C_f, \qquad (23)$$

where L represents the length of inundated roadway, H is the total head upstream measured above the crown of the roadway and C_f and C_s are coefficients of discharge for free flow and with submergence, respectively. Where the depth of flow varies along the roadway, it is advisable to divide the inundated portion into reaches and compute the discharge over each reach separately. The process, of course, can be reversed to aid in determining backwater for a combination of bridge and roadway.

The overtopping of roadways bears a connotation of the past but this sort of thinking should not be discarded; it has far reaching possibilities in present and future design. The present tendency, for Interstate and primary roads, is to construct approach embankments well above the 50-year flood, or highest flood level of record, and depend on the bridge to pass all flood waters, including the super flood. A limit must be set on the length of bridge for economic reasons, which is usually proportioned for about a 50-year flood, but where topography is favorable, this same bridge with embankments set at a lower predetermined level may handle a 1,000-year flood safely. An excellent example of this type of design is the bridge across the Missouri River near Roche-

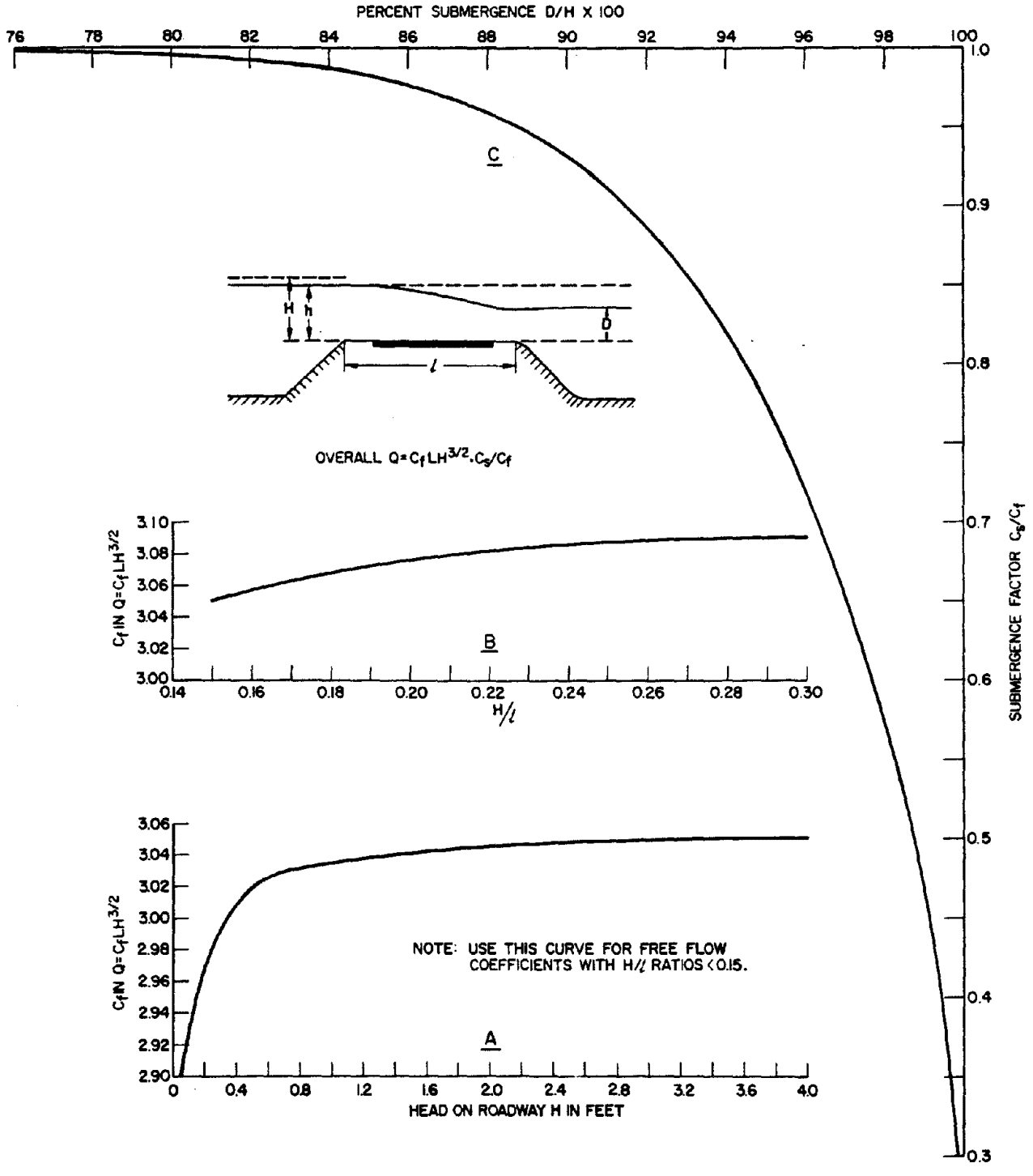

Figure 24.—Discharge coefficients for flow over roadway embankments.

port, Mo., on Interstate 70. A profile across the valley looking upstream is shown on figure 25. The bridge is located well above high water, the approach embankment on the left is set at about the 75-year flood level, yet there is adequate sight distance throughout. This is the ideal valley cross section and the bridge and embankment have been tailor made to fit the site. The arrangement will accommodate any flood that is likely to occur with a minimum of damage. Computation of flow across this

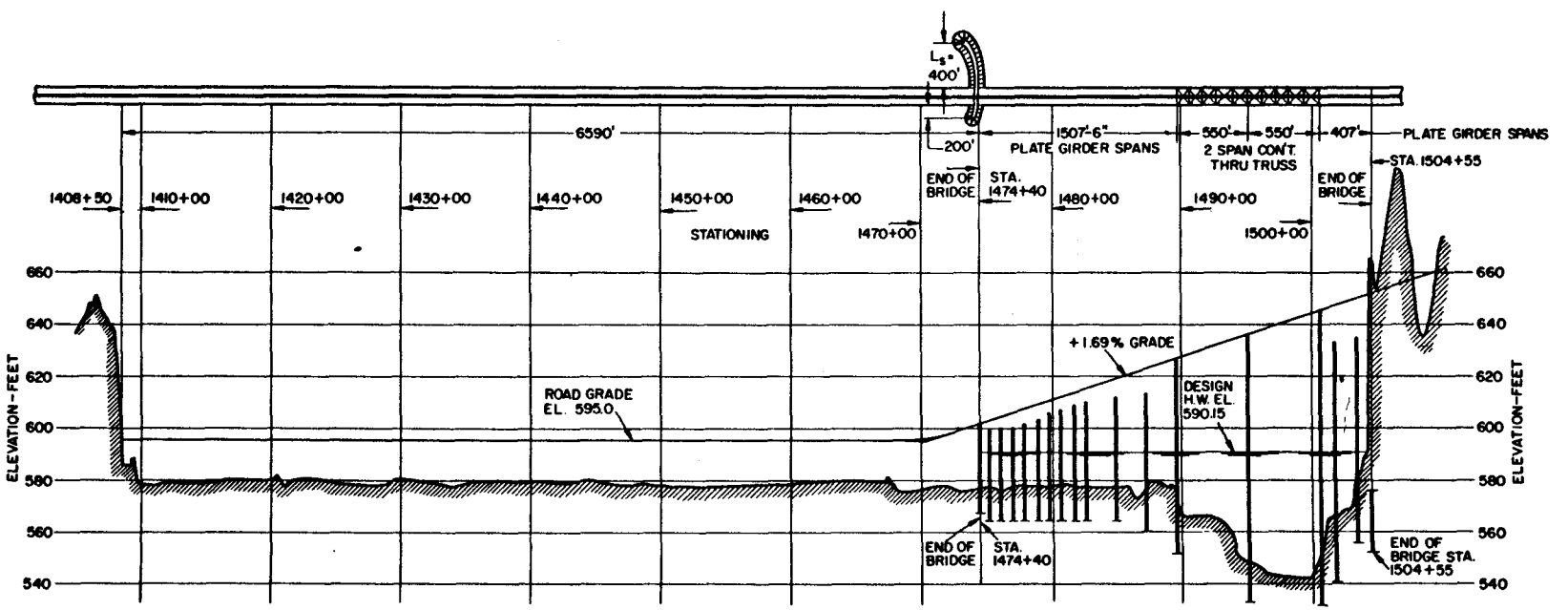

Figure 25.—Missouri River Bridge on route I–70.

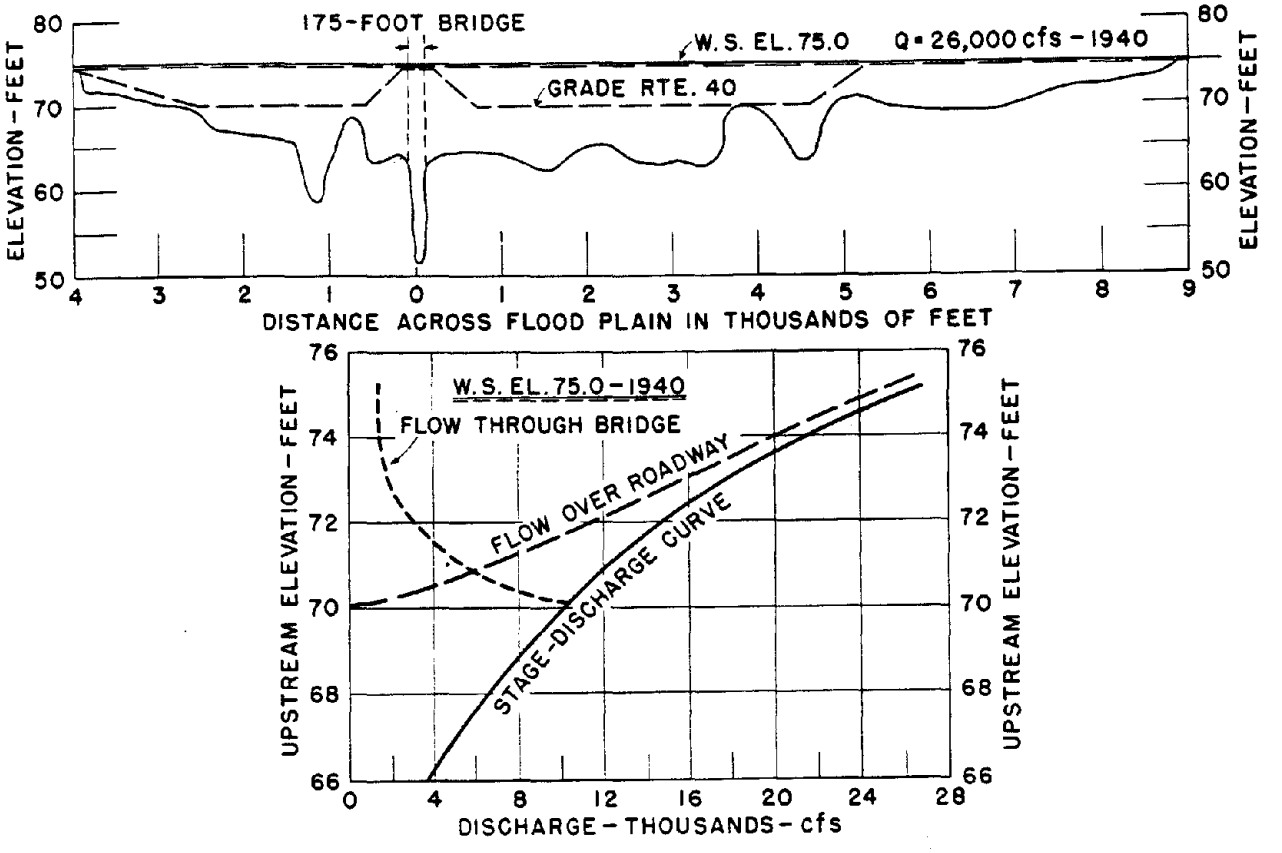

Figure 26.—Nottoway River Bridge on Virginia Route 40.

roadway is shown in example 9 (ch. XII). The manner in which a crossing of this kind functions has been explained in reference 6; a portion of the explanation is repeated in section 8.6.

8.6 Nottoway River Bridge. The crossing of the Nottoway River on State Route 40 near Sussex, Va., is an actual case on which reliable field observations and measurements were made.

"The 175-ft. bridge shown in figure 26 has withstood several severe floods, one with a recurrence interval exceeding 100 years. The capacity of the bridge itself is approximately 10,000 c.f.s., however, a flood of 26,000 c.f.s., or approximately 2½ times the capacity, was accommodated with no damage to the bridge. Only minor repairs were required to the downstream shoulders of the embankments.

"The solid line in figure 26 represents the stage-discharge relationship for the river at the bridge site. Discharges of up to 10,000 c.f.s. were carried under the bridge. As the stage reached El. 70, flow began to spill over the road. With flow over the roadway established, resistance decreased, resulting in a corresponding reduction in both backwater upstream from the bridge and differential head across the embankment. In turn, reduction in backwater caused the flow under the bridge to decrease. By the time the stage reached El. 75, water flowed to a depth of 5 ft. over the roadway. Flow over the embankment at this point reached 24,000 c.f.s. whereas flow under the bridge fell to less than 2,000 c.f.s.

"The backwater upstream from the bridge reached a maximum of 0.37 ft. for the stage at El. 70. The differential head across the embankment was approximately double this amount for the same stage but fell to 0.015 ft. as the stage reached El. 75. Measurements indicated that the highest mean velocity attained under the bridge was 4 f.p.s. at approximately El. 70, decreasing to 0.7 f.p.s. as the stage approached El. 75. The velocity over the roadway reached a maximum of approximately 2 f.p.s. at El. 70.3, decreasing to approximately 0.7 f.p.s. for river stage at El. 75.

"The greatest test withstood by the bridge foundations occurred, therefore, not at the peak flow, but at 10,000 c.f.s. For greater flows the discharge and velocity under the bridge decreased. The greatest threat to the superstructure occurred at the peak of the flood when timber and debris lodged against

it, but with the low velocities prevailing at that time even this was not serious. The outstanding factor contributing to the safety of the bridge is the surprisingly large capacity of the roadway when it is operating as a submerged broad-crested weir." (*6*)

The above case is for a rather short bridge on a secondary road involving low velocities, but the principle is the same regardless of size, provided there is sufficient width of flood plain to warrant such a design. It is recommended that this safety valve idea be kept in mind and used where applicable. The roadway in this case would be located slightly above the flood level for which the bridge is designed. The bridge should have sufficient clearance so that the lowest part of the superstructure remains above high water at all times.

The following comment made by F. A. Kilpatrick of the U.S.G.S. is worthy of mention here. "My observations of the Colorado 1965 floods and the damage to the Interstate System would seem to point out the advantages of such thinking, especially where the restoration of traffic can be accomplished as quickly as was the case in the western States. After the Colorado floods, the embankments were restored in 1 to 2 days, the bridges only after many months and millions of dollars."

Chapter IX.—SPUR DIKES

9.1 Introduction. Where approach embankments encroach on wide flood plains and constrict the normal flood flow, special attention should be given to scour, particularly in the vicinity of bridge abutments. Flow from the flood plain travels along the embankment, and enters the constriction as a concentrated jet normal to the direction of flow in the main channel. In so doing the severity of the contraction is increased at the abutment, the effective length of bridge opening is reduced, and the possibility of scour at the junction of the two jets is great. This action is illustrated in the aerial photograph of figure 27. Concentration of flow is from right to left along the upstream side of the embankment; the river flow is from top to bottom. The low water channel is to the left of the photograph. Where borrow pits and ditches exist along the upstream side of a bridge embankment, flow from the flood plain favors this path of least resistance; the result is often an unusually high flow concentration along the embankment. This is specifically the condition which existed along the upstream side of the embankment shown in the photograph on figure 27. Note the violent mixing action where the side jet and the main flow converge, the ineffectiveness of the first span, and also witness that scour has been responsible for the loss of a portion of the bridge.

The scour hole measured after the flood is shown on figure 28. The deepest part is 25 feet below the river bed, yet it is certain that the scour extended considerably deeper during the peak of the flood, which demonstrates the transport power of turbulent curvilinear flow. It took the highway maintenance crew several weeks of probing to locate the missing bridge spans and piers which were found buried deep in the bed of the stream. This condition can be alleviated to some extent on new bridges by prohibiting borrow pits on the upstream side of embankments and forbidding the cutting of trees back of the toe of the fill slope. For cases where channeling along an embankment is already present or cannot

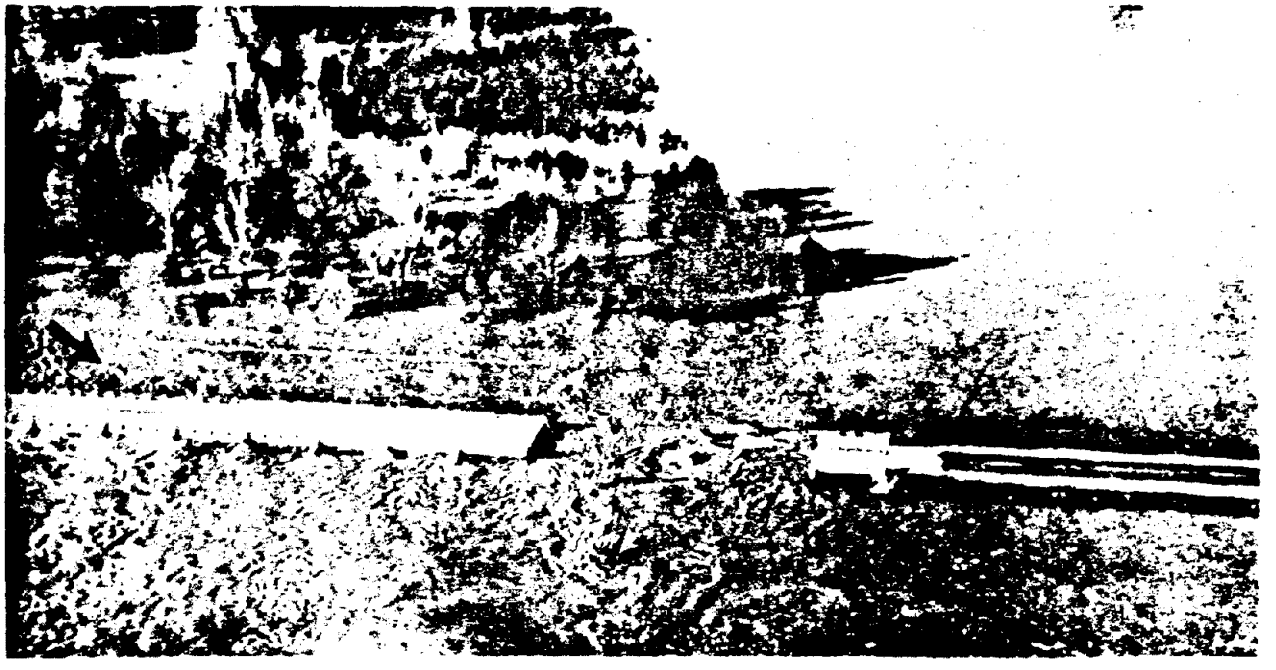

Figure 27.—Flow concentration along upstream side of embankment at Big Nichols Creek.

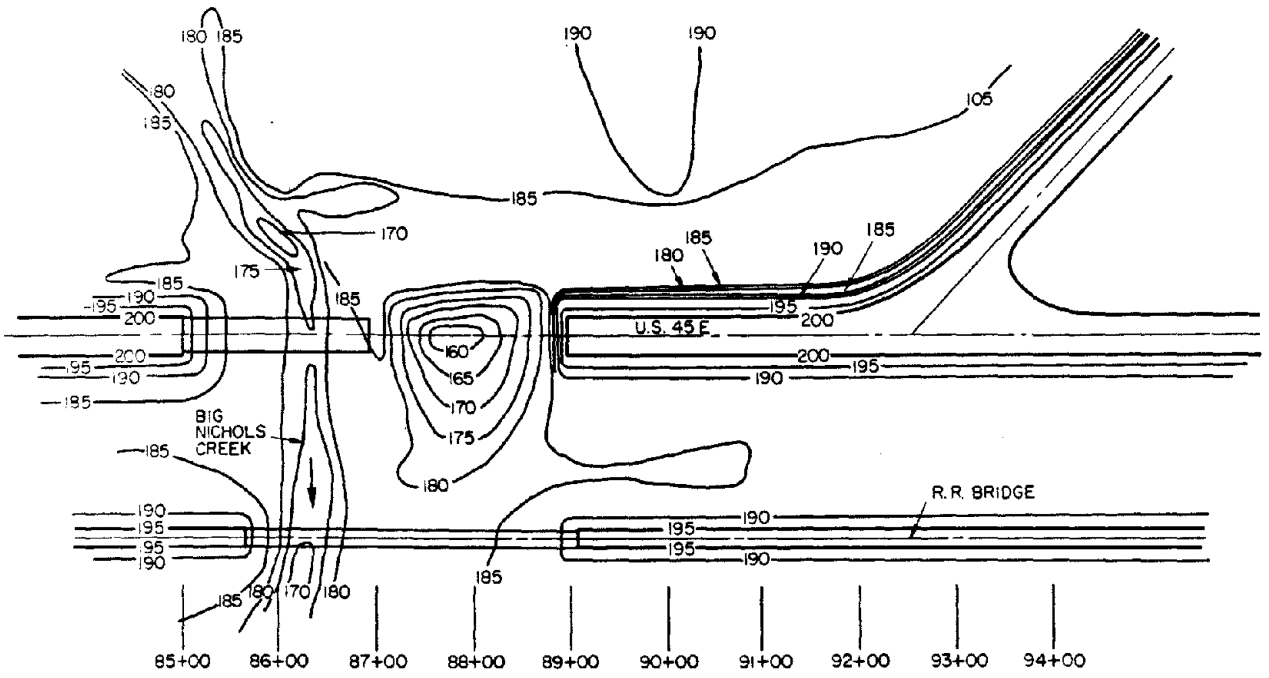

Figure 28.—Extent of scour measured after the flood at Big Nichols Creek.

be avoided, the situation can usually be remedied by constructing a spur dike as shown in the model in figure 29.

9.2 Function and geometry of spur dike. Where approach embankments divert considerable flood plain flow through the bridge opening, a spur dike, properly proportioned, is effective in reducing the gradient and velocity along the embankment by moving the mixing action of the merging flow away from the abutment to the upstream end of the dike.

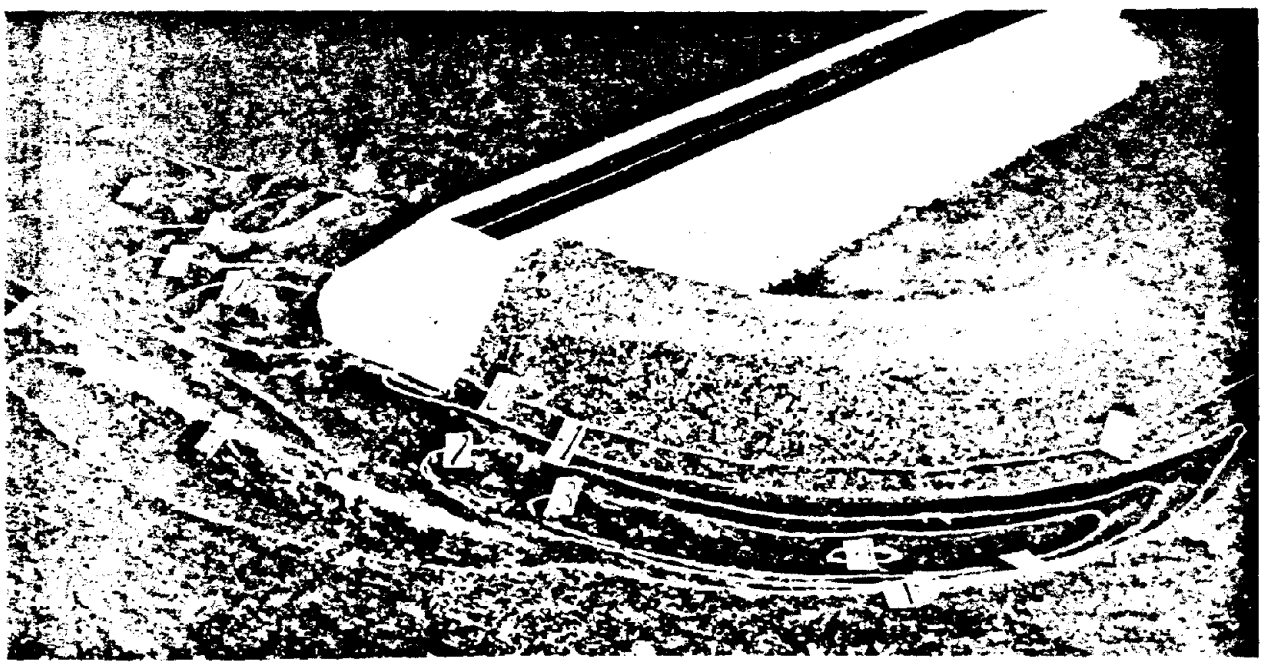

Figure 29.—Model of a spur dike.

The combined flow is directed so that the entire waterway under the bridge is utilized and the depth of scour in the vicinity of the bridge abutment and at adjacent piers is reduced. Scour, if it occurs, is moved upstream away from the bridge structure as shown on figure 29. Although any spur dike is usually helpful in reducing scour from merging flood plain flow, a dike of proper proportions is needed to keep scour at the bridge abutment to a minimum and properly align the flow through the end spans of the bridge.

Three principal considerations are involved in proportioning a spur dike: geometry, height and length. Laboratory studies (*19* and *25*) showed that a dike shaped in the form of a quarter of an ellipse, with ratio of major (length) to minor (offset) axes of 2.5:1 performed as well or better than any shape tested. The height of spur dike is based on anticipated high water. It should have sufficient height and freeboard to avoid overtopping and be protected from wave action. With the exception of dikes constructed entirely of stone or earth dikes properly armored with graded stone facing, overtopping will usually result in serious damage or complete destruction of a dike because the difference in level across the dike is usually sufficient to produce erosive velocities. The remaining dimension, length of dike, will be considered in detail in the following section. It may be said, however, that since field information on the operation of spur dikes is meager, the tendency at present is to lean toward over design rather than under design.

9.3 Length of spur dike. The information for determining the length of spur dike was obtained from model studies performed at Colorado State University (*19* and *25*), field data collected by the U.S. Geological Survey during floods in the State of Mississippi (*39*), and field observations by D. E. Schneible (*30*) during floods. Additional model information may be found in references 2 and 27 of the selected bibliography. The usable experimental and field information presently available on spur dikes is summarized in table C–1 and plotted on figure C–1. A discussion of the method of plotting, the variables involved, and the reliability of the data can be found in appendix C. For design purposes, figure C–1 has been reproduced, omitting the points, as figure 30. The parameters are a spur dike discharge ratio, Q_f/Q_{100}, relating the flow over the left or the right flood plain to a specific portion of the flow under the bridge, a representative velocity adjacent to the abutment of the bridge, and the length of spur dike needed. The discharge ratio is shown as the ordinate, the length of dike as the abscissa, and the family of curves are for different values of the velocity, V_{n2}.

Definitions of the symbols used are:

Q = Total discharge of stream (c.f.s.).

Q_f = Lateral or flood plain flow (one side) measured at section 1 (c.f.s.).

Q_{100} = Discharge in 100 feet of stream adjacent to abutment, measured at section 1 (c.f.s.).

b = Length of bridge opening (ft.).

A_{n2} = Water area under bridge referred to normal stage (sq. ft.).

$V_{n2} = \dfrac{Q}{A_{n2}}$ = Average velocity through bridge opening (f.p.s.).

$\dfrac{Q_f}{Q_{100}}$ = Spur dike discharge ratio.

L_s = Top length of spur dike (measured as shown on figure 30 (ft.).

The shape of the dike will conform to the equation of one quarter of an ellipse with 2.5:1 ratio of major to minor axis.

$$\frac{X^2}{L_s^2} + \frac{Y^2}{(0.4L_s)} = 1 \qquad (24)$$

or

$$L_s = (X^2 + 6.25Y^2)^{1/2}$$

It can be observed from figure 30 that the length of a spur dike should be increased with an increase in flood plain discharge, with an increase in velocity under the bridge, or both. The chart is read by entering the ordinate with the proper value of Q_f/Q_{100}, moving horizontally to the curve corresponding with the computed value of V_{n2} and then downward to obtain from the abscissa the length of spur dike required. As a general rule, if the length read from the abscissa is less than 30 feet, a spur dike is not needed. For chart lengths from 30 to 100 feet, it is recommended that a spur dike no less than 100 feet long be constructed. This length is needed to direct the curvilinear flow around the end of the dike so that it will merge with the main channel flow and establish a straight course down river before reaching the bridge abutment. Curvilinear flow can have several times the capacity to scour than that of parallel flow, depending on the radius of curvature, velocity, depth of flow and other factors. Holding the depth of flow and other factors

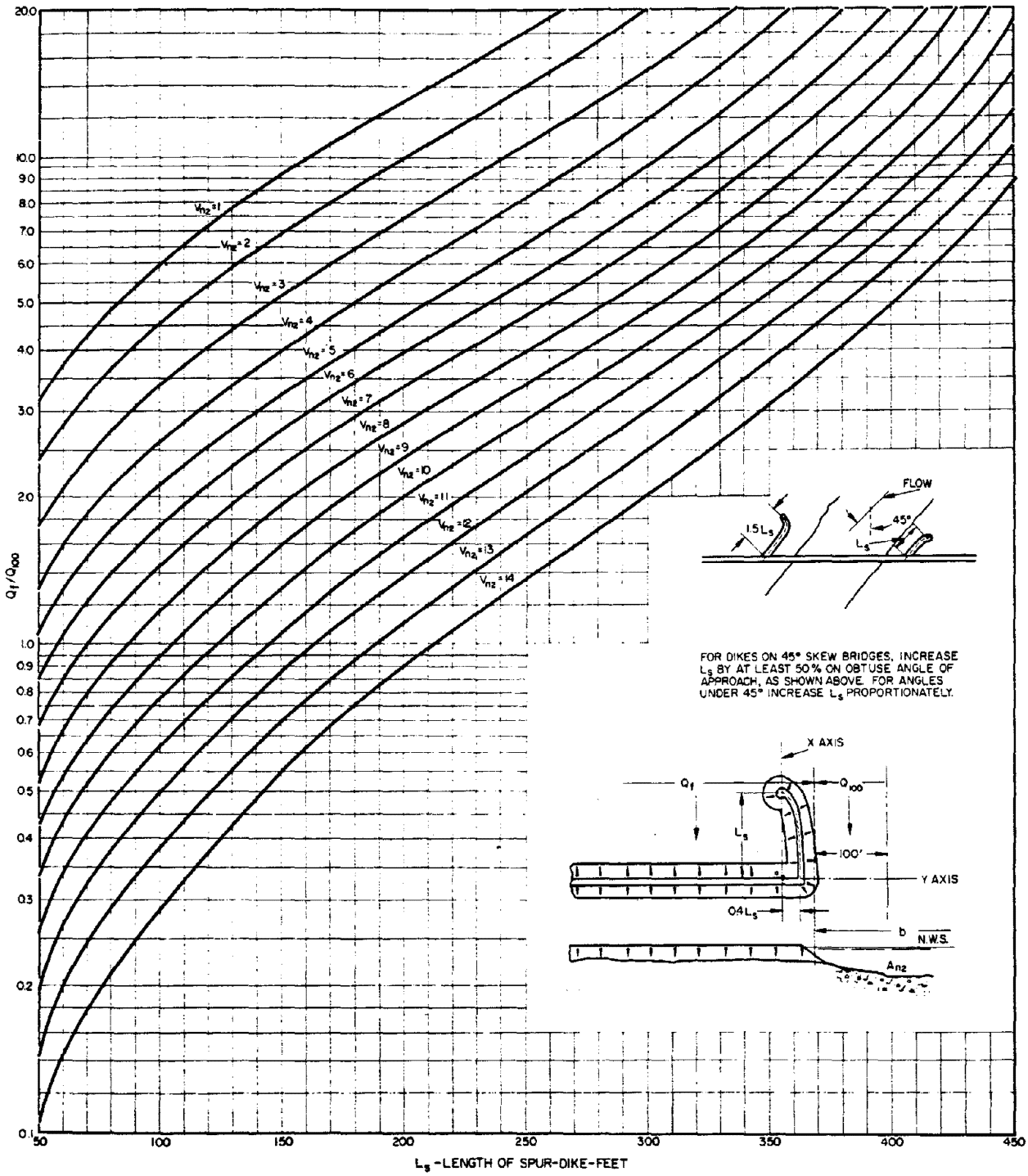

Figure 30.—Chart for determining length of spur dikes.

the same, the depth of scour will increase with decrease in radius of curvature. For this reason the deepest scour produced by a spur dike occurs near the nose where the radius of curvature is sharpest.

Figure 31 shows a case where spur dikes are indispensable on the Tarbela Bridge on the Indus River in West Pakistan (*42*). The average velocity under the bridge will be about 14 f.p.s. for the design flood of 750,000 c.f.s. For bridges skewed at an angle of 45°, it is recommended that the forward dike (see

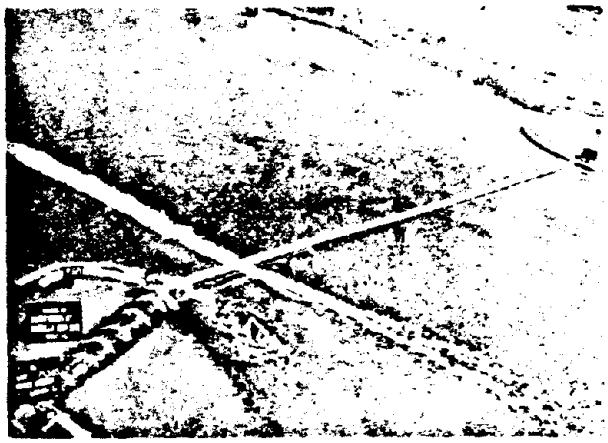

Figure 31.—Spur dikes on model of Tarbela Bridge, Indus River, West Pakistan.

sketch, fig. 30) be lengthened by 50 percent over the value given by the design chart. For lesser angles, the forward dike may be lengthened in proportion. Figure 32 shows a spur dike at a bridge on the Susquehanna River near Nanticoke, Pa., during the flood of March 1964. The spur dike, which is constructed entirely of rock, is 300 feet long and the bridge is skewed at an angle of 45° with the river. This dike was built before the model studies, therefore, it is not elliptical in plan and the flow does not follow the nose as well as it should. It has proven very effective, however, as evidenced by comparisons of the scour at abutment and adjacent piers after two floods, one before and the other after the dike was constructed.

9.4 Other considerations. The method of proportioning spur dikes for use at bridge abutments is illustrated by example 10 of chapter XII. There is no direct relation between length of spur dike and length of bridge; for this reason only the first 100 feet of waterway adjacent to the abutment in question is considered. A better choice of parameters might be desirable for figure 30, preferably expressed in dimensionless form. These points were given consideration in preparing the chart, but experimental and field data are insufficient to warrant greater refinement at this time. After a sufficient number and variety of field structures have been proportioned in accordance with figure 30, its worth may be evaluated from the performance of these spur dikes under flood water conditions. Modifications will by then be in order, and it may be desirable to present the overall information in an entirely different manner. From a review of the dimensions of spur dikes constructed to date (see columns 18 and 19 of table C–1), a method lending some standardization to design appears to be of immediate importance at this time. It was for this reason that figure 30 is presented.

Figure 33 shows in detail a general plan and cross section of a spur dike as usually constructed. Prior to the introduction of the design chart, figure 30, there was no definite criteria for determining length of spur dike so 150 feet was recommended by D. E. Schneible (*30*) as a standard length. There is still no objection to considering 150 feet a minimum length on the basis that a long dike can sustain considerable damage and still remain effective while damage to a short dike may result in a complete loss.

Spur dikes may be constructed entirely of rock provided the facing is of sufficient size to resist displacement by the current. Dikes constructed of earth should be compacted to the same standards as the roadway embankment and should extend above expected high water. Protection may be limited to the areas shown on figure 33 if rock is expensive and the remaining portions of dike will support vegetation. Where rock is used as a facing on an earth dike, it should be well graded and a filter blanket should be used if the relative gradations of the rock and of the spur dike material require it. Design of filter blankets and riprap protection are described in BPR Hydraulic Engineering Circular No. 11 (*16*). In special cases where the cost of facing for a spur dike is prohibitive, it can be constructed with a sod cover or minimum protection with a plan for repair or replacement after each high water occurrence with the risk that it would protect the bridge for one flood.

The following points should be kept in mind:

1. Keep trees as close to the toe of the spur dike embankment as construction will permit.

Figure 32.—Spur dike on 45° skewed bridge over Susquehanna River at Nanticoke, Pa.

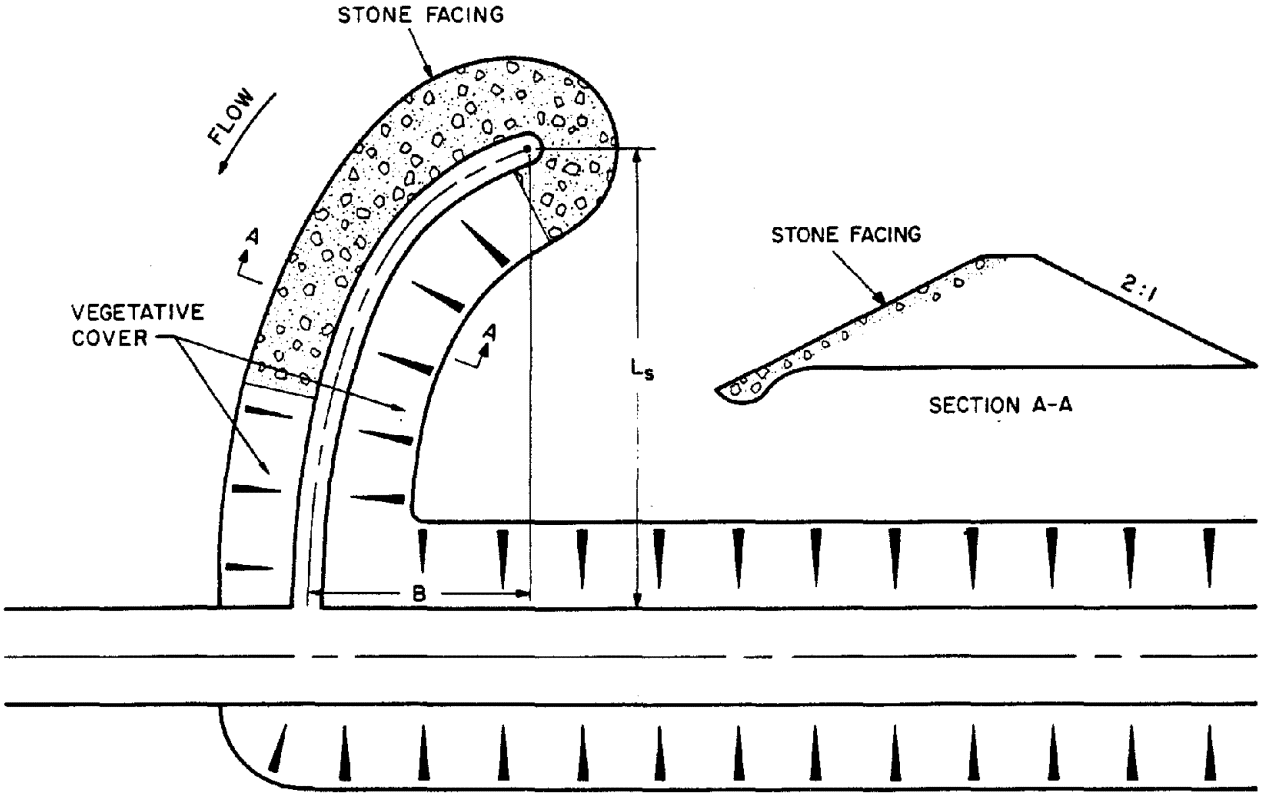

Figure 33.—Plan and cross section of spur dike.

2. Do not allow the cutting of channels or the digging of borrow pits near spur dikes or along the upstream side of embankments.

3. If drainage is important, put small pipe through spur dike or embankment to drain pockets left behind dikes after flood recedes.

A 14-minute motion picture (16 mm. film) entitled, "Spur Dikes," demonstrating the theory and performance of these elliptical shaped embankments during high water, is available on loan from the Federal Highway Administration, Publications and Visual Aids Branch, Washington, D.C. 20591.

Chapter X.—FLOW PASSES THROUGH CRITICAL DEPTH (TYPE II)

10.1 Introduction. The computation of backwater for bridges on streams with fairly steep gradients, by the method outlined up to this point, may result in unrealistic values. When this occurs, it is probably a sign that the flow encountered is type II (see fig. 4), and the backwater analysis for subcritical or type I flow no longer applies. The water surface for type IIA flow passes through critical stage under the bridge but returns to normal or subcritical flow some distance downstream. In the case of type IIB flow, the water surface passes through critical stage under the bridge and then dips below critical stage downstream. One analysis that applies to both types is found in section A.2, appendix A. The sole source of data for type II flow is from model studies, which cover but a limited range of contraction ratios.

10.2 Backwater coefficients. Design information for other than type I flow has been in demand and some designers have expressed confusion in attempting to apply the type I analysis to other types of flow. It has been decided, therefore, to present a tentative backwater coefficient curve (fig. 34) based on the information at hand. The expression for the backwater coefficient in this case is:

$$C_b = \frac{h_1^* + \bar{y} - y_{2c}}{\alpha_2 V_{2c}^2/2g} + \frac{\alpha_1}{\alpha_2}\left(\frac{V_1}{V_{2c}}\right)^2 - 1 \qquad (25)$$

Where

$\bar{y}$ = Normal depth in constriction or A_{n2}/b (ft.)
y_{2c} = Critical depth in constriction or A_{2c}/b (ft.)
V_{2c} = Critical velocity in constriction or Q/A_{2c} (f.p.s.)
α_2 = Velocity head coefficient for the constriction

The backwater coefficient has been assigned the symbol C_b to differentiate it from the coefficient for subcritical flow.

The curve of figure 34 accounts for the contraction ratio only, which is the major factor involved. The effect of piers, eccentricity, and skew have not been evaluated because of the tentative nature of the curve. The incremental coefficients on figures 7, 8, and 10 for piers, eccentricity and skew, are not applicable to type II flow problems.

The backwater for type II flow, with no allowance

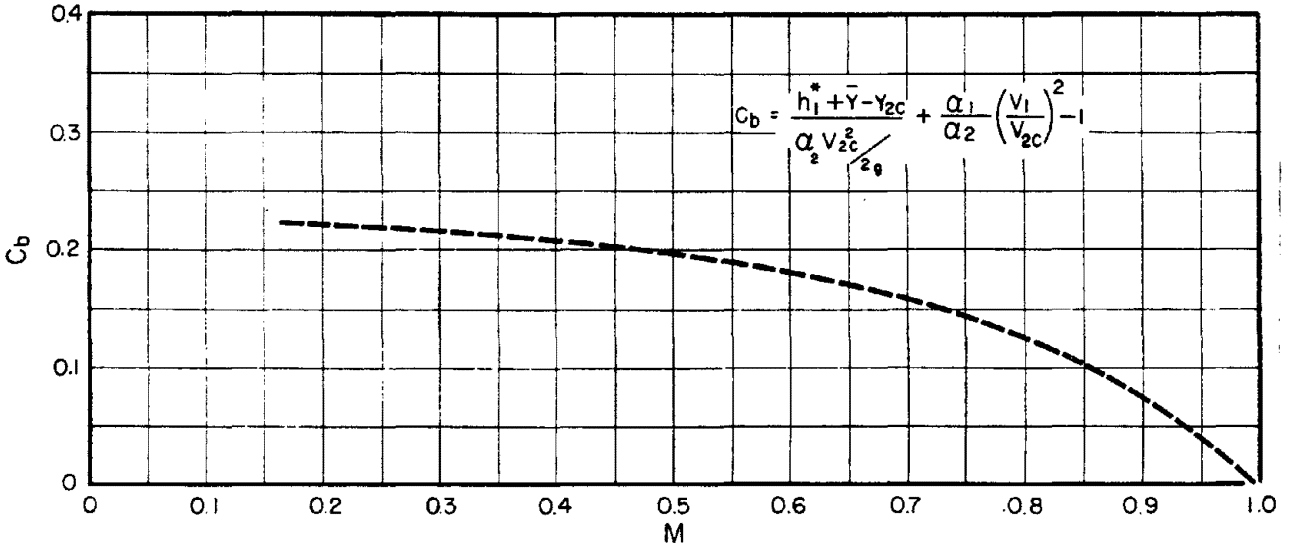

Figure 34.—Tentative backwater coefficient curve for type II flow.

for piers, eccentricity and skew, is then:

$$h_1^* = \alpha_2 \frac{V^2_{2c}}{2g}(C_b + 1) - \alpha_1 \frac{V^2_1}{2g} + Y_{2c} - \bar{Y} \quad (26)$$

10.3 Recognition of flow type. The prime difficulty here will be to determine which type of flow will occur at a proposed bridge site in the field prior to starting the backwater computations. No definite answers can be given since most problems encountered of this nature will be borderline cases. As a suggestion try the type I approach for computing backwater first. Should the result appear unrealistic, repeat the backwater computation using the type II approach. It is more than likely that the difference in the two results will be great enough to readily spot the erratic one. Stating it another way, if the backwater for the type II flow results in a lower value than for the type I computation, the flow definitely will be type II.

The extent of the model information and the plotted points may be inspected in table A–1 and figure A–3, respectively. Example 13, chapter XII, briefly illustrates the computational procedure suggested.

Chapter XI.—PRELIMINARY FIELD AND DESIGN PROCEDURES

11.1 Evaluation of flood hazards. Bureau of Public Roads' instructions require that after January 1, 1968, all Federal and Federal-aid highway plans submitted for approval shall show the magnitude, frequency, and pertinent water surface elevations for the design flood and, if available, similar data for the maximum flood of record for all structures and roadway embankments that cross flood plains or encroach on rivers and streams having a design flood of more than 500 c.f.s. Similar information for structures designed for lesser discharges are to be recorded in the project design files. In addition, the instructions require that highway structures that encroach on or cross the flood plain of a drainage course shall not cause a significant adverse effect to developments on the flood plain, and at the same time the structure shall be capable of withstanding the design flood flow with minimum damage.

On interstate projects, all bridges and culverts are to accommodate floods of at least a 50-year frequency or the greatest flood of record, whichever is greater, with runoff based on land development 20 years hence and backwater limited to an amount which will not result in damage to upstream property or the highway. Where the greatest flood of record is considerably larger than the 50-year flood and the cost to provide for such an exceptional flood without damage or flooding to the roadway or adjacent property is shown by analysis to be excessive for the protection given, a lesser flood, but not less than the flood of 50-year frequency, may be used for design. The effect of flood-control structures on reducing floods should be considered in determining the design flood.

For Federal-aid projects other than interstate, similar requirements apply as in the above paragraphs except that design floods may be less than a 50-year frequency where conditions warrant lower standards. The flood frequency selected for design should be consistent with the magnitude of damage to adjacent property and the importance of the highway.

11.2 Site study outline. The following outline is presented to aid in organizing and collecting the necessary field data for a bridge site investigation:

1. Location map to show proposed highway alignment and reach of river to be studied.

(*a*) U.S.G.S. Quadrangle sheet or map of equal detail.

(*b*) Aerial photographs.

2. Vicinity map showing flood flow patterns, cross sections of stream, location of proposed bridge and relief openings, and alignment of piers.

(*a*) Map showing 1- or 2-foot contours, stream meanders, vegetation and manmade improvements.

(*b*) In some cases, cross sections perpendicular to flood flow are acceptable in lieu of the map in (*a*); at least three cross sections are desirable: one on the centerline of the proposed bridge, one upstream and one downstream from the proposed bridge at from 500- to 1,000-foot intervals.

3. A full description of existing bridges both upstream and downstream from proposed crossing (including relief and overflow structures).

(*a*) Type of bridge, including span lengths and pier orientation.

(*b*) Cross section beneath structure, noting stream clearance to superstructure and skew or direction of current during floods.

(*c*) All available flood history—high water marks with dates of occurrence, nature of flooding, damages and source of information.

(*d*) Photographs of existing bridges, past floods, main channels and flood plains and information as to nature of drift, ice, streambed and stability of banks.

4. Factors affecting water stage at bridge site.

(*a*) High water from other streams.

(*b*) Reservoirs—existing or proposed and approximate date of construction.

(*c*) Flood control projects.

(*d*) Tide.

(*e*) Other controls.

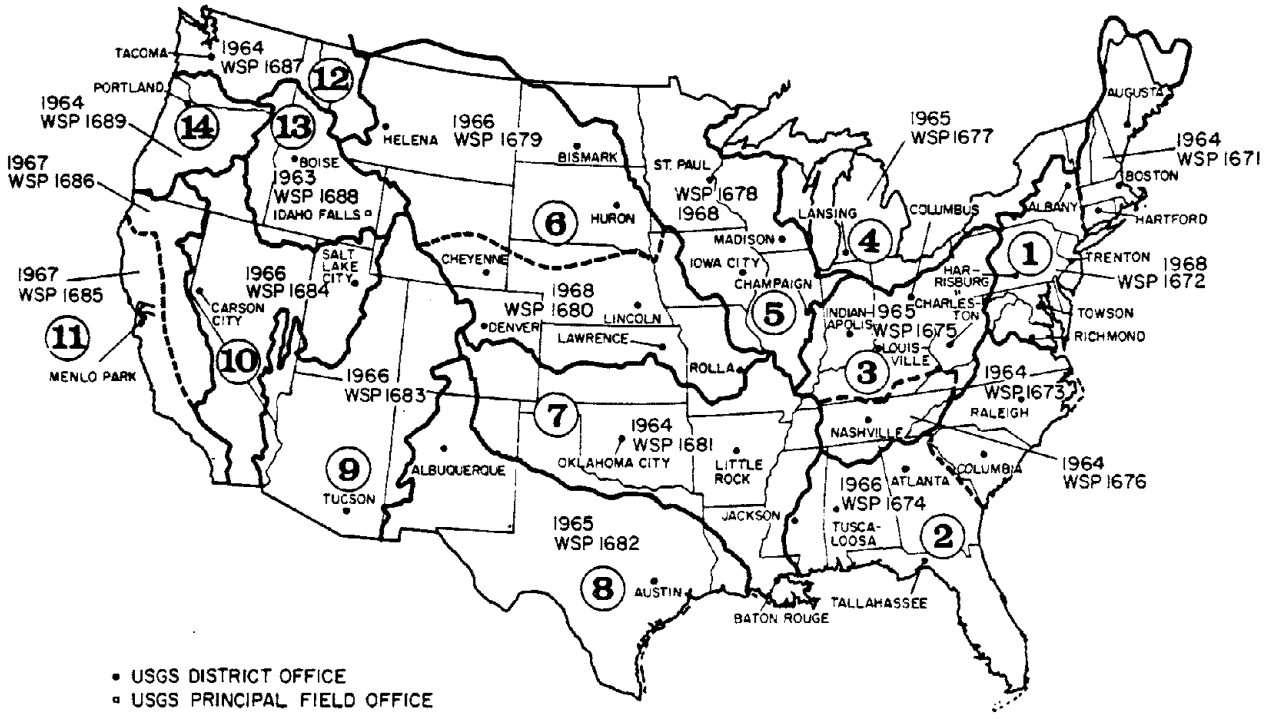

Figure 35.—Status of U.S. Geological Survey nationwide flood frequency project.

11.3 Hydrological analysis outline. Site inspection should be made by engineer making hydrological and hydraulic analysis.

1. List flood records available on river being studied.
2. Determine drainage area above proposed crossing from available maps.
3. Plot flood frequency curve for the site.
4. Plot a stage-discharge curve for the site.
5. Prepare chart showing distribution of flood flow and velocities for several discharges or stages in natural channel without proposed bridge. (n-values used in this computation should be selected by an experienced hydraulic engineer.)

The following sections contain information which may prove of value in compiling the above listed material.

11.4 Flood magnitude and frequency. A complete discussion of estimating flood frequency is beyond the scope of this publication, but sources of data will be cited. The frequency and magnitude of floods may be determined from gaging station records, if available, on the river in question. In the absence of such records, a regional flood frequency study may be made or may already be available from studies made by the U.S. Geological Survey or others.

The Geological Survey has prepared two series of water-supply papers that summarize streamflow in the United States as measured continuously or periodically at stream-gaging stations. The first series of these compilation reports contains monthly data from the beginning of record for each station through September 1950 ("Compilation of records of surface waters of the United States through September 1950"). The second series of reports contains similar data for the period October 1950 through September 1960.

Recently a nationwide series of water-supply papers was completed on the "Magnitude and frequency of floods in the United States." The reports contain tables of maximum known floods at gaging stations and curves for estimating the probable magnitude of floods of frequencies ranging up to 50 years for most streams (gaged or ungaged) for discharges not materially affected by regulation or diversion.[1] A map outlining the boundaries of the nationwide flood frequency project, recently completed, is included as figure 35. The heavy lines outline the geographical areas studied and the part numbers are those used in the annual reports on

[1] All three series of reports are available for reference at many public and university libraries. Those reports still in print may be purchased from the Superintendent of Documents, Government Printing Office, Washington, D.C. 20402.

surface-water supply of the United States. The number of the water supply paper applicable to each area is shown on the map together with the date of publication. Also indicated are locations of U.S.G.S. district and principal field offices where additional field information may be available. Inquiries can be made of the surface water branch office of the State in question.

The Bureau of Public Roads has made studies to determine peak rates of runoff from small watersheds. Reference 15 describes a research study limited to watersheds of 25 square miles or less, located east of the 105th meridian. Hydraulic Engineering Circular No. 2 (*12*)[2] describes a flood estimating procedure based on an analysis of 55 streamflow records and drainage areas ranging from 0.03 to 762 square miles in the Piedmont Plateau, which embodies the area between the Appalachian Mountains and the Atlantic coastal plain, extending from Alabama to New Jersey.

11.5 Stage discharge. It is important that the normal stage of a river for the design flood be determined as accurately as possible at the bridge site. This may be accomplished in several ways, but where possible it is best to establish it from a stage-discharge rating curve based on stream-gaging records collected in the vicinity of the bridge site. Such records are available in the files of the U.S. Geological Survey. A typical stage-discharge curve, figure 40, accompanies example 4 in chapter XII. The scale at the top of the graph also shows flood recurrence intervals. Where stage-discharge records are lacking for the stream in question, the usual procedure is to locate high water marks of floods by consulting people who live in the vicinity of the proposed bridge site. Flood information supplied by local residents is often inaccurate, but may be considered reliable if confirmed by other residents.

It is then necessary to find a means of relating stage to discharge. This can be done by the slope-area method, a simplified variation of which will be found illustrated in examples 1 and 4. Extreme care must be exercised both in the collection of field data and in the manner in which it is processed if glaring discrepancies are to be avoided in the final result. In many cases where records are lacking, it is advisable to arrange for the installation and maintenance of a temporary stream gage at or near the bridge site several years in advance of construction. Even a single reliable point at an intermediate stage can be of inestimable value in the preparation of a stage-discharge curve.

11.6 Channel roughness. A matter of prime importance in bridge backwater or slope-area computations is the ability to evaluate properly the roughness of the main channel and of the flood plains; both are subject to extreme variations in vegetal growth and depth of flow. As a guide, values of the Manning roughness coefficient, n, as commonly encountered in practice, are tabulated for various conditions of channel and flood plain in table 1. Since the practicing engineer in this country is familiar with the Manning roughness coefficient, the Manning equation has been chosen for use here. In interpreting roughness coefficients from table 1, it should be kept in mind that the value of n for a small depth of flow, especially on a flood plain covered with grass, weeds, and brush, can be considerably larger than that for greater flow depths over the same terrain (*34* and *35*). On the other hand, as the stage rises in a stream with an alluvial bed, sand waves develop which can increase the value of n (*4*). It is, therefore, suggested that the notes accompanying table 1 be carefully considered along with the tabulation. An especially useful guide for choosing channel roughness coefficients is reference 41.

11.7 Bridge backwater design procedure. The following is a brief step-by-step outline for determining the backwater produced by a bridge constriction:

1. Determine the magnitude and frequency of the discharge for which the bridge is to be designed from sources cited (sec. 11.4).
2. Determine the stage of the stream at the bridge site for the design discharge (sec. 11.5).
3. Plot a representative cross section of stream for design discharge at section 1, if not already done under step 2. If stream channel is essentially straight and cross section substantially uniform in the vicinity of the bridge, the natural cross section of the stream at the bridge site may be used for this purpose.
4. Subdivide the cross section plotted in step 3 according to marked changes in depth of flow and changes in roughness. Assign values of Manning roughness coefficient, n, to each subsection (table 1). Experience and careful judgment are necessary in selecting these values.
5. Compute conveyance and then discharge in each subsection (method is demonstrated in examples).

[2] Available in limited numbers from Office of Engineering and Operations, Bureau of Public Roads, Washington, D.C. 20591.

Table 1.—Manning's roughness coefficient for natural stream channels[1].

	Manning's n range
A. **Minor streams** (surface width at flood stage < 100 ft.):[2]	
1. Fairly regular section:	
a. Some grass and weeds, little or no brush	0.030–0.035
b. Dense growth of weeds, depth of flow materially greater than weed height	0.035–0.05
c. Some weeds, light brush on banks	0.035–0.05
d. Some weeds, heavy brush on banks	0.05–0.07
e. Some weeds, dense willows on banks	0.06–0.08
f. For trees within channel with branches submerged at high stage, increase all above values by	*0.01–0.02*
2. Irregular section, with pools, slight channel meander; channels (a) to (e) above, increase all values about	*0.01–0.02*
3. Mountain streams, no vegetation in channel, banks usually steep, trees and brush along banks submerged at high stage:	
a. Bottom of gravel, cobbles, and few boulders	0.04–0.05
b. Bottom of cobbles with large boulders	0.05–0.07
B. **Flood plains** (adjacent to natural streams):	
1. Pasture, no brush:	
a. Short grass	0.030–0.035
b. High grass	0.035–0.05
2. Cultivated areas:	
a. No crop	0.03–0.04
b. Mature row crops	0.035–0.045
c. Mature field crops	0.04–0.05
3. Heavy weeds, scattered brush	0.05–0.07
4. Light brush and trees:[3]	
a. Winter	0.05–0.06
b. Summer	0.06–0.08
5. Medium to dense vegetation:[3]	
a. Winter	0.07–0.11
b. Summer	0.10–0.16
6. Dense willows, summer, not bent over by current	0.15–0.20
7. Cleared land with tree stumps, 100–150 per acre:	
a. No sprouts	0.04–0.05
b. With heavy growth of sprouts	0.06–0.08
8. Heavy stand of timber, a few down trees, little undergrowth:	
a. Flood depth below branches	0.10–0.12
b. Flood depth reaches branches (n increases with depth)[4]	0.12–0.16
C. **Major stream** (surface width at flood stage > 100 feet): Roughness coefficient is usually less than for minor streams of similar description on account of less effective resistance offered by irregular banks or vegetation on banks. Values of n may be somewhat reduced. Follow general recommendations[1] if possible. The value of n for larger streams of mostly regular section, with no boulders or brush, may be in the range	0.028–0.33

[1] For calculations of stage or discharge in natural stream channels, it is recommended that the designer consult the local District Office of the U.S. Geological Survey to obtain data regarding values of n applicable to streams of any specific region. Where the recommended procedure is not followed, the table values may be used as a guide.

With channel of alinement other than straight, loss of head by resistance forces will be increased. A small increase in value of n may be made to allow for the additional loss of energy.

[2] The tentative values of n cited are principally derived from measurements made on fairly short but straight reaches of natural streams. Where slopes calculated from flood elevations along a considerable length of channel, involving meanders and bends, are to be used in velocity calculations by the Manning formula, the value of n must be increased to provide for the additional loss of energy caused by bends. All values in the table must be so increased. The increase may be in the range of perhaps 3 to 15 percent.

[3] The presence of foliage on trees and brush under flood stage will materially increase the value of n. Therefore, roughness coefficients for vegetation in leaf will be larger than for bare branches. For trees in channel or on banks, and for brush on banks where submergence of branches increases with depth of flow, n will increase with rising stage.

[4] For important work and where accurate determination of water profiles is necessary, the designer is urged to consult reference 41 to select n by comparison with specific conditions.

6. Using cumulative conveyance and discharge at section 1, compute slope of stream, S_0. Should the computed slope vary more than 25 percent from the actual slope, reassign values of the roughness factor, n, and repeat conveyance computations.

7. Determine value of kinetic energy coefficient, α_1 (method is illustrated in examples, chapter XII).

8. Plot natural cross section under proposed bridge based on normal water surface for design discharge, and compute gross water area (including area occupied by piers).

9. Compute bridge opening ratio, M (sec. 1.10), observing modified procedure for skewed crossings (sec. 2.7).

10. Obtain value of K_b from base curve in figure 6 for symmetrical normal crossings.

11. If piers are involved, compute value of J (sec. 2.4) and obtain incremental coefficient, ΔK_p, from figure 7 (note method outlined for skewed crossings, sec. 2.5).

12. If eccentricity is severe, compute value of e (sec. 2.6) and obtain incremental coefficient, ΔK_e, from figure 8.

13. If a skewed crossing is involved, observe

proper procedure in previous steps, then obtain incremental coefficient, ΔK_a, for proper abutment type from figure 10.

14. Determine total backwater coefficient, K^*, by adding incremental coefficients to base curve coefficient, K_b.

15. Estimate α_2 from figure 5, then make allowance for any unusual topographic, vegetative or approach condition which may lead to further asymmetrical velocity distribution in the bridge constriction.

16. Compute backwater by expression (4), section 2.1.

17. Determine distance upstream to maximum backwater from figure 13 and convert backwater to water surface elevation at section 1 if computations are based on normal stage at bridge.

It is now possible to place the above basic information on punch cards and do all or part of the above procedure and computations by electronic computer (*13*).

Chapter XII.—ILLUSTRATIVE EXAMPLES

A better understanding of the procedures for computing bridge backwater can be gained from the illustrative examples in this chapter. Some of the procedures to be explained in detail have been computerized (*13*), however, the point cannot be over emphasized that to properly appreciate and utilize the computer programs, one should first become familiar with the long hand methods. The examples deal with the following phases of design:

Example 1 comprises a simple normal crossing; the steps closely follow the outline of design procedure listed in chapter XI.

Example 2 treats example 1 as a dual crossing.

Example 3 should help clarify the procedure recommended for skewed crossings.

Example 4 is an eccentric crossing which demonstrates how backwater computations may be systematized for a typical bridge waterway problem where a range in bridge length and in flood discharge is to be studied. This example serves to demonstrate that the length, and hence the cost, of a bridge at a given site varies within wide limits depending on the amount of backwater considered tolerable.

Example 5 is included to demonstrate an approximate calculation for backwater at bridge sites where abnormal stage-discharge conditions prevail.

Example 6 illustrates how scour under a bridge affects the backwater.

Examples 7 and 8 demonstrate how discharge or differential water level across bridge embankments can be determined when portions of the superstructure are in the flow.

Example 9 considers favoring flow over bridge embankments to serve as a safety valve for the bridge during superfloods.

Example 10 demonstrates a proposed method for the design of spur dikes at bridges.

Example 11 deals with type II flow which passes through critical stage under the bridge.

Example 1

12.1 Example 1: Normal crossing. *Given.*—The channel crossing shown in figure 36 with the following information: Cross section of river at bridge site showing areas, wetted perimeters, and values of Manning, n; normal water surface for design = El. 28.0 ft. at bridge; average slope of river in vicinity of bridge S_0 = 2.6 ft./mi. or 0.00049 ft./ft.; cross section under bridge showing area below normal water surface and width of roadway = 40 ft.

The stream is essentially straight, the cross section relatively constant in the vicinity of the bridge, and the crossing is normal to the general direction of flow.

Find.—

(*a*) Conveyance at section 1.
(*b*) Discharge of stream at El. 28.0 ft.
(*c*) Velocity head correction coefficient, α_1.
(*d*) Bridge opening ratio, M.
(*e*) Backwater produced by the bridge.
(*f*) Water surface elevation on upstream side of roadway embankment.
(*g*) Water surface elevation on downstream side of roadway embankment.

Computation (*1a*). Under the conditions stated, it is permissible to assume that the cross sectional area of the stream at section 1 is the same as that at the bridge. The approach section is then divided into subsections at abrupt changes in depth or channel roughness as shown in figure 36. The conveyance of each subsection is computed as shown in columns 1 through 8 of table 2 (see also sec. 1.9). The summation of the individual values in column 8 represents the overall conveyance of the stream at section 1 or K_1 = 879,489. Note that the water interface between subsections is not included in the wetted perimeter. Table 2 is set up in short form

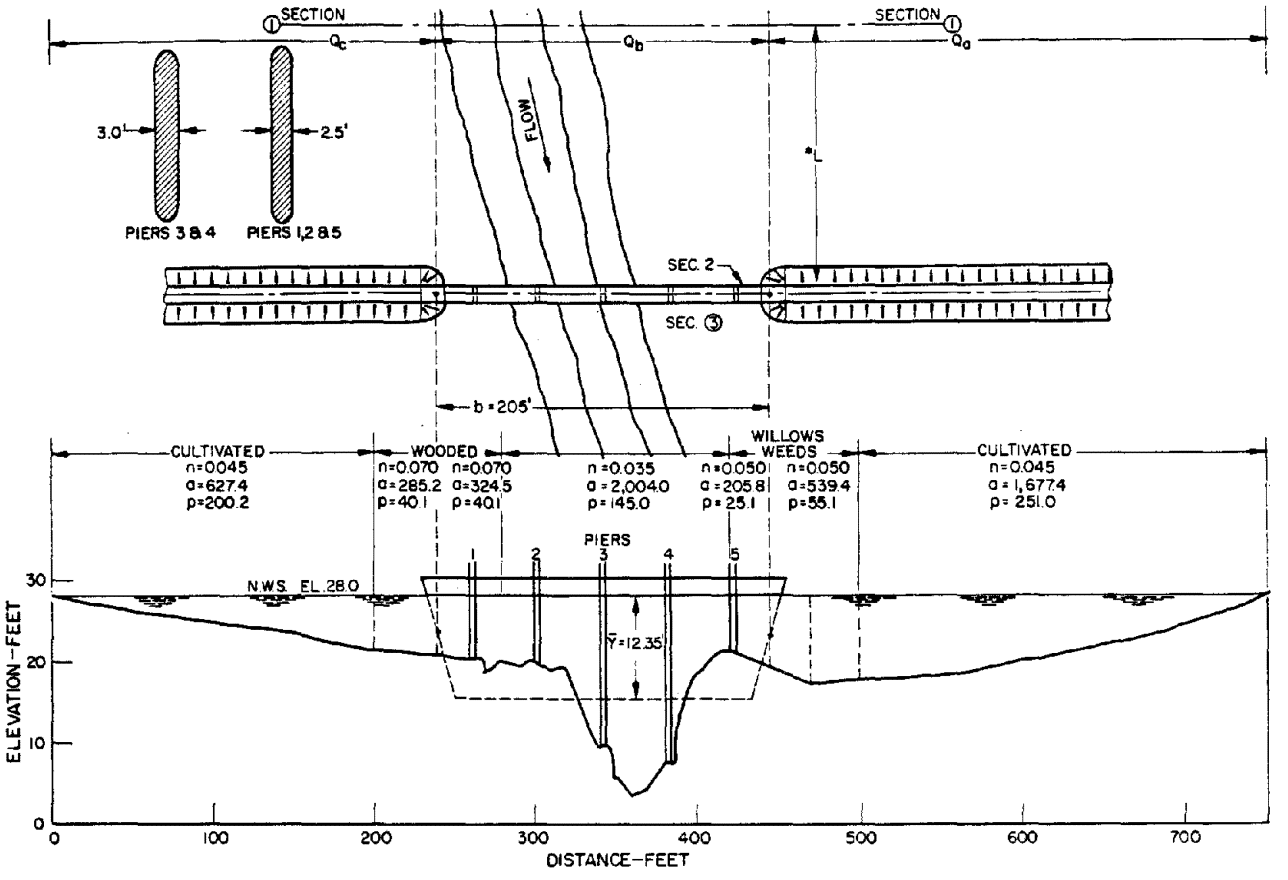

Figure 36.—Example 1: Plan and cross section of normal crossing.

to better demonstrate the method. The actual computation would involve many subsections corresponding to breaks in grade or changes in channel roughness.

Computation (1b). Since the slope of the stream is known (2.6 ft./mi.) and the cross sectional area is essentially constant throughout the reach under consideration, it is permissible to solve for the discharge by what is known as the slope-area method or:

$$Q = K_1 S_0^{1/2} = 879{,}489(0.00049)^{1/2} = 19{,}500 \text{ cfs.}$$

It should be noted that the procedure in examples 3 and 4 conforms more nearly to what is usually required in practice.

Computation (1c). To compute the kinetic energy coefficient (sec. 1.11), it is first necessary to complete columns 9, 10, and 11 of table 2; then, using expression (3a) (sec. 1.11):

$$\alpha_1 = \frac{\sum qv^2}{QV_{n1}^2} = \frac{374{,}895}{19{,}500(19{,}500/5{,}664)^2} = 1.62$$

where $\sum qv^2$ is the summation of column 11, and V_{n1} represents the average velocity for normal stage at section 1.

Computation (1d). The sum of the individual discharges in column 9 must equal 19,500 c.f.s. The factor M, as stated in section 1.10, is the ratio of that portion of the discharge approaching the bridge in width b, to the total discharge of the river; using expression (1) (sec. 1.10):

$$M = \frac{Q_b}{Q} = \frac{12{,}040}{19{,}500} = 0.62$$

Entering figure 5 with $\alpha_1 = 1.62$ and $M = 0.62$, the value of α_2 is estimated as 1.40.

Computation (1e). Entering figure 6 with $M = 0.62$, the base curve coefficient is $K_b = 0.72$ for bridge waterway of 205 ft.

As the bridge is supported by five solid piers, the incremental coefficient (ΔK_p) for this effect will be determined as described in section 2.4. Referring to figure 36 and table 2, the gross water area under the bridge for normal stage, A_{n2}, is 2,534 sq. ft. and

Table 2.—Example 1: Sample computations.

$S_0 = 0.00049$

	Sub-section	n	$\frac{1.49}{n}$	a	p	$r = \frac{a}{p}$	$r^{2/3}$	$k = \frac{1.49}{n} ar^{2/3}$	$q = Q\frac{k}{K_1}$	$v = \frac{q}{a}$	qv^2
				sq. ft.	ft.	ft.			cfs	fps	
	(1)	(2)	(3)	(4)	(5)	(6)	(7)	(8)	(9)	(10)	(11)
	Computation (1a)								Computation (1c)		
Q_a	0–200	0.045	33.0	627.4	200.2	3.134	2.142	44,349	983.3	1.57	2,424
	200–240	.070	21.2	285.2	40.1	7.112	3.698	22,359	495.7	1.74	1,501
	240–280	.070	21.2	324.5	40.1	8.092	4.031	27,732	614.8	1.89	2,196
Q_b	280–420	.035	42.5	2,004.0	145.0	13.821	5.759	490,492	10,875.2	5.43	320,654
	420–445	.050	29.7	205.8	25.1	8.199	4.066	24,852	551.0	2.68	3,958
Q_c	445–500	.050	29.7	539.4	55.1	9.789	4.576	73,309	1,625.4	3.01	14,726
	500–750	.045	33.0	1,677.4	251.0	6.683	3.548	196,396	4,354.6	2.60	29,436
				$A_n = 5,663.7$ sq. ft.				$K_1 = 879,489$	$Q = 19,500.0$ c.f.s.		$\Sigma qv^2 = 374,895$

$A_{n2} = 2,534$ sq. ft. $\qquad Q_b = 12,040$ c.f.s.

the area obstructed by the piers, A_p, is 180 sq. ft.; so:

$$J = \frac{A_p}{A_{n2}} = \frac{180}{2,534} = 0.071.$$

Entering figure 7A with $J = 0.071$ for solid piers, the reading from ordinate is $\Delta K = 0.13$. This value is for $M = 1.0$. Now enter figure 7B and obtain the correction factor σ, for $M = 0.62$ which is 0.84. The incremental backwater coefficient for the five piers, $\Delta K_p = \Delta K\sigma = 0.13 \times 0.84 = 0.11$.

The overall backwater coefficient:

$$K^* = K_b + \Delta K_p = 0.72 + 0.11 = 0.83,$$

$$V_{n2} = \frac{Q}{A_{n2}} = \frac{19,500}{2,534} = 7.70 \text{ f.p.s.}$$

and

$$\frac{V^2_{n2}}{2g} = 0.92 \text{ ft.}$$

Using expression (4a) (sec. 2.1), the approximate backwater will be:

$$K^* \frac{\alpha_2 V^2_{n2}}{2g} = 0.83 \times 1.40 \times 0.92 = 1.07 \text{ ft.} \qquad (4a)$$

Substituting values in the second half of expression (4) for difference in kinetic energy between sections 4 and 1 (sec. 2.1) where $A_{n1} = 5664$ sq. ft. $= A_4$, $A_1 = 6384$ sq. ft., and $A_{n2} = 2534$ sq. ft.,

$$\alpha_1 \left[\left(\frac{A_{n2}}{A_4}\right)^2 - \left(\frac{A_{n2}}{A_1}\right)^2 \right] \frac{V^2_{n2}}{2g} \qquad (4b)$$

or

$$1.62 \left[\left(\frac{2,534}{5,664}\right)^2 - \left(\frac{2,534}{6,384}\right)^2 \right] 0.92 = 1.62 \times 0.042 \times 0.92 = 0.06 \text{ ft.}$$

Then total backwater produced by the bridge is

$$h_1^* = 1.07 + 0.06 = 1.13 \text{ ft.} \qquad (4)$$

Computation (1f). The statement was made (in sec. 4.1) that the water surface on the upstream side of the roadway embankment will be essentially the same as that at section 1. Thus, to determine the backwater elevation it is first necessary to locate the position of section 1, which is accomplished with the aid of figure 13.

From preceding computations:

$$b = 205 \text{ ft.}$$

and

$$\bar{y} = \frac{A_{n2}}{b} = \frac{2,534}{205} = 12.36 \text{ ft.}$$

It is necessary to assume the total drop across the embankments for a first trial (Δh is assumed as 1.9

ft.). Entering figure 13 with

$$\frac{\Delta h}{\bar{y}} = \frac{1.90}{12.36} = 0.154$$

and

$$\bar{y} = 12.36,$$

$$\frac{L^*}{b} = 0.78$$

and

$$L^* = 0.78 \times 205 = 160 \text{ ft.}$$

The drop in channel gradient between sections 1 and centerline of roadway is then $S_0 L_{1\text{-}℄} = 0.00049(160 + 30) = 0.093$ ft. The water surface elevation at section 1 and along the upstream side of the roadway embankment will be:

$$\text{El. } 28.0 + S_0 L_{1\text{-}℄} + h^*_1 = 28.0 + 0.09 + 1.13$$
$$= \text{El. } 29.2 \text{ ft.}$$

Computation (*1g*). The first step in determining the water surface elevation at section 3 is to compute the backwater for the bridge in question without piers, as explained in chapter III:

$$h_b^* = K_b \frac{\alpha_2 V^2_{n2}}{2g} = 0.72 \times 1.40 \times 0.92 = 0.93 \text{ ft.}$$

Entering figure 12 with $M = 0.62$, the differential level ratio for the bridge (without piers) is:

$$D_b = \frac{h_b^*}{h_b^* + h_3^*} = 0.58,$$

so

$$h_3^* = h_b^* \left(\frac{1}{D_b} - 1\right) = 0.93 \left(\frac{1}{0.58} - 1\right) = 0.67 \text{ ft.} \quad (6)$$

The placing of piers in a waterway results in no change in the value of h^*_3 provided other conditions remain the same (sec. 3.3), so h^*_3 (with piers) also equals 0.67 ft. The water surface elevation on the downstream side of the roadway embankment will be essentially

$$\text{El. } 28.0 - 0.67 = 27.33 \text{ ft.}$$

The drop in water surface across the embankment is then

$$\Delta h = 29.22 - 27.33 = 1.89 \text{ ft.}$$

Since Δh was assumed as 1.90 ft., the computed water surface elevations above are satisfactory. Should the computed value of Δh be materially different from that assumed, another trial will be necessary.

Example 2

12.2 Example 2: Dual bridges. *Given.*—A second bridge, identical to that of example 1, is to be constructed parallel and 300 feet, between centerlines, downstream from the first bridge. The stream is essentially straight and of uniform cross section throughout this reach. Assuming no erosion at the constriction.

Find.—

(*a*) The backwater upstream from the first bridge for a flood of 19,500 c.f.s.
(*b*) The water surface elevation along upstream side of roadway embankment of the first bridge.
(*c*) The water surface elevation along downstream side of roadway embankment of second bridge (assuming elevation of roadway the same for both bridges).

Computation (*2a*). From example 1, $M = 0.62$, $h^*_1 = 1.13$ ft., $J = 0.071$, $S = 0.00049$, $b = 205$ ft., $A_{n2} = 2{,}534$ sq. ft., $A_{n1} = 5{,}664$ sq. ft., $h^*_3 = 0.67$ ft., $\bar{y} = 12.36$ ft. and $l = 40$ ft.

$$\text{The parameter } \frac{L_d}{l} = \frac{300 + 40}{40} = 8.50.$$

Entering figure 14 with L_d/l of 8.50, the backwater multiplication factor $\eta = 1.49$. The backwater upstream from the first bridge for the combination is then:

$$h^*_d = \eta h^*_1 = 1.49 \times 1.13 = 1.68 \text{ ft.}$$

Computation (*2b*). With normal stage of El. 28.0 ft. given at site of upstream bridge, it is necessary to determine drop in channel between centerline of first bridge and a new section 1. Assuming Δh in this case as 2.80,

$$\frac{\Delta h}{\bar{y}} = \frac{2.80}{12.36} = 0.226.$$

Entering figure 13 with the above value and $\bar{y} = 12.36$, $L^*/b = 0.92$ and $L^* = 0.92 \times 205 = 188$ ft. The fall in the channel between section 1 and centerline of first bridge is $S_0 L_{1\text{-}℄} = 0.00049(188 + 30) = 0.11$. The water surface elevation at section 1 and along the upstream side of the roadway embank-

ment of the first bridge will be:

$$\text{El. } 28.0 + S_0L_{1-\mathbb{C}} + h_d^* = 28.0 + 0.11 + 1.68$$
$$= \text{El. } 29.8 \text{ ft.}$$

Computation (*2c*). Entering figure 15 with L_d/l = 8.50, the differential level multiplication factor, $\xi = \psi h_{3B}/\psi h = 1.41$. For the single bridge in example 1:

$$\psi h = h^*_1 + h^*_3 = 1.13 + 0.67 = 1.80 \text{ ft.}$$

For the two bridges

$$\psi h_{3B} = \xi\psi h = 1.41 \times 1.80 = 2.54 \text{ ft.}$$
$$L_{1-3B} = 188 + 300 + 40 = 528 \text{ ft.}$$
$$S_0L_{1-3B} = 0.00049 \times 528 = 0.26 \text{ ft.}$$
$$\Delta h_{3B} = \psi h_{3B} + S_0L_{1-3B} = 2.54 + 0.26$$
$$= 2.80 \text{ ft.}$$

Checking back, the assumed value of Δh_{3B} was 2.80 feet so there is no need for repetition. The approximate water surface elevation on the downstream side of the second bridge will be

$$\text{El. } 29.79 - \Delta h_{3B} = 29.79 - 2.80 = 27.0 \text{ feet.}$$

Example 3

12.3 Example 3: Skewed crossing. Suppose it is decided to construct a skewed bridge, figure 37, on the site chosen in example 1, rather than the normal crossing. *Given.*—The quantities from example 1; Q = 19,500 c.f.s. for N.W.S. = 28.0, b = 205, S_0 = 0.00049, α_1 = 1.62, M = 0.62, A_4 = 5,664 sq. ft., A_1 = 6,384 sq. ft. and l = 40 ft.

Find.—

a. Length of skewed bridge required to produce essentially 1.1 feet of backwater as occurred in example 1.
b. The backwater for bridge length chosen.
c. The approximate water level at point A on section 1.

Computation (*3a*). The design discharge and normal stage at bridge site are known. The same procedure demonstrated in example 1 is followed, with exceptions as noted. First, the general direction of flow in the river at the bridge site for the design flood, without constriction, is determined. Next, the position and extent of roadway embankments and the type of abutment are superimposed on the stream as illustrated in figure 9. The angle of skew is measured, which is 40° in this case; then the bridge opening is projected upstream, normal to the direction of flow, to section 1.

Entering figure 11, which has been reproduced from reference 3, with $\phi = 40°$ and $M = 0.62$,

$$\frac{b_s \cos\phi}{b} = 0.935,$$

$$b_s \cos\phi = 0.935 \times 205 = 192 \text{ ft.,}$$

and

$$b_s = \frac{192}{0.766} = 250 \text{ ft. (approx.).}$$

Computation (*3b*). The actual backwater produced by the skewed bridge, 250 feet long, will be computed as a check on the above determination as well as to demonstrate the method of procedure. Conveyance and area are both plotted with respect to distance across flood plain at section 1 on figure 38. The information needed to construct the chart came directly from table 2 which was prepared in connection with the solution of example 1.

The first step is to locate the position of the skewed bridge on figure 38 and lay off the projected length, $b_s \cos\phi$, as shown. Then M is computed as follows:

$$M = \frac{k_s}{K_1} = \frac{600{,}000 - 70{,}000}{879{,}489} = 0.60.$$

From figure 6, the backwater coefficient, K_b = 0.77.

Note that an extra pier has been added and all are parallel to the direction of flow. The area obstructed by piers, A_p, is now 220 sq. ft. The projected area under the bridge referenced to normal water surface, from figure 38 is

$$A_{n2_s} = 3{,}400 - 1{,}000 = 2{,}400 \text{ sq. ft.}$$

and

$$J = \frac{A_p}{A_{n2}} = \frac{220}{2{,}400} = 0.092.$$

Consulting figure 7, the incremental backwater coefficient for piers

$$\Delta K_p = 0.18 \times 0.8 = 0.15.$$

Entering figure 10A with M = 0.60 and $\phi = 40°$,

$$\Delta K_s = -0.19.$$

The total backwater coefficient for the skewed

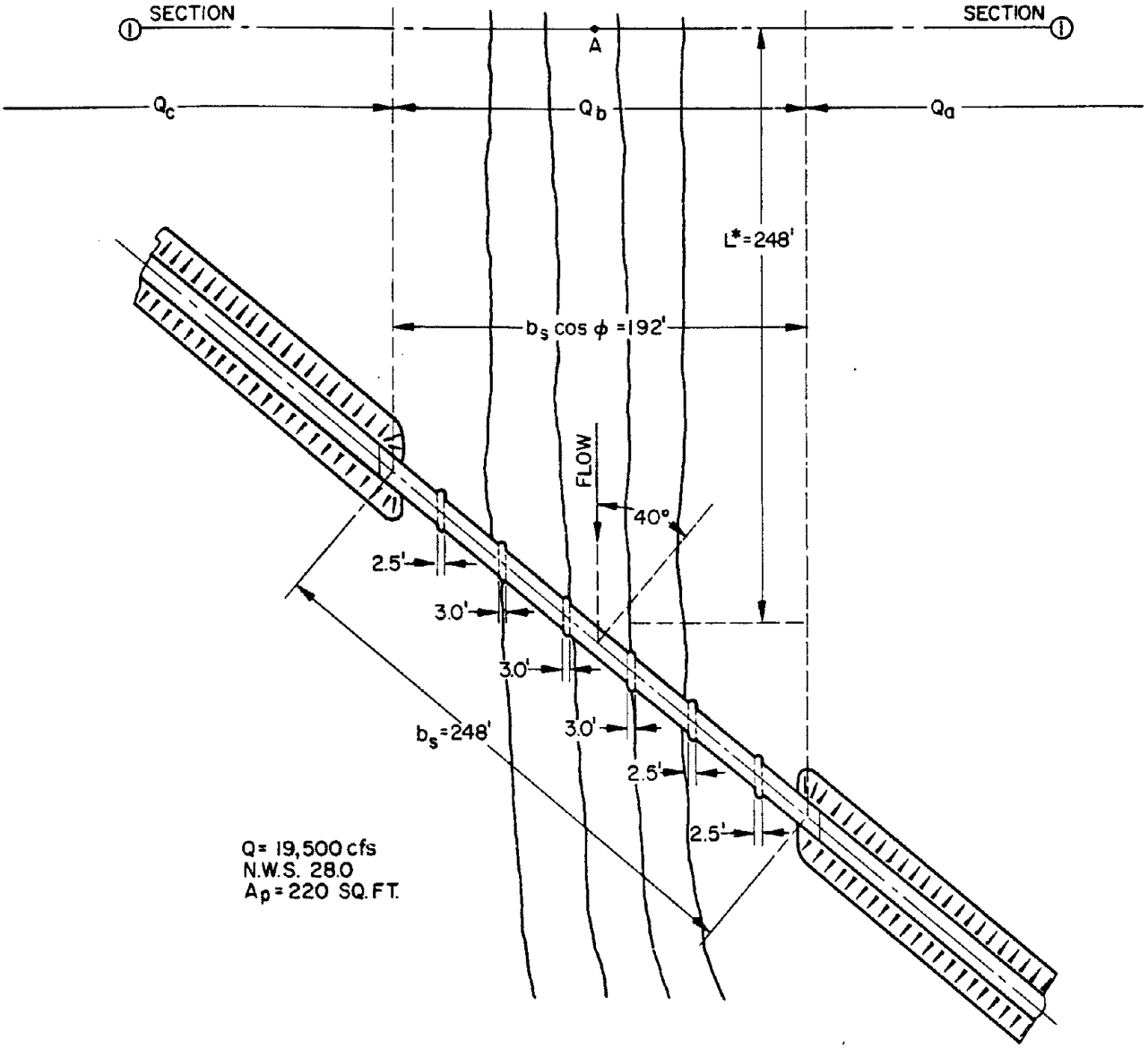

Figure 37.—Example 3: Plan for skewed crossing.

bridge is then

$$K^* = K_b + \Delta K_p + \Delta K_s = 0.77 + 0.15 - 0.19 = 0.73,$$

$$V_{n2} = \frac{Q}{A_{n2}} = \frac{19{,}500}{2{,}400} = 8.13 \text{ f.p.s.},$$

$V^2_{n2}/2g = 1.03$

and from figure 5,

$\alpha_2 = 1.40.$

Using expression (4a) (sec. 2.1) the approximate backwater will be

$$K^* \frac{\alpha_2 V^2_{n2}}{2g} = 0.73 \times 1.40 \times 1.03 = 1.05 \text{ ft.} \quad (4a)$$

Substituting values in the second half of expression (4),

$$\alpha_1 \left[\left(\frac{A_{n2}}{A_4} \right)^2 - \left(\frac{A_{n2}}{A_1} \right)^2 \right] \frac{V^2_{n2}}{2g}$$

$$= 1.62 \left[\left(\frac{2{,}400}{5{,}664} \right)^2 - \left(\frac{2{,}400}{6{,}384} \right)^2 \right] 1.03$$

$$= 1.62 \times 0.037 \times 1.03 = 0.062. \quad (4b)$$

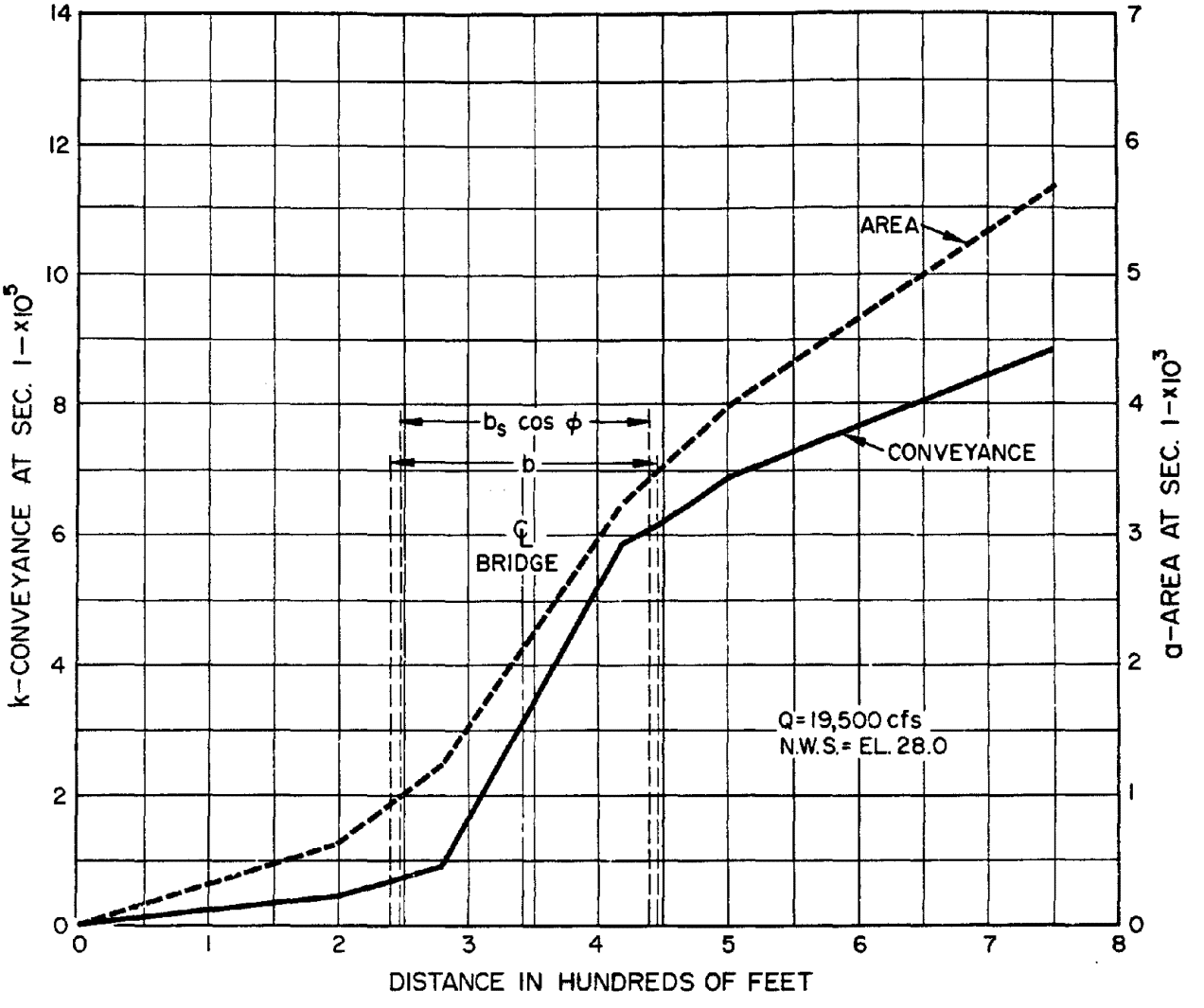

Figure 38.—Examples 1-3: Conveyance and area at section 1.

The total backwater for the skewed bridge is

$$h_1^* = 1.05 + 0.06 = 1.11 \text{ ft.} \qquad (4)$$

Computation (3c). For skewed crossings the distance to maximum backwater, L^*, has been chosen arbitrarily as equal to b_s, so:

$$S_0 L_{1\text{-}℄} = 0.00049(250 + 30) = 0.14 \text{ ft.}$$

The water level at point A is thus

$$\text{El. } 28.0 + h_1^* + S_0 L_{1\text{-}℄} = 28.0 + 1.11 + 0.14$$

$$= \text{El. } 29.2 \text{ ft.}$$

In the case of a skewed crossing, the water level along the upstream face of the two embankments will be different and neither need correspond to that at point A.

Example 4

12.4 Example 4: Eccentric crossing. The following example is intended to show in part how a computer program may be utilized to predict backwater at a given bridge site for a range of discharges and bridge lengths.

Given.—A representative cross section of the river and flood plain at the bridge site shown on figure 39 and the following information: The river is straight for a considerable distance both upstream and downstream from the site and has an average slope of 0.00024 foot per foot. One field measurement is available from the site for a discharge of 98,300 c.f.s. with river stage at elevation 653.0. The abutment on the right side of the river is a 2:1 spill-through type. The bed of the river and flood plain consist of sand and loam overlying a limestone base.

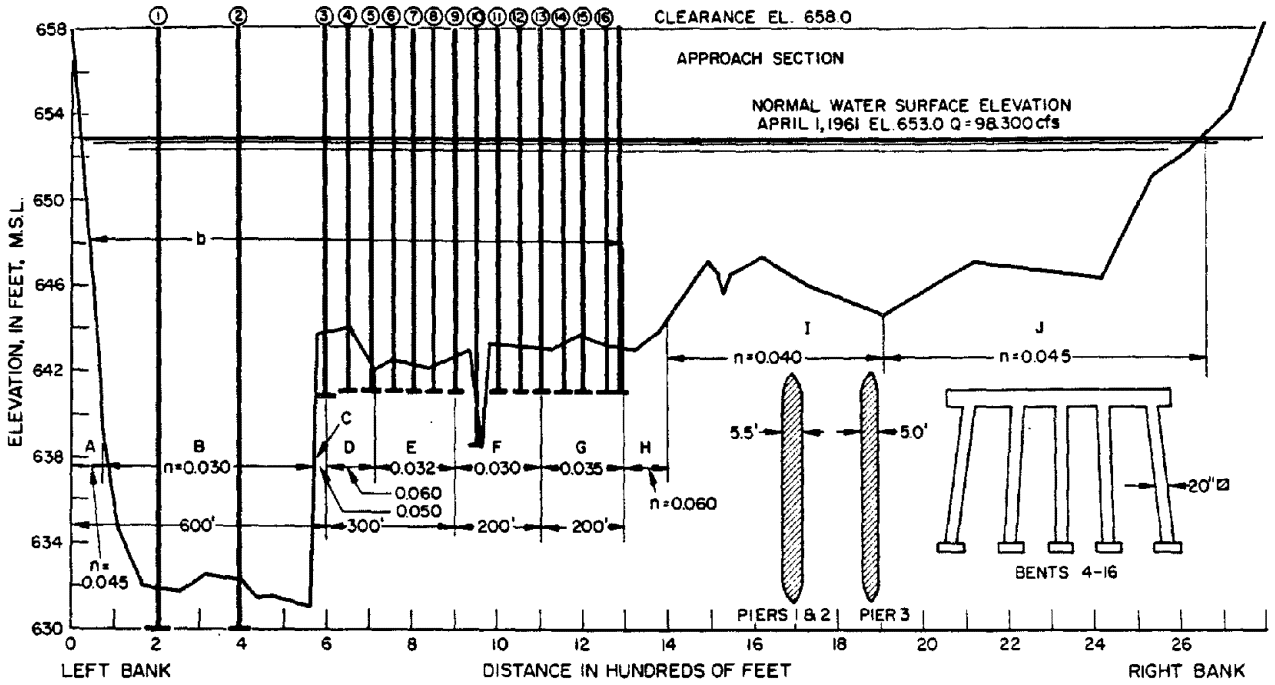

Figure 39.—Example 4: Cross section of eccentric river crossing.

Find.—Prepare a hydraulic chart showing bridge backwater related to discharge for bridge lengths of 600 to 1300 feet and for flood frequencies ranging from 10 to approximately 100 years, assuming no appreciable scour or erosion under the bridge.

Computation (*4a*). Tabulate distances, elevations and values of n for each break in grade throughout the cross section of figure 39 for the preparation of punch cards. The process is described in detail in the electronic computer program for bridge waterways (*13*). Next tabulate the maximum and minimum water surface elevations together with interval elevations to be investigated. For example, computations will be made for water levels from elevation 656 to 647 at intervals of 3 feet. Four bridge lengths will be investigated for each river stage; and the computer will tabulate bridge backwater for each case. The bridge lengths chosen are 600, 900, 1,100, and 1,300 feet. For this example, the bridge will consist of three spans of 200 feet each over the main channel, while the remainder will be divided into spans of 50 feet each supported on pile bents. A sample backwater computation for one bridge length and one river stage is shown as table 3.

The stage-discharge curve for the unobstructed river, which can be plotted by the computer, is re-

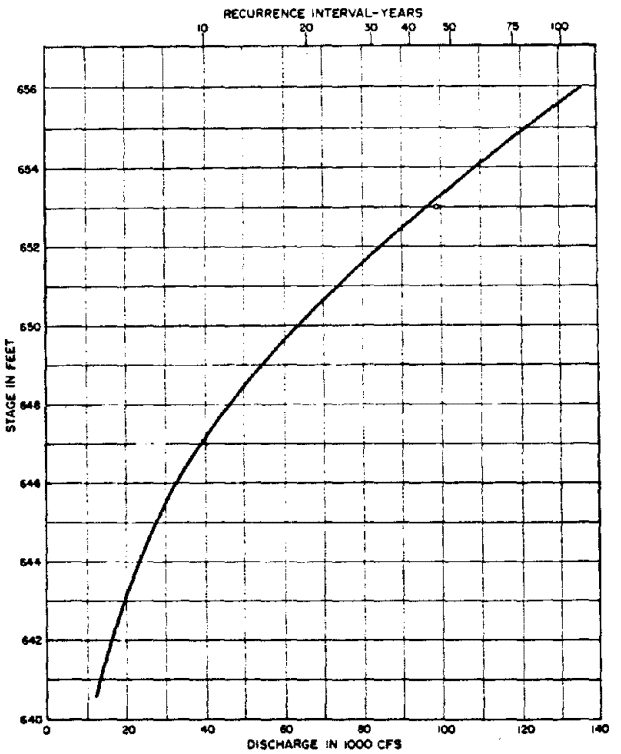

Figure 40.—Example 4: Stage-discharge curve for river at bridge site.

Table 3.—Computer sheet for one stage and one bridge length.

INPUT DATA

Stage elevation ..... 653 ft. Design discharge ..... 98,300 c.f.s.
Slope of river ..... 0.00024 f.p.f.

RESULTANT DATA

X beginning	X ending	Mannings n	Area	Wetted per	Hyd. radius	Conveyance	Discharge	Velocity
21.87	70.00	0.0450	264.69	49.37	5.36	26,777.31	415.04	1.57
70.00	565.00	.0300	10,115.00	495.80	20.40	3,741,236.90	57,989.18	5.73
565.00	600.00	.0500	420.00	39.46	10.64	60,400.46	936.20	2.23
600.00	715.00	.0600	1,096.00	115.04	9.53	122,000.11	1,891.00	1.73
715.00	900.00	.0320	1,986.00	185.01	10.73	448,822.39	6,956.74	3.51
900.00	1,100.00	.0300	2,063.00	201.11	10.26	482,467.58	7,478.25	3.62
1,100.00	1,300.00	.0350	1,929.50	200.01	9.65	371,275.27	5,754.77	2.99
1,300.00	1,400.00	.0600	984.00	101.08	9.74	111,120.76	1,722.38	1.75
1,400.00	1,910.00	.0400	3,527.50	510.13	6.91	475,673.89	9,372.95	2.09
1,910.00	2,660.00	.0450	3,976.50	750.12	5.30	399,249.75	6,188.37	1.56

Total area ..... 26,362.19 sq. ft. Total discharge ..... 96,704.88 c.f.s.
Total conveyance ..... 6,239,024.40 c.f.s.

BRIDGE INFORMATION INPUT

Bridge length 900
Left Abutment position ..... $XAB(1)$ ..... 0 $YAB(1)$ 658.00
$XAB(2)$ ..... 0 $YAB(2)$ 0
Right abutment position ..... $XAB(3)$ ..... 868.8 $YAB(3)$ 642.4
$XAB(4)$ ..... 900.0 $YAB(4)$ 642.80
Bridge opening at water surface 840
Base backwater curve used 1

CALCULATED INFORMATION

Portion of discharge left of opening (Q_a) ..... 0 c.f.s.
Portion of discharge thru opening (Q_b) ..... 68,199.62 c.f.s.
Portion of discharge right of opening (Q_c) ..... 28,504.73 c.f.s.
Area of piers below water surface ..... 368 sq. ft.
Alpha 1 ..... 1.69
Alpha 2 ..... 1.50
Total backwater coefficient 0.71
Bridge backwater opening below normal depth (A_{n2}) ..... 13,900 sq. ft.
Mean velocity thru bridge opening (V_{n2}) ..... 6.96 f.p.s.
Discharge ratio (M) 0.705
Backwater approximation No. 1 ..... 0.800
Final backwater approximation 0.830
Number of iterations to obtain final backwater 3

produced on figure 40. In this particular case one field measurement made at the bridge site on April 1, 1961, is available where a discharge of 98,300 c.f.s. was measured at a stage of 653.0 feet. Upon plotting this point on figure 40, it is found that it misses the curve obtained by the slope area method by only a slight margin so the stage-discharge curve is considered valid at least in the high stage range. This demonstrates the value of one or more reliable measurements at the proposed bridge site made during overbank flow. As pointed out earlier, once a bridge site is chosen every effort should be made to obtain a stage-discharge correlation at the site prior to construction of the bridge, even though it may result in only one or two points. Should a marked difference occur between the point or points obtained from measurement at the site and the stage-discharge curve determined by the slope area method, a reevaluation of the channel roughness is advisable.

Table 4.—Summary of computer calculations.

Q c.f.s.	Stage (feet)	Bridge length (feet)	K_1 $\times 10^3$	K_b $\times 10^3$	M	A_{n2} sq. ft.	V_{n2} f.p.s.	J	K^*	b ft.	α_1	α_2	h_1^* ft.	L^* ft.	S_0L^* ft.	$h_1^* + S_0L^*$	Water surface elevation at section 1 (feet)
(1)	(2)	(3)	(4)	(5)	(6)	(7)	(8)	(9)	(10)	(11)	(12)	(13)	(14)	(15)	(16)	(17)	(18)
134,500	656.0	600	8,690	4,850	0.560	12,500	10.75	0.0211	1.14	545	1.65	1.35	2.85	1,168	0.28	3.13	659.13
.....	.....	900	.....	5,600	.645	16,450	8.18	.0270	.88	845	....	1.40	1.33	1,416	.34	1.67	657.67
.....	.....	1,100	.....	6,270	.722	19,000	7.08	.0285	.70	1,045	....	1.45	.82	1,464	.35	1.17	657.17
.....	.....	1,300	.....	6,880	.792	21,600	6.23	.0293	.52	1,245	....	1.50	.49	1,420	.34	.83	656.83
96,704	653.0	600	6,239	3,830	.615	10,800	8.95	.0205	.94	540	1.69	1.45	1.75	1,025	.25	2.00	655.00
.....	.....	900	.....	4,400	.705	13,900	6.96	.0265	.71	840	....	1.50	.83	1,210	.29	1.12	654.12
.....	.....	1,100	.....	4,880	.785	15,050	6.06	.0277	.52	1,040	....	1.55	.48	1,210	.29	.77	653.77
.....	.....	1,300	.....	5,250	.844	17,850	5.42	.0289	.40	1,240	....	1.60	.30	1,215	.29	.59	653.59
63,800	650.0	600	4,106	2,920	.710	9,100	7.03	.0230	.65	525	1.74	1.55	.80	755	.18	.98	650.98
.....	.....	900	.....	3,240	.790	11,300	5.65	.0276	.48	825	....	1.60	.39	925	.22	.67	650.61
.....	.....	1,100	.....	3,520	.857	12,700	5.02	.0288	.35	1,025	....	1.65	.24	965	.23	.47	650.47
.....	.....	1,300	.....	3,720	.905	14,050	4.55	.0299	.28	1,225	....	1.70	.16	1,030	.25	.41	650.41
38,700	647.0	600	2,495	2,115	.848	7,400	5.24	.0238	.31	515	1.56	1.45	.23	455	.11	.34	647.34
.....	.....	900	.....	2,250	.903	8,700	4.45	.0278	.24	815	....	1.50	.2	620	.15	.27	647.27
.....	.....	1,100	.....	2,365	.950	7,550	4.05	.0288	.21	1,015	....	1.53	.09	730	.18	.27	647.27
.....	.....	1,300	.....	2,440	.978	10,250	3.78	.0302	.18	1,215	....	1.55	.07	850	.20	.27	647.27

A summary of the pertinent computerized data has been hand tabulated in table 4. From this table the following have been plotted:

Figure 41A.—Curves giving cumulative water areas across the unobstructed river, from left to right, for four stages of the river,

Figure 41B.—A curve showing the velocity head coefficient, α_1 with respect to discharge, and

Figure 42. —Curves showing cumulative conveyance across the unobstructed river, from left to right, for the same stages as in figure 41a.

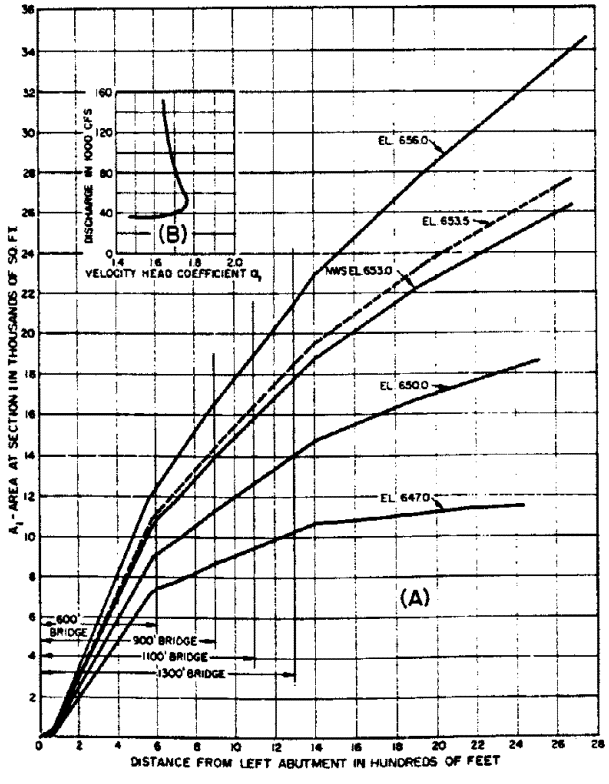

Figure 41.—Example 4: Area and velocity-head coefficient.

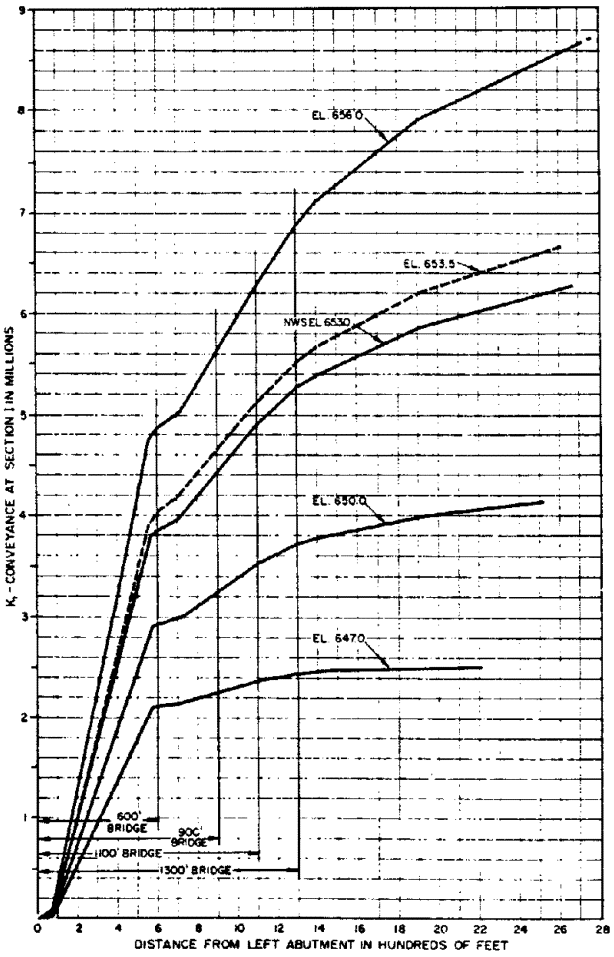

Figure 42.—Example 4: Conveyance at section 1.

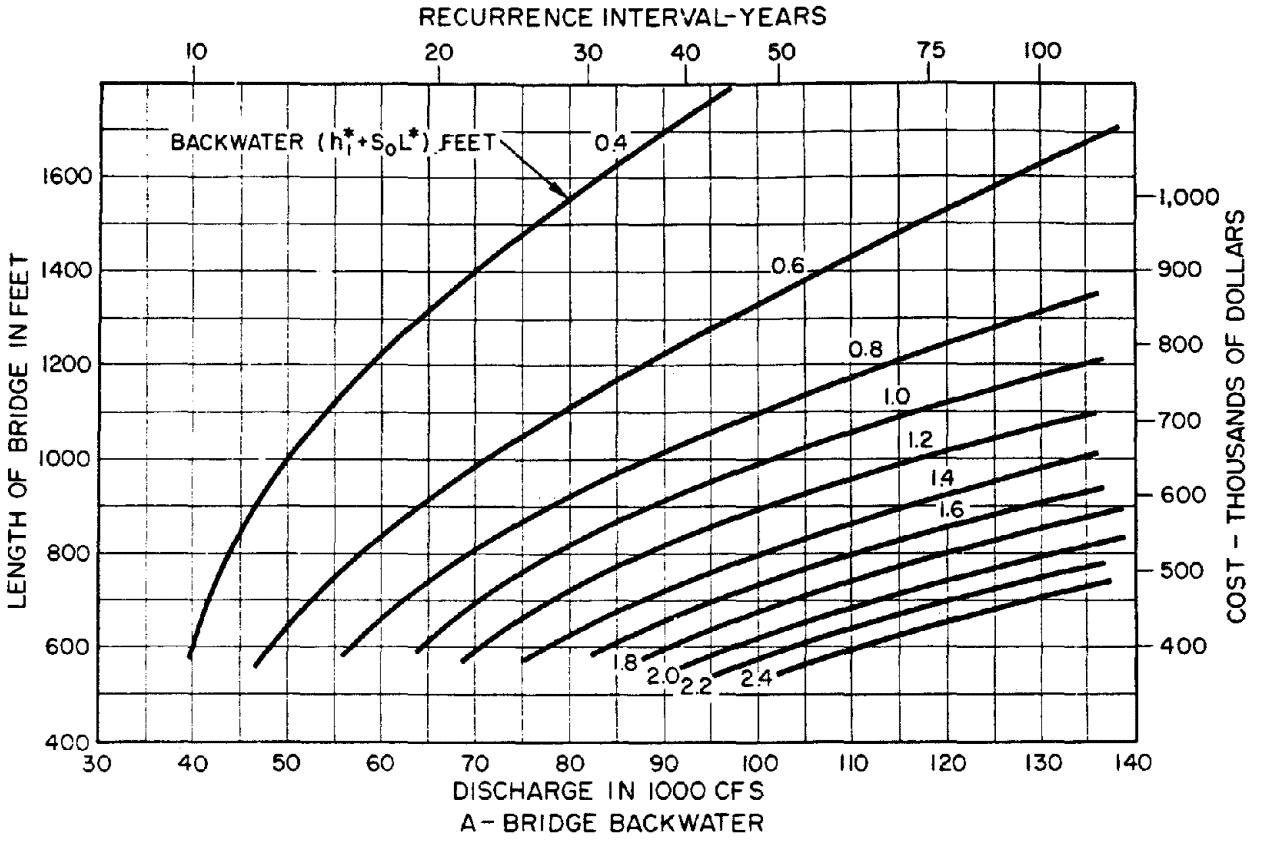

Figure 43.—Example 4: Composite backwater curves.

A composite hydraulic design chart, plotted from information contained in columns 1, 3, and 17 of table 4, is presented as Figure 43. The designer can read from this chart the length of bridge required to pass various flows with a given backwater. A scale of bridge cost can also be added on the right-hand side as shown. For convenience the recurrence interval is included at the top of the chart. To illustrate use of the resulting chart; suppose it is decided to design the bridge for a 50-year recurrence interval. If 1.5 feet of backwater can be tolerated, the bridge can be 780 feet long at a cost of $520,000. While if the backwater must be limited to 0.6 foot, the bridge length required would be 1,350 feet at a cost of $870,000 or $350,000 more. Thus an arbitrary decision to stay within a certain limiting rise of water surface can mean a relatively large increase in the length and cost of a bridge. A hydraulic design chart of this type is very useful for conveying information to others who are responsible for making decisions.

Another way of plotting the same information but expressing the backwater as water level along the upstream embankment, is demonstrated on figure 44. These curves were plotted from the values in columns 1, 3, and 18 of table 4. In this case the water surface at section 1, and along the upstream embankment, can be read for any discharge and bridge length.

Example 5

12.5 Example 5: Abnormal stage-discharge. The method of computation of backwater for other than a normal stage-discharge relation for a stream, will be illustrated by the following example.

Given.—The stream crossing used in example 1 (fig. 36) in which normal stage, roughness factors, discharge, and all dimensions remain the same except for an abnormal condition existing downstream which has increased the stage at the bridge site by 2 feet to elevation 30.0.

Find.—For this abnormal condition (assuming no scour):

a. The approximate backwater which will be produced by the bridge constriction and

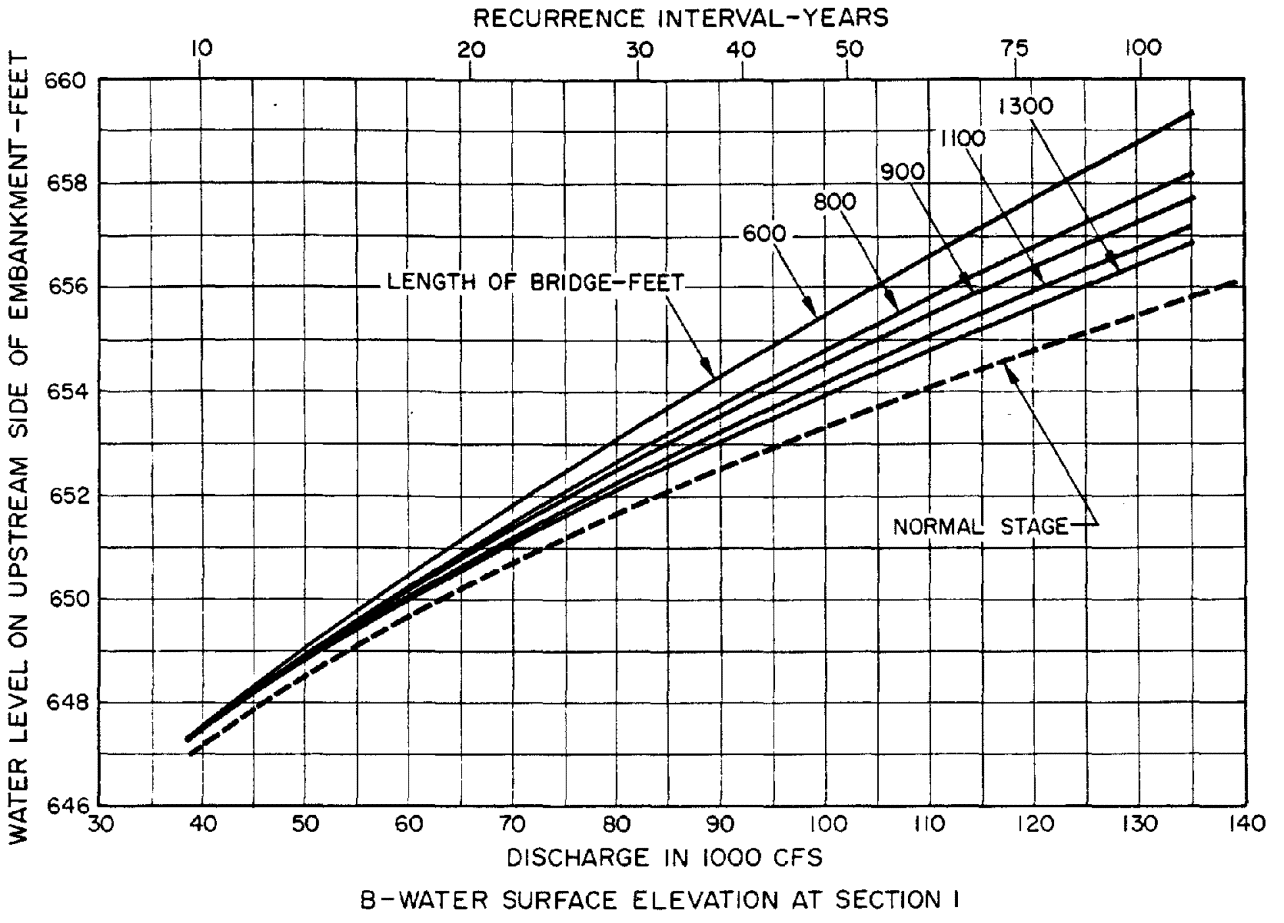

Figure 44.—Example 4: Water surface at section 1.

b. The approximate water surface differential which can be expected to occur across the embankments.

Computation (5a). The following values are tabulated from example 1 (sec. 12.1): Normal stage at bridge = 28.0 ft.;

Q = 19,500 c.f.s., b = 205 ft., M = 0.62,
A_{n2} = 2,534 ft.^{2}, V_{n2} = 7.70 f.p.s.,
A_p = 180 ft.^{2}, J = 0.071,
K^* = 0.83, K_b = 0.72, D_b = 0.58,
h_1^* = 1.13 ft., h_3^* = 0.67 ft.,
α_1 = 1.62, α_2 = 1.40 and
Δh = 1.89.

For a stage 2 feet higher than the normal of example 1, the pertinent quantities are (see fig. 16):

Stage at bridge = 30.0 feet,

Q = 19,500 c.f.s., b = 209 ft., M = 0.62
A_{2A} = 3,000 ft.^{2}, V_{2A} = 6.50 f.p.s.
A_p = 207 ft.^{2} and J = 0.069.

The backwater in this case will be computed according to expression (14) (sec. 6.3), using the same value of K^* as in example 1:

$$h_{1A}^* = K^* \alpha_2 \frac{V_{2A}^2}{2g} \qquad (14)$$

The approximate backwater for the abnormal stage of El. 30.0 will be

$$h_{1A}^* = 0.83 \times 1.40 \times \frac{(6.50)^2}{2g} = 0.76 \text{ ft.},$$

which is 67 percent of the value computed for normal stage in example 1.

Computation (5b). To obtain the differential level ratio it will first be necessary to recompute the backwater (excluding the effect of piers):

$$h_{bA}^* = K_b \alpha_2 \frac{V_{2A}^2}{2g} = 0.72 \times 1.40 \times \frac{(6.50)^2}{2g} = 0.66 \text{ ft.},$$

Table 5.—Example 6: Sample computations—properties of natural stream

[Q = 9,640 c.f.s.; Measured S_0 = 0.00208; Normal stage elevation = 23.9 ft.]

Subsection	Computation (6a)							Computation (6b)		
	n	$\frac{1.49}{n}$	a	p	$r=\frac{a}{p}$	$r^{2/3}$	k	q	v	qv^2
(1)	(2)	(3)	(4)	(5)	(6)	(7)	(8)	(9)	(10)	(11)
			sq. ft.	*ft.*	*ft.*			*c.f.s.*	*f.p.s.*	
Q_a 1	0.08	18.6	268	222	1.21	1.14	5,690	259	0.97	244
Q_a 2	.06	24.8	267	159	1.68	1.41	9,340	425	1.59	1,072
Q_a 3	.05	29.7	354	108	3.28	2.21	23,200	1,056	2.98	8,890
Q_b 4	.04	37.1	555	121	4.59	2.76	56,900	2,590	4.67	56,200
Q_c 5	.05	29.7	750	290	2.59	1.89	42,000	1,912	2.55	12,420
Q_c 6	.055	27.0	1,636	780	2.10	1.64	72,400	3,295	2.01	13,300
Q_c 7	.08	18.6	118	110	1.07	1.05	2,300	103	.87	78
Total			A_{n1}=3,948				K_1=211,830			Σqv^2=92,204

From figure 12,

$$D_b = \frac{h_{bA}^*}{h_{bA}^* + h_{3A}^*} = 0.58$$

so

$$h_{3A}^* = h_{bA}^* \left(\frac{1}{D_b} - 1\right) = 0.66 \left(\frac{1}{0.58} - 1\right) = 0.48. \tag{15}$$

The drop in channel gradient from section 1 to 3,

$$S_0 L_{1-3} = 0.00049(160 + 40) = 0.10 \text{ ft.},$$

then the approximate difference in water surface elevation across the embankment is

$$\Delta h_A = h_{1A}^* + S_0 L_{1-3} + h_{3A}^*$$
$$= 0.76 + 0.10 + 0.48 = 1.34 \text{ ft.}$$

or 71 percent of that for example 1. The above computations are approximate.

Example 6

12.6 Example 6: Backwater with scour. The following is an unusual but actual case involving scour under a bridge during flood for which reliable field data were obtained by the U.S. Geological Survey. This bridge site was chosen for an example because it effectively illustrates the marked effect scour can produce on backwater.

Given.—The cross section of the stream measured 170 feet upstream from the bridge, as shown in figure 45A; the cross section under the bridge showing normal water surface, initial bed surface, normal water area, and extent and area of scour during peak flow (fig. 45B); and the profile of the stream at the bridge (fig. 45C). The streambed consists of sand underlaid with gravel and shale. At the peak of flood, essentially all loose material was flushed out of the constriction. The pile bents and abutments are embedded in concrete foundations which are keyed into the hardpan, as shown in figure 45B. The average slope of the stream in this reach is 11 feet to the mile, S_0 = 0.00208, and the discharge, measured by current meter during the peak of the flood, was 9,640 c.f.s. No flow occurred over the road.

Find.—The drop across the embankment and the water surface elevations expected along the upstream and downstream sides of the embankments (with scour) for the peak discharge of 9,640 c.f.s.

The procedure will involve the following steps:

a. Determine the backwater, h_1^*, which would exist without scour.

b. Compute the value of the backwater, h_{1s}^* (with scour).

c. Compute the value of h_{3s}^* (with scour).

d. Compute water surface elevations on upstream and downstream sides of embankment and Δh_s, the drop in water surface across the embankments (with scour).

Computation (6a). Normal stage is determined by trial. The river cross section, taken 170 feet upstream from the bridge, is representative of the stream for several miles upstream and downstream. This is divided into subsections as shown in figure 45A and

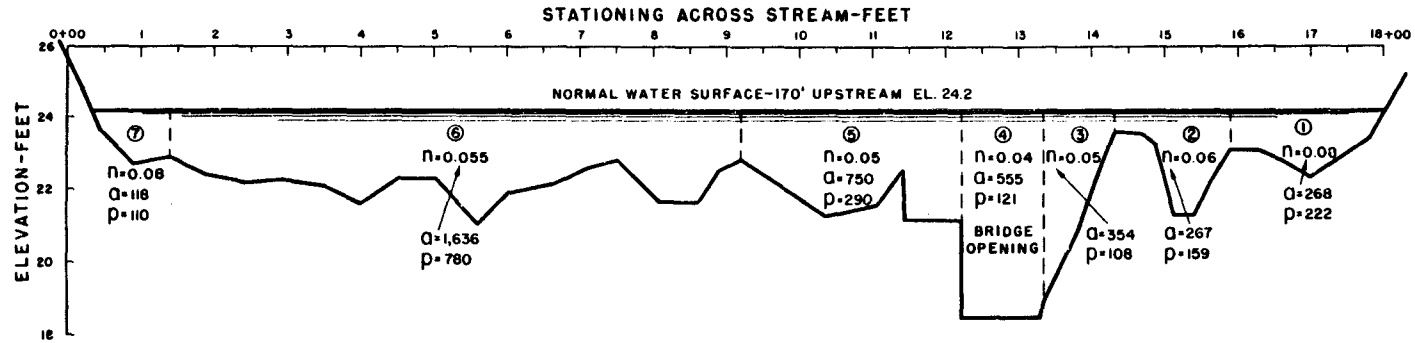

A-CROSS SECTION OF STREAM 170 FEET UPSTREAM FROM BRIDGE (LOOKING UPSTREAM)

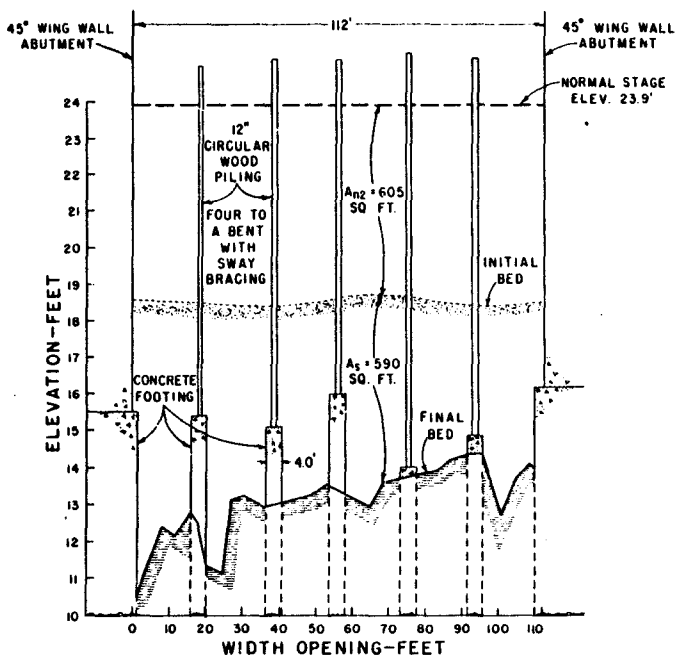

B-CROSS SECTION UNDER BRIDGE (LOOKING UPSTREAM)

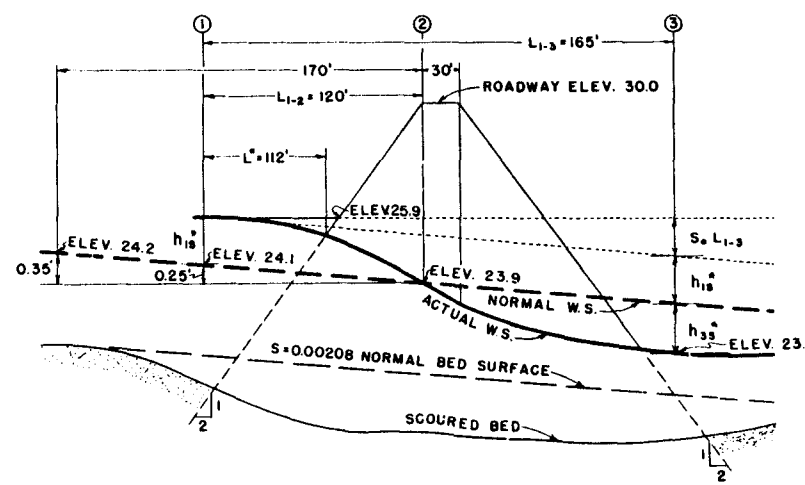

C-PROFILE AT BRIDGE

Figure 45.--Example 6: Backwater with scour.

an appropriate value of n is assigned to each subsection. Assuming normal stage as El. 24.2 at the approach cross section (fig. 45C) for a discharge of 9,640 c.f.s., areas, wetted perimeters, and roughness factors are recorded and conveyance values are computed (col. 1–8, table 5). Columns 9, 10, and 11 are next completed and the velocity head correction coefficient and the value of M determined:

$$\alpha_1 = \frac{\Sigma q v^2}{Q V_1^2} = \frac{92{,}204}{9{,}640\left(\frac{9{,}640}{3{,}948}\right)^2} = 1.61; \text{ and}$$

$$M = \frac{Q_b}{Q} = \frac{2{,}590}{9{,}640} = 0.27.$$

Figure 45B shows the initial streambed under the bridge at approximately elevation 18.5 feet, and figure 45C indicates that normal stage at the bridge is elevation 23.9 feet and $\bar{y} = 23.9 - 18.5 = 5.4$ feet.

Assuming a pier width of 1.67 feet, to allow for sway bracing and trash:

$$A_p = 45 \text{ sq. ft.}; A_{n2} = 605 \text{ sq. ft.}; \text{ and}$$

$$J = \frac{A_p}{A_{n2}} = \frac{45}{605} = 0.074.$$

The velocity under the bridge, without scour, would be

$$V_{n2} = \frac{Q}{A_{n2}} = \frac{9{,}640}{605} = 15.95 \text{ f.p.s.}$$

Checking for the type of flow, the Froude number, without scour, would be

$$F_n = \frac{V_{n2}}{(g\bar{y})^{1/2}} = \frac{15.95}{(32.2 \times 5.4)^{1/2}} = 1.21,$$

which indicates that the flow would be supercritical under the bridge. The curves on figure 6 are for subcritical flow. The best that can be done for this case is to refer to the type II flow on figure 34. Since incremental coefficients for piers are not available for this type of flow, compensation for this effect will be made by using the net water area under the bridge rather than the gross area;

$$q = \frac{Q}{b_N} = \frac{9{,}640}{103.5} = 93 \text{ c.f.s./ft.},$$

$$Y_{2c} = \left(\frac{q^2}{g}\right)^{1/3} = \left[\frac{(93)^2}{32.2}\right]^{1/3} = 269^{1/3} = 6.46 \text{ ft.},$$

$$V_{2c} = \frac{q}{Y_{2c}} = \frac{93}{6.46} = 14.40 \text{ f.p.s., and}$$

$$V^2_{2c}/2g = 3.22 \text{ ft.}$$

From figure 5, $\alpha_2 = 1.18$. Approximate values for

$$A_1 = 3{,}948 + 5.0 \times 2{,}200 = 14{,}948 \text{ ft.}^2$$

$$V_1 = \frac{Q}{A_1} = \frac{9{,}640}{14{,}948} = 0.645 \text{ f.p.s. and}$$

$$V_1^2/2g = 0.0065.$$

Entering figure 34 with $M = 0.27$, the backwater coefficient for type II flow, $C_b = 0.22$. Substituting values in the expression,

$$h_1^* = \alpha_2 V^2_{2c}/2g(C_b + 1) + y_{2c} - \bar{y} - \alpha_1 V_1^2/2g \tag{26}$$

the backwater without scour would be,

$$h_1^* = 1.18 \times 3.22(0.22 + 1) + 6.46 - 5.40 - 1.61 \times 0.0065 = 5.69 \text{ ft.}$$

Computation (6b). From figure 45B, the gross area of scour under the bridge (including piers), $A_s = 590$ sq. ft. Since the piers are not of uniform width throughout, it is advisable to use net areas in computing the ratio A_s/A_{n2}. Thus:

$$\frac{A_s}{A_{n2}} \text{ (net)} = \frac{590 - 60}{605 - 45} = \frac{530}{560} = 0.95.$$

Entering figure 20 with above value,

$$C = \frac{h_{1s}^*}{h_1^*} = 0.32.$$

The backwater with scour is then reduced to

$$h_{1s}^* = 0.32 \times 5.69 = 1.82 \text{ ft.} \tag{17}$$

Computation (6c). From figure 12 with $M = 0.27$:

$$D_b = \frac{h_b^*}{h_b^* + h_3^*} = 0.86, \text{ or}$$

$$h_3^* = h_b^*\left(\frac{1}{D_b} - 1\right) = h_b^*\left(\frac{1}{0.86} - 1\right) = 0.163\, h_b^* \tag{6}$$

With scour,

$$h_{3s}^* = 0.163 \times 1.82 = 0.30 \text{ ft. (approx.)}$$

Computation (6d). Assuming maximum backwater occurs one bridge length upstream, the water surface

at section 1 and along the upstream side of the embankment is

$$\text{El. } 24.1 + h_{1s}^* = 24.1 + 1.82 = \text{El. } 25.9 \text{ ft.}$$

The drop in level across the embankment is

$$\Delta h_s = h_{1s}^* + h_{3s}^* + S_0 L_{1-3}$$

$$= 1.82 + 0.30 + 0.34 = 2.46 \text{ ft.}$$

so the water surface along the downstream side of the embankment is

$$\text{El. } 25.9 - 2.46 = 23.4 \text{ ft.}$$

The following tabulation shows a comparison of the computed values with those determined by measurement in the field:

	Measured	*Computed*
Δh, ft.	2.6	2.46
Elevation upstream	25.8	25.9
Elevation downstream	23.2	23.4

The agreement between measured and computed values is beyond expectations. While one example is not enough to prove the case, it does support the reasonableness of the conclusions drawn from the model experiments in the laboratory. The calculations are rough and some portions of the procedure could be subject to question. However, this example, an extreme case, serves well to illustrate how scour affects backwater.

Example 7

12.7 Example 7: Upstream bridge girder in the flow. When computing general backwater curves for a river, as is common practice for the Corps of Engineers, it is necessary to know within reasonable limits the amount of ponding which occurs at bridges which constrict the flow during floods. The bridge backwater, the downstream water surface, and the drop in level across bridge embankments, where clearance of superstructure is not a problem, have been treated in the preceeding examples. Examples 7 and 8 pertain to bridges in which the flow is in contact with the superstructure.

Given.—Plan and cross section of the bridge of example 1 (fig. 36) and the centerline profile shown on figure 46A: For this example, suppose that the superstructure is lowered so the bottom of the upstream girder is at elevation 28.0 or at the normal water surface.

Find.—

(*a*) The approximate water surface along the upstream face of the embankment.
(*b*) The approximate water surface along the downstream face of the embankment.
(*c*) The drop in water level across the bridge embankment without scour.

Computation (*7a*). The pertinent quantities from example 1 are:

$Q = 19{,}500$ c.f.s., $S_0 = 0.00049$, $\bar{Y} = 12.35$ ft.
$b = 205$ ft., $W_p = 14$ ft., $A_{n1} = 5{,}664$ ft.^{2}
$V_{n1} = 19{,}500/5{,}664 = 3.45$ f.p.s., $\alpha_1 = 1.62$ and $\alpha_1 V^2_{n1}/2g = 0.30$ ft.

The discharge expression for case I, chapter VIII is:

$$Q = C_d b_N Z \left[2g\left(Y_u - \frac{Z}{2} + \alpha_1 \frac{V_1^2}{2g}\right)\right]^{1/2} \text{ or } \quad (20)$$

$$Y_u = \frac{Q^2}{2g b_N^2 Z^2 C_d^2} + \frac{Z}{2} - \frac{\alpha_1 V_1^2}{2g}$$

As a first trial, assume $y_u/Z = 1.12$; enter the upper curve on figure 21 with this value, and read $C_d = 0.380$.

Substituting in equation 20,

$$Y_u = \frac{(19{,}500)^2}{64.4(191 \times 12.35)^2(0.380)^2} + \frac{12.35}{2} - 0.30$$

$$= \frac{1.061}{(0.38)^2} + 6.18 - 0.30$$

$$= 7.37 + 6.18 - 0.30 = 13.25 \text{ ft.}$$

In figure 21 $h_u^* = y_u - \bar{y}$

$$h_u^* = 13.25 - 12.35 = 0.9 \text{ ft.}$$

Then $A_1 = 5{,}664 + 770(0.9) = 6{,}357$ ft.^{2}

$$V_1 = 19{,}500/6{,}357 = 3.07 \text{ f.p.s.}$$

$V_1^2/2g = 0.146$ and

$\alpha_1 V_1^2/2g = 1.62 \times 0.146 = 0.236.$

The corrected value of

$$y_u = 7.37 + 6.18 - 0.236 = 13.31 \text{ ft. and}$$

$$y_u/Z = 13.31/12.35 = 1.078$$

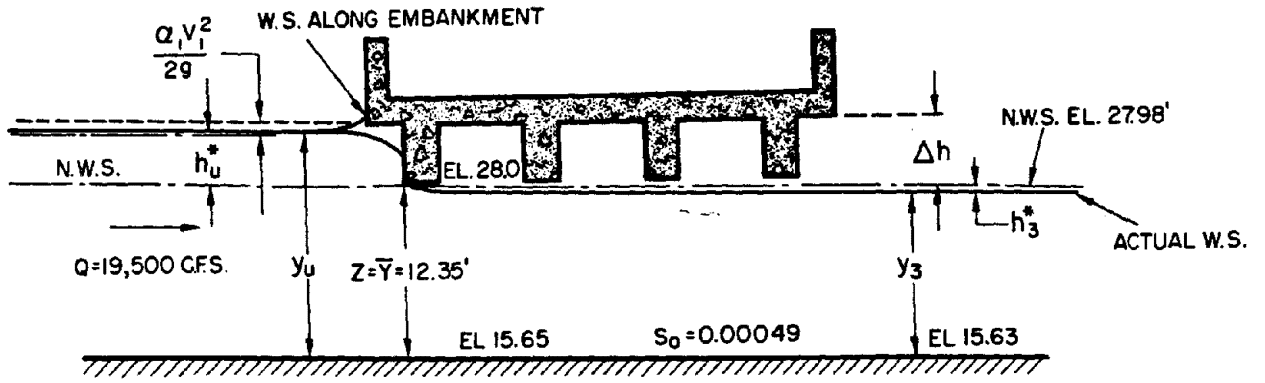

A-EXAMPLE 7 (CASE I)

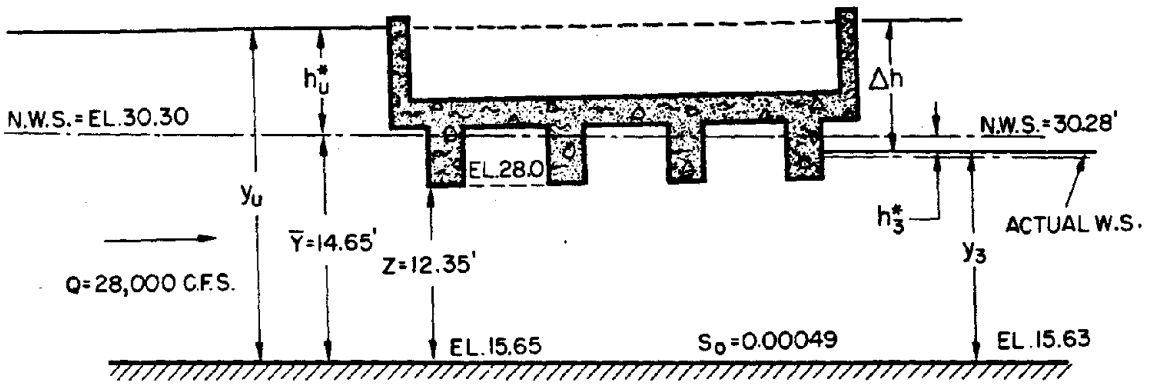

B-EXAMPLE 8 (CASE II)

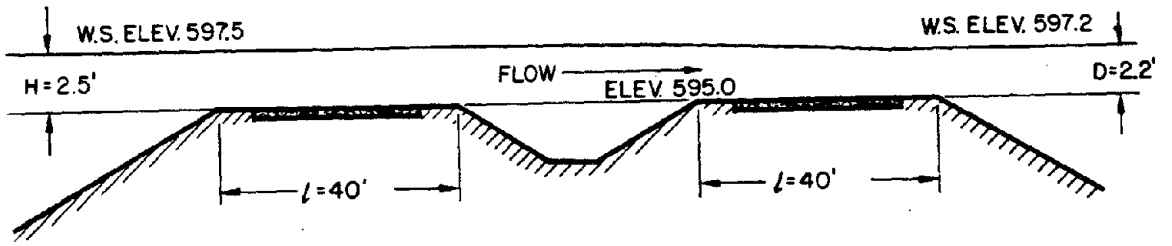

C-EXAMPLE 9

Figure 46.—Examples 7, 8, and 9: Bridge backwater under less common conditions.

which does not agree with the assumed value (1.12). Next assume $y_u/Z = 1.10$, then $C_d = 0.370$ (fig. 21).

$$y_u = 1.061/(0.37)^2 + 6.18 - 0.24$$
$$= 7.75 + 6.18 - 0.24 = 13.69 \text{ ft.}$$
$$h_u^* = 13.69 - 12.35 = 1.34 \text{ ft. and}$$
$$A_1 = 5{,}664 + 1.34 \times 770 = 6{,}696 \text{ ft.}^2$$
$$V_1 = 19{,}500/6{,}696 = 2.91 \text{ f.p.s.}$$

$V_1^2/2g = 0.132$ and
$\alpha_1 V_1^2/2g = 1.62 \times 0.131 = 0.212$

The corrected value of

$$y_u = 7.75 + 6.18 - 0.212 = 13.72 \text{ ft.}$$
$$h_u^* = 13.72 - 12.35 = 1.37 \text{ ft. and}$$
$$y_u/Z = 13.72/12.35 = 1.11$$

which is sufficiently close to the assumed value (1.10).

The water surface on the upstream side of the embankment will be

$$\text{El. } 15.65 + Y_u + \frac{\alpha_1 V_1^2}{2g} = 15.65 + 13.72 + 0.21$$

$$= \text{El. } 29.6 \text{ ft.}$$

Computation (*7b*). Entering the lower curve on figure 21 with $C_d = 0.37$ and reading downward, $y_u/y_3 = 1.125$ and $y_3 = 13.72/1.125 = 12.19$ ft.

The water surface along the downstream side of the embankment is: El. 15.63 + 12.19 = El. 27.8 ft. or approximately 0.2 foot below normal stage.

Computation (*7c*). The water surface differential across the bridge embankment Δh = El. 29.6 − El. 27.8 = 1.8 feet.

The above computation is quite sensative since the example falls within the transition zone (fig. 21) where the curves are steep.

Example 8

12.8 Example 8: Superstructure partially inundated. *Given.*—The same stream and bridge arrangement as for example 7 except the discharge is increased to 28,000 c.f.s. A profile on the centerline of channel is shown on figure 46B. Normal water surface is now at elevation 30.30 at the upstream bridge girder.

The pertinent data (fig. 46B) are Q = 28,000 c.f.s., $\bar{Y}$ = 14.65 ft., Z = 12.35 ft., b_N = 191 ft., and

$$A_{2N} = 2{,}358 \text{ ft.}^2$$

Find.—

(*a*) The drop in level across the bridge embankment.

(*b*) Water surface elevation on the upstream side of the embankment.

(*c*) Water surface elevation on the downstream side of the embankment, assuming no appreciable scour under the bridge.

Computation (*8a*). The equation applicable in this case is:

$$Q = C_d b_N Z (2g\Delta h)^{1/2} \text{ or} \qquad (21)$$

$$\Delta h = \frac{Q^2}{2g b_N^2 Z^2 C_d^2}$$

where the discharge coefficient (C_d) is constant at a value of 0.80. Substituting values in the latter expression,

$$\Delta h = \frac{(28{,}000)^2}{64.4(191 \times 12.35)^2(0.80)^2}$$

$$= \frac{784{,}000{,}000}{358{,}332{,}741 \times 0.64} = 3.42 \text{ ft.}$$

(*Computation 8b*). Entering figure 22B with $\Delta h/\bar{y} = 3.42/14.65 = 0.233$, $y_u/\bar{y} = 1.13$ so,

$$y_u = 1.13 \times 14.65 = 16.55 \text{ ft.}$$

The water surface elevation on the upstream side of the embankment should be:

$$\text{El. } 15.65 + 16.55 = 32.20 \text{ feet.}$$

The bridge backwater in this case will be,

$$\text{El. } 32.20 - \text{El. } 30.30 = 1.90 \text{ feet.}$$

Computation (*8c*). The water surface elevation on the downstream side of the embankment will be:

El. 32.20 − Δh = 32.20 − 3.42 = El. 28.8 feet. or 1.5 feet below normal stage.

An interesting point is that increasing the discharge from 19,500 c.f.s. to 28,000 c.f.s. changed the backwater, h_u*, from 1.37 to 1.90 feet while Δh changed from 1.8 to 3.42 feet. In other words, the hydraulic capacity of the structure is markedly increased with orifice flow.

Example 9

12.9 Example 9: Flow over roadway embankment. This example is presented to demonstrate computation of flow over a roadway embankment serving as a weir or a by-pass during a superflood.

Given.—The roadway profile across the valley shown on figure 25, and a cross section of the roadway, figure 46C.

Find.—The flow over the roadway embankment with upstream water surface at elevation 597.5 and downstream water surface at elevation 597.2.

From figure 25, the effective length of weir is from station 1470 + 00 to 1408 + 50 or 6,150 feet. From figure 46C, the effective width of the divided highway will be considered as 2*l* or 80 feet.

The value of the abscissa for entering curve B (fig. 24) will be:

$$H/l = \frac{2.5}{80} = 0.031.$$

Since curve B is not applicable for such a low value of H/l, curve A should be used. Entering curve A with $H = 2.5$ feet, the free flow coefficient of discharge is about 3.05.

From figure 46C, the percent submergence is:

$$\frac{D}{H} = \frac{2.2}{2.5} \times 100 = 88 \text{ percent.}$$

Entering curve C (fig. 24) with the above value, the submergence factor $C_s/C_f = 0.92$.

Substituting the above information in the weir equation

$$Q = C_f L H^{3/2} C_s/C_f \qquad (23)$$

gives the flow over the roadway as

$Q = 3.05 \times 6150 \times (2.5)^{3/2} \times 0.92 = 68{,}400$ c.f.s. (approximately).

Of interest here is the fact that 88 percent submergence decreased the free flow discharge by only 8 percent.

To prepare a chart such as that shown on figure 26 for another stream which has both flow under the bridge and over the roadway, first plot the stage-discharge curve for the river and note the overflow embankment elevation.

It is next necessary to compute the backwater level, water surface downstream, and flow over roadway for successive stages of the river. Overtopping of the roadway reduces the overall resistance to flow, so the drop in water surface across the embankment usually decreases with increase in discharge. Thus as the stage of the river rises, flow over the roadway increases while flow under the bridge often decreases due to the reduction in differential across the embankment. (See the discussion in section 8.6.)

Example 10

12.10 Design of spur dike. *Given.*—The bridge of example 4. Because of the extreme eccentricity of the crossing, it appears that a spur dike might be needed on the flood plain end of the bridge (fig. 39). Suppose the bridge chosen for the crossing is 1,100 feet long, the design discharge is 102,500 c.f.s. (for 50-year flood), the design water surface is elevation 653.5 feet, and the right abutment is a spillthrough type with 2:1 side slopes.

Find.—

(*a*) If a spur dike is needed.

(*b*) If needed, determine the length and compute the centerline coordinates for laying out an elliptical dike with axes ratio of 2.5:1.

Computation (*7a*). Most of the necessary computations were performed in the solution of example 4. The discharge on the flood plain, Q_f, is obtained from the conveyance curves of figure 42 for stage at El. 653.5 as follows:

$$Q_f = \frac{K_{(25+50)} - K_{(10+80)}}{K_1} Q$$

$$= \frac{6{,}660{,}000 - 5{,}080{,}000}{6{,}660{,}000} 102{,}500 = 24{,}313 \text{ c.f.s.}$$

The discharge in the first 100 feet of river channel next to the right abutment is:

$$Q_{100} = \frac{K_{(10+80)} - K_{(9+80)}}{K_1} Q$$

$$= \frac{5{,}080{,}000 - 4{,}800{,}000}{6{,}660{,}000} 102{,}500 = 4{,}309 \text{ c.f.s.}$$

The spur dike discharge ratio is

$$\frac{Q_f}{Q_{100}} = \frac{24{,}313}{4{,}309} = 5.64$$

The velocity used in this application is the average velocity under the bridge, without correction factor, or

$$V_{n2} = \frac{Q}{A_{n2}} = \frac{102{,}500}{16{,}200} = 6.33 \text{ f.p.s.,}$$

where A_{n2} is obtained directly from figure 41 at Sta. 10 + 80.

Entering figure 30 with $Q_f/Q_{100} = 5.64$ and $V_{n2} = 6.33$ f.p.s., the recommended length of spur dike is $L_s = 260$ feet.

Computation (*7b*). The equation (sec. 9.3) for a 2.5:1 ellipse is

$$\frac{x^2}{L_s^2} + \frac{y^2}{(0.4L_s)^2} = 1 \qquad (24)$$

For a dike length of 260 feet expression (24) becomes:

$$\frac{x^2}{(260)^2} + \frac{y^2}{(104)^2} = 1$$

The coordinates for establishing the centerline of the

Table 6.—Computer sheet (example 11).

INPUT DATA

Stage elevation ..... 92.50 ft. Design discharge ..... 4,325 c.f.s.
Slope of river ..... 0.0380 f.p.f.

RESULTANT DATA

X beginning	X ending	Mannings n	Area	Wetted per	Hyd. radius	Conveyance	Discharge	Velocity
139.00	264.80	.0350	109.93	126.15	.8713	4,258.01	830.03	7.55
264.80	275.00	.0351	13.26	10.20	1.2989	668.33	130.28	9.82
275.00	296.63	.0350	28.84	21.95	1.3138	1,468.87	286.33	9.92
354.68	359.50	.0351	9.15	5.90	1.5507	519.33	101.23	11.05
359.50	413.00	.0350	91.35	53.62	1.7035	5,532.26	1,078.43	11.80
505.76	525.00	.0350	9.61	19.25	.4993	256.93	50.08	5.20
525.00	534.60	.0351	10.08	9.60	1.0497	440.79	85.92	8.52
534.60	645.24	.0350	164.33	111.39	1.4752	9,042.07	1,762.62	10.72

Total area ..... 436.57 sq. ft. Total discharge ..... 4,324.96 c.f.s.
Total conveyance ..... 22,186.62 c.f.s.

BRIDGE INFORMATION INPUT

Bridge length (feet) 72.30
Left abutment position ..... $XAB(1)$ ..... 354.7 $YAB(1)$ 93.5
$XAB(2)$ ..... 0 $YAB(2)$ 0
Right abutment position ..... $XAB(3)$ ..... 0 $YAB(3)$ 0
$XAB(4)$ ..... 427 $YAB(4)$ 92.5
Bridge opening at water surface 70.15
Base backwater curve used 3

CALCULATED INFORMATION

Portion of discharge left of opening (Q_a) ..... 1,246.65 c.f.s.
Portion of discharge thru opening (Q_b) ..... 1,179.67 c.f.s.
Portion of discharge right of opening (Q_c) ..... 1,898.63 c.f.s.
Area of piers below water surface ..... 2.60 sq. ft.
Alpha 1 ..... 2.0
Alpha 2 ..... 1.25
Total backwater coefficient 1.564
Bridge waterway opening below normal depth (A_{n2}) ..... 100.50 sq. ft.
Mean velocity thru bridge opening (V_{n2}) ..... 43.03 f.p.s.
Discharge ratio (M) 0.272
Backwater approximation No. 1 ..... 45.034 ft.
Final backwater approximation ..... 46.691 ft.
Number of iterations to obtain final backwater 3

spur dike are tabulated in the following table. (See sketch on figure 30 for location of x and y axes.)

x	y	x	y	x	y
0	104.00	120	92.26	220	55.43
20	103.69	140	87.64	230	48.50
40	102.76	160	81.98	240	40.00
60	101.19	180	75.05	250	28.57
80	98.95	200	66.45	255	20.3
100	96.00	210	61.32	260	0

The dike usually constructed, where climate will support vegetation and velocities are not in excess of those the vegetative cover will withstand, is shown on figure 33 and described in section 9.4 Where velocities are excessive for the cover or in areas where the climate will not support a vegetative cover, it may be advisable to riprap the entire front face of the spur dike. In determining the maximum size of stone for the nose of the dike, velocities of from two to three times V_{n2} are suggested.

Example 11

12.11 Bridge backwater with supercritical flow. *Given.*—The tabulation, table 6, a computer sheet for the computation of bridge backwater at a proposed bridge in New Mexico on a stream with

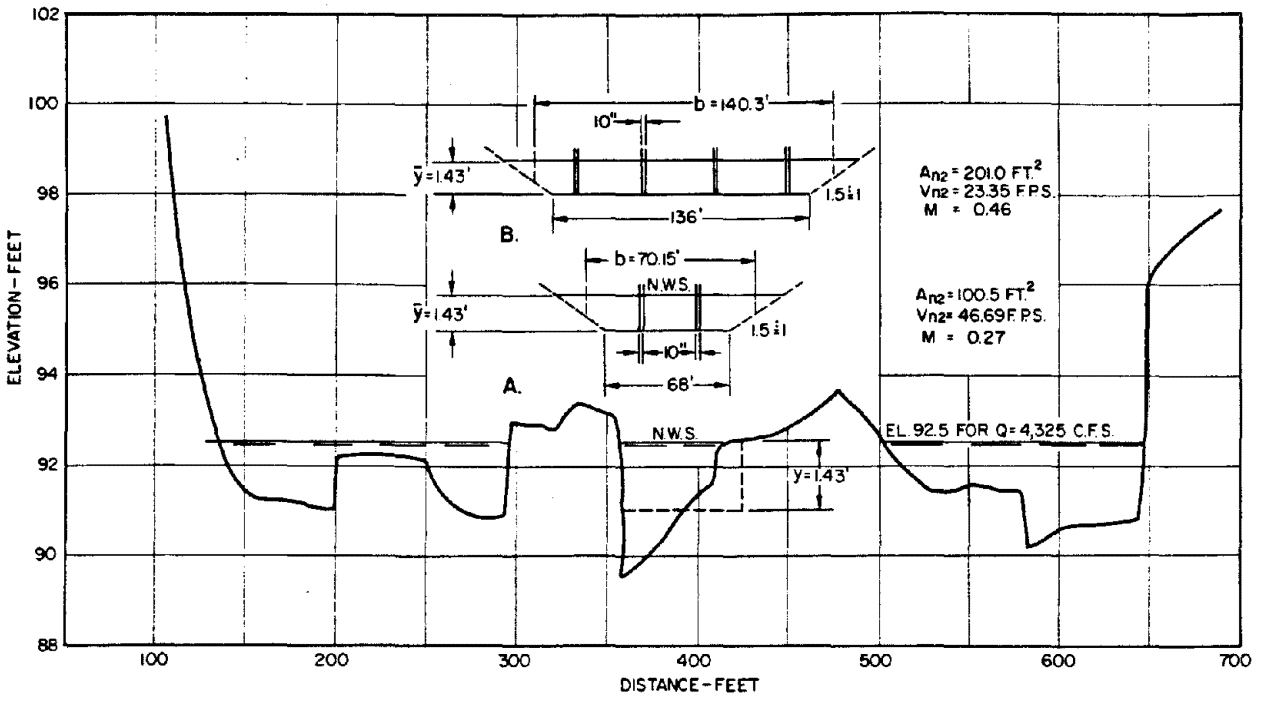

Figure 47.—Example 11: Bridge backwater with supercritical flow.

$S_0 = 0.0380$. Expression (4), Chapter II, for type I flow was first used and resulted in a ridiculous figure of 46.69 feet for the backwater. (See table 6.) This cannot occur with the present program (*13*, p. 15) which will not compute backwater when the flow is supercritical, but will print out a message "Design Method Invalid."

Find.—The recomputed backwater using expression (26), chapter X, for type II flow. A cross section of the stream and a cross section at the bridge opening are shown on figure 47. Pertinent quantities from the cross section and table 6 are:

$Q = 4{,}325$ c.f.s. for stage at elevation 92,50 ft.,

$M = 0.27$, $A_{n1} = 437$ ft.², $A_{n2} = 100.50$ ft.²,

$b = 70.15$ ft., $J = 0.026$, $\bar{y} = 1.43$, $\alpha_1 = 2.0$

and from figure 5,

$$\alpha_2 = 1.25.$$

To compensate for the two 10-inch piers, since incremental pier coefficients are not available for supercritical flow, the net area, A_{n2N}, will be used in the computation rather than the customarily used gross area, thus

$$A_{n2N} = 100.50 - 2.60 = 97.9 \text{ ft.}^2$$

The channel under the bridge is considered trapezoidal with area equivalent to that of the actual cross section (see fig. 47). Solving for critical depth:

$$q = \frac{Q}{b} = \frac{4{,}325}{70.15 - 1.67} = 63.2 \text{ c.f.s./ft. and}$$

$$y_{2c} = \left[\frac{(63.2)^2}{32.2}\right]^{1/3} = [124]^{1/3} = 4.99 \text{ ft.}$$

The critical velocity in the constriction is then

$$V_{2c} = \frac{q}{y_{2c}} = \frac{63.2}{4.99} = 12.67 \text{ f.p.s. and}$$

$$V^2_{2c}/2g = 2.49 \text{ feet.}$$

The normal velocity in the constriction is

$$V_{n2} = \frac{Q}{A_{n2N}} = \frac{4{,}325}{97.9} = 44.2 \text{ f.p.s.}$$

The velocity for normal depth at section 1 will be

$$V_{n1} = \frac{Q}{A_{n1}} = \frac{4{,}325}{437} = 9.90 \text{ f.p.s. and}$$

$$V^2_{n1}/2g = 1.52 \text{ ft.}$$

From figure 34, the backwater coefficient for $M = 0.27$ is $C_b = 0.22$ for type II flow. Substituting the above values in the backwater expression for

supercritical flow:

$$h_1^* = \alpha_2 \frac{V_{2c}^2}{2g}(c_b + 1) + y_{2c} - \bar{y} - \alpha_1 \frac{V_1^2}{2g} \quad (26)$$

$$h_1^* = 1.25 \times 2.49(0.22 + 1) + 4.99 - 1.43 - 2.0 \times 1.52$$

$$= 4.32 \text{ ft.}$$

It is necessary now to recompute the following:

$$A_1 = 437 + 4.32 \times 525 = 437 + 2{,}268$$

$$= 2{,}705 \text{ ft.}^2,$$

$$V_1 = \frac{Q}{A_1} = \frac{4{,}325}{2{,}705} = 1.60 \text{ f.p.s. and}$$

$$V_1^2/2g = 0.040 \text{ ft.}$$

Recomputing the backwater

$$h_1^* = 3.80 + 4.99 - 1.43 - 2.0 \times 0.040 = 7.28 \text{ ft.}$$

With $h_1^* = 7.28$ feet and $V = 44.2$ f.p.s., the waterway for the bridge, shown on figure 47, is inadequate, even should scour considerably enlarge the waterway.

Should the waterway be doubled in width (fig. 47B), which would require widening the center channel or relocating the bridge, the quantities would be as follows:

$Q = 4{,}325$ c.f.s., $A_{n1} = 437$ ft.^{2}, $\alpha_1 = 2.0$
$b = 140.3$ ft., $M = 0.46$, $\alpha_2 = 1.45$,
$\bar{y} = 1.43$ ft., $A_{n2} = 201.0$ ft.^{2}
$A_{n2N} = 201.0 - 5.2 = 195.8$ ft.^{2}
$q = 31.75$ c.f.s./ft., $y_{2c} = 3.12$ ft.,
$V_{2c} = 10.15$ f.p.s.,
$V_{2c}^2/2g = 1.60$ ft., $V_{n1} = 9.90$ f.p.s.,
$V_{n1}^2/2g = 1.52$ ft., $V_{n2N} = 22.1$ f.p.s.

and from figure 34, $C_b = 0.200$ for type II flow. Substituting in expression (26)

$$h_1^* = \alpha_2 V_{2c}^2/2g(C_b + 1) + y_{2c} - \bar{y} - \alpha_1 V_1^2/2g$$
$$h_1^* = 1.45 \times 1.60(0.200 + 1) + 3.12 - 1.43 - 2.0 \times 1.52$$
$$= 2.78 + 3.12 - 1.43 - 3.04 = 1.43 \text{ ft.}$$

Recomputing A_1 assuming $h_1^* = 4.0$ feet,

$$A_1 = 437 + 4.0 \times 525 = 2{,}537 \text{ ft.}^2,$$

$$V_1 = \frac{Q}{A_1} = \frac{4{,}325}{2{,}537} = 1.71 \text{ f.p.s. and}$$

$$V_1^2/2g = 0.045$$

Replacing the last term in expression (26) with the recomputed velocity head at section 1,

$$h_1^* = 2.78 + 3.12 - 1.43 - 2.0 \times 0.045$$

$$= 4.38 \text{ ft. of backwater.}$$

Checking on the type of flow, the depth at section 1 would be

$$\bar{y} + h_1^* = 1.43 + 4.38 = 5.81 \text{ ft.}$$

The water surface is above y_{2c} at section 1, passes through y_{2c} in the constriction, and thereon remains below y_{2c}. Thus, after enlargement of the waterway the flow is still type II.

Chapter XIII.—DISCUSSION OF PROCEDURES AND LIMITATIONS OF METHOD

13.1 Review of design methods. The design charts and methods which have been presented are applicable to a wide variety of bridge backwater problems. Some of the procedures may appear more involved and lengthy than necessary; this was done to make clear each step of the computations. Once the designer becomes familiar with the method, he can use the electronic computer to solve bridge backwater problems. This requires a copy of the BPR computer program HY–4–69 which is available upon request.

It may be well to review some of the limitations already mentioned to avoid misuse of the material presented and to discuss the information used to develop the design methods and curves.

1. The method of computing backwater as presented is intended to be used for relatively straight reaches of streams having subcritical flow and approximately uniform slope. When the flow passes through critical depth, see chapter X. Field measurements indicate that a stream cross section can vary considerably without causing serious error in computing backwater.

2. It was found that scale models are not suitable for the study of streams with large width to depth ratios. Such streams must be studied in the field. Since preparation of the first edition of this publication, the U.S. Geological Survey has collected considerable field information on backwater at bridges during floods in the State of Mississippi. This field information has served to point up the limitations of the model study (*18*) and supply information which the model study could not. The field studies (*39*), which included long bridges and wide flood plains, are mainly responsible for the changes which appear in this edition. Of course there is still much to be learned from additional field measurements, particularly in locations with heavy vegetal growth.

3. As the length of a bridge is increased, it stands to reason that the type or shape of abutment should have less effect on the backwater. The model study consistently showed slightly less backwater for spill-through than for 45° wingwall abutments, but the model represented very short bridges. After studying the field results, the differentiation between abutment types was dropped except for those producing severe contraction on short bridges.

4. The design information applies specifically to the normal stage-discharge condition, although one exception was made in demonstrating an approximate solution for a particular type of abnormal stage in example 5. In cases where the slope of the water surface is either flatter or steeper than the slope of the bed (abnormal or subnormal stage discharge), it is suggested that the method developed by the U.S. Geological Survey (*8*, *26*) for indirect flow measurement be tried. The reason for this suggestion is the fact that the U.S. Geological Survey performed their model tests in a flume with horizontal floor. The Bureau of Public Roads tests (*18*) were made in a sloping flume; uniform flow was always established before the channel was constricted (with the exception of the tests described in chapter VI).

The Geological Survey method was developed for the express purpose of utilizing bridge constrictions as flow measuring devices. By knowing the stream and bridge cross sections and measuring the drop across the embankment, Δh, the discharge occurring at the time can be computed directly but the computation of backwater requires a trial solution. The Bureau of Public Roads method, described in this publication, permits a direct solution for backwater but requires a trial solution for discharge. It is evident by now that some backwater solutions are sufficiently complex without involving a trial solution. The differences in the two methods are outlined in a discussion by Messers Izzard and Bradley (*31*).

5. Plausible questions will arise in connection with the manner in which the foregoing design information was presented. For example, why was the gross rather than the net area used for determining the contraction ratio and the normal velocity under the bridge for cases where piers were involved? Why

were skewed crossings treated as they were? Are the incremental backwater coefficients applicable to very short bridges with wide piers? Any one of several methods could have been presented with the same accuracy; the choice made in each case was simply the one appearing the most logical and straightforward to the research staff of the Bureau of Public Roads at the time. What must be borne in mind is that the empirical curves for various coefficients were derived by treating the model data in certain ways. It follows that exactly the same process must be used in reverse if faithful and intelligent answers are to be obtained for bridges in the field.

6. For the case where a high flow concentration parallels an embankment, such as depicted in figure 27, the water surface along the upstream side of the embankment will have a falling characteristic and the drop across the embankment will vary depending on where the measurement is taken. It is important to avoid digging borrow pits or to allow channeling of flow of any kind adjacent to the upstream side of bridge embankments. Clearing of the right-of-way beyond the toe of the embankment should not be permitted as trees and brush act most effectively to deter channeling. Where the condition is already present, the situation can be corrected by the use of spur dikes which can be proportioned according to the method described in chapter IX.

7. Questions will arise as to the permissible amount of backwater which can be tolerated under various situations. This is principally a policy matter and should be based on sound economic considerations. If backwater produced by a bridge threatens flooding of improved property, the estimated damage from this source over the expected life of the bridge should be weighed against the initial cost of a longer or shorter bridge. Figure 43 illustrates the costliness of reducing backwater beyond a certain economic limit.

Should the bridge be located in open country where backwater damage is of little or no concern, a shorter bridge may serve the purpose but there is still a practical limit to the permissible backwater. The velocity head at section 2 is roughly:

$$h_1^* + \alpha_1 \frac{V_1^2}{2g}$$

or

$$V_2 = (2gh_1^* + \alpha_1 V_2^2)^{1/2}$$

Assuming $V_1 = 3$ f.p.s. and $\alpha_1 = 1.0$, a backwater of 1 foot would produce an approximate velocity:

$$V_2 = [64.4(1.0) + 9(1.0)]^{1/2} = 8.5 \text{ f.p.s.}$$

Holding upstream conditions the same, 2 feet of backwater would produce a velocity of approximately 11.5 f p.s. and 3 feet of backwater about 14 f.p.s. For bridge sites where scour is not to be encouraged, 1 foot of backwater may be an upper limit. On the other hand, for sites with stable river channels, the backwater can be increased accordingly. Also, in cases where the bed is of a movable nature but foundation conditions are favorable, there is considerable latitude in the initial backwater that can be allowed, as was demonstrated in example 6. In general the stability of the material supporting or protecting the abutments and piers will most likely govern the velocity that can be tolerated and thus the backwater.

8. Streams with extremely sinuous channels on wide flood plains introduce a special case for which the present design procedure may prove inadequate, partly because of uncertainty regarding flow distribution at any cross section. This phase needs further study.

9. For cases where islands or other major obstructions occur in the main channel at or upstream from a bridge, the procedure will require some modification. If these obstructions extend under the bridge it may be possible to treat them in the same manner as piers.

10. For the computation of backwater where the flow of a stream is divided between the main channel bridge and several relief bridges, the methods described in this publication are valid for each bridge provided the flow is divided properly between bridges. (See ref. 40.) The field data available bear out this statement. The principle was first verified by the U.S. Geological Survey after completion of an extensive laboratory model study (*38*).

11. A current trend is toward constructing bridges longer and embankments higher than in the past. From the hydraulic and long-range economic points of view, this practice may or may not be sound. Only a reliable engineering economic analysis, in which all factors of importance are considered, can lead to the correct answer for any one site. Young (*1*) discusses some of the economic factors which come into play during floods; much remains to be done in compiling data on flood damage costs, magnitude and frequency of floods, scour data, flood risk factors, and in perfecting a sound and acceptable method of economic analysis. Since backwater is reflected in one way or another in practically every

phase of the bridge waterway problem, it is hoped that the information contained in this publication will aid in promoting a more logical approach to bridge waterway design.

13.2 Further research recommended. Additional field measurements are needed on practically all phases of the bridge backwater problem such as:

(*a*) Dual bridges
(*b*) Skewed bridges
(*c*) Eccentric bridges
(*d*) Effect of scour on backwater
(*e*) Effect of spur dikes on backwater
(*f*) Optimum length of spur dikes
(*g*) Effect of heavy vegetal cover, both upstream and downstream, on the backwater, and
(*h*) Bridge backwater when the flow passes through critical stage in the constriction (flow type II).

Flow in the constriction is considered supercritical if the Froude number, $V_{n2}/(g\bar{y})^{1/2}$ is greater than unity where,

V_{n2} = mean velocity in constriction—f.p.s. and

$\bar{Y} = \frac{A_{n2}}{b}$ = normal flow depth in constriction—ft.

The above expression has definite meaning in a rectangular channel but is not readily applicable to the irregular cross sections found in streams and rivers. Thus, one of the problems involved in proposals *h*, is prior identification of the type of flow to be expected.

SELECTED BIBLIOGRAPHY

(*1*) ASCE, "Economics of Self-Protection of Highways Against Flood Damage," by J. C. Young, *Journal of Highway Division*, HW 3, October 1956, Paper 1075.

(*2*) ASCE, "Effect of Spur Dikes on Flow Through Contractions," by E. R. Hedman, *Journal of Hydraulics Division*, Vol. 91, HY–4, July 1965, Paper 4412.

(*3*) ASCE, *Journal of Hydraulics Division*, Vol. 92, HY–2, March 1966, p. 430. (Discussion of ref. 2 by L. A. Herr.)

(*4*) ASCE, "Systematic Changes in the Beds of Alluvial Rivers," by W. C. Carey and M. D. Keller, *Journal of Hydraulics Division*, Vol. 83, HY–4, August 1957, Paper 1331.

(*5*) ASCE Trans., "Flood Erosion Protection for Highway Fills," by C. P. Posey, Vol. 122, 1957, p. 531.

(*6*) ASCE Trans. Vol. 122, 1957, p. 544. (Discussion of ref. 5 by C. F. Izzard and J. N. Bradley.)

(*7*) ASCE Trans., Vol. 122, 1957, p. 548. (Discussion of ref. 5 by C. E. Kindsvater.)

(*8*) ASCE Trans., "Tranquil Flow Through Open Channel Constrictions," by C. E. Kindsvater and R. W. Carter, Vol. 120, 1955, p. 955.

(*9*) ASCE Trans., *Backwater Effects of Open-Channel Constrictions*, by H. J. Tracy and R. W. Carter, Vol. 120, 1955, p. 993.

(*10*) Bradley, J. N., "The Use of Backwater in the Design of Bridge Waterways", *Public Roads*, Vol. 30, No. 10, October 1959, p. 221.

(*11*) Bradley, J. N., "Use of Backwater in Designing Bridge Waterways," *Highway Research Board Bulletin 242*, Washington, D.C., 1960, p. 57.

(*12*) Bureau of Public Roads, *Estimating Flood Discharges in the Piedmont Plateau*, by W. D. Potter, Hydraulic Engineering Circular No. 2, Washington, D.C., November 1960, 21 pp.

(*13*) Bureau of Public Roads, *Hydraulics of Bridge Waterways*, by K. H. Welty, M. L. Corry, and J. L. Morris, Electronic Computer Program HY–4–69, Washington, D.C., 1969.

(*14*) Bureau of Public Roads, *Hydraulic Charts for the Selection of Highway Culverts*, by L. A. Herr, Hydraulic Engineering Circular No. 5, Washington, D.C., U.S. Government Printing Office, December 1965, 54 pp.

(*15*) Bureau of Public Roads, *Peak Rates of Runoff From Small Watersheds*, by W. D. Potter, Hydraulic Design Series No. 2, Washington, D.C., U.S. Government Printing Office, April 1961, 35 pp.

(*16*) Bureau of Public Roads, *Use of Riprap for Bank Protection*, by J. K. Searcy, Hydraulic Engineering Circular No. 11, Washington, D.C., U.S. Government Printing Office, June 1967, 43 pp.

(*17*) Chow, Ven Te, *Open Channel Hydraulics*, New York, McGraw-Hill, 1959, p. 226.

(*18*) Colorado State University, Civil Engineering Section, *Backwater Effects of Piers and Abutments*, by H. K. Liu, J. N. Bradley, and E. J. Plate, Report CER57HKL10, October 1957, 364 pp.

(*19*) Colorado State University, Civil Engineering Section, *Hydraulic Model Study of Spur Dikes for Highway Bridge Openings*, by S. S. Karaki, Report CER59SSK36, September 1959, 47 pp.

(*20*) Colorado State University, Civil Engineering Section, *Mechanics of Local Scour, Part II, Bibliography*, by S. S. Karaki and R. M. Haynie, CER-63SSK46, Fort Collins, Colo., November 1963, 51 pp.

(*21*) Colorado State University, Civil Engineering Dept., Engineering Research Center, *Mechanics of Local Scour*, by H. W. Shen, V. R. Schneider, and S. S. Karaki, CER66HWS22, Fort Collins, Colo., June 1966, 58 pp.

(*22*) Corry, M. L. and W. Sanger, "Ultrasonic Instrument for Determining Scour at Bridge Piers," *Public Roads*, Vol. 35, No. 4, October 1968, p. 91.

(*23*) Iowa Highway Research Board, *Scour Around Bridge Piers and Abutments*, by E. M. Laursen, and A. Toch, Bulletin 4, May 1956, 60 pp.

(*24*) Iowa Highway Research Board, *Scour at Bridge Crossings*, by E. M. Laursen, Bulletin 8, August 1958, 53 pp.

(*25*) Karaki, S. S. "Laboratory Study of Spur Dikes for Highway Bridge Protection," *Highway Research Board Bulletin 286*, Washington, D.C., 1961, p.31.

(*26*) Kindsvater, C. E., R. W. Carter, and H. J. Tracy, *Computation of Peak Discharge at Contractions*, U.S. Geological Survey Circular 284, Washington, D.C., 1953, 35 pp.

(*27*) Lehigh University Institute of Research, *Spur Dikes Prevent Scour at Bridge Abutments*, by J. B. Herbich, Fritz Engineering Laboratory Report 280.20, Bethlehem, Pa., December 1966.

(*28*) National Hydraulic Laboratory, *Etude Des Affouillements Autour Des Piles De Ponts*, (Study of scour around bridge piers), Series A, Chatou, France, October 1956.

(*29*) Sanden, E. J., *Scour at Bridge Piers and Erosion of River Banks*, Department of Highways, Province of Alberta, Canada, 3 October 1960.

(*30*) Schneible, D. E., *Field Observations on Performance of Spur Dikes at Bridges*, Philadelphia, Pa., 17–21 October 1966. (Paper presented at ASCE Transportation Engineering Conference.)

(*31*) State University of Iowa, *Field Verification of Model Tests on Flow Through Highway Bridges and Culverts*, by C. F. Izzard and J. N. Bradley, Studies in Engineering, Bulletin 39, June 1958, p. 225. (Proceedings 7th Hydraulics Conference.)

(*32*) Tainish, J. *Investigation of Forces on Submerged Bridge Beams*, Report No. 108, New South Wales, Australia, March 1965.

(*33*) U.S. Department of Agriculture, *Bridge Piers as Channel Obstructions*, by D. L. Yarnell, Technical Bulletin No. 442, Washington, D.C., U.S. Government Printing Office, November 1934, 52 pp.

(*34*) U.S. Department of Agriculture, *Flow of Water in Drainage Channels*, by C. E. Ramser, Technical Bulletin No. 129, Washington, D.C., U.S. Government Printing Office, November 1929, 102 pp.

(*35*) U.S. Department of Agriculture, *Flow of Water in Channels Protected by Vegetative Linings*, by W. O. Ree and V. J. Palmer, Technical Bulletin No. 967, Washington, D.C., U.S. Government Printing Office, February 1949, 115 pp.

(*36*) U.S. Department of Agriculture, *Pile Trestles as Channel Obstructions*, by D. L. Yarnell, Technical Bulletin, No. 429, Washington, D.C., U.S. Government Printing Office, July 1934.

(*37*) U.S. Geological Survey, *Discharge Characteristics of Embankment-Shaped Weirs*, by C. E. Kindsvater, Water Supply Paper 1617–A, Washington, D.C., U.S. Government Printing Office, 1964, 114 pp.

(*38*) U.S. Geological Survey, *Flow Through Openings in Width Constrictions*, by J. Davidian, P. H. Carrigan, Jr., and J. Shen, Water Supply Paper 1369-D, Washington, D.C., U.S. Government Printing Office, 1962, 32 pp.

(*39*) U.S. Geological Survey, "Hydraulic Performance of Bridges in the State of Mississippi," by B. L. Neely, Jr., Jackson, Miss., 30 June 1966. (Unpublished report.)

(*40*) U.S. Geological Survey, *Measurement of Peak Discharge at Width Constrictions by Indirect Methods*, by H. F. Matthai, Techniques of Water Resources Investigations, Book 3, Chapter A4, Washington, D.C., U.S. Government Printing Office, 1967, 44 pp.

(*41*) U.S. Geological Survey, *Roughness Characteristics of Natural Channels*, by H. H. Barnes, Jr., Water Supply Paper 1849, Washington, D.C., U.S. Government Printing Office, 1967, 213 pp.

(*42*) Water and Power Development Authority, *Hydraulic Model Studies, Tarbela Dam Project, Part II*, Lahore, West Pakistan, October 1965.

(*43*) Yarnell, D. L., and F. A. Nagler, "Flow of Water Over Railway and Highway Embankments," *Public Roads*, Vol. 11, No. 2, April 1930, p. 30.

Appendix A.—DEVELOPMENT OF EXPRESSIONS FOR BRIDGE BACKWATER

The three types of flow encountered in connection with bridges constricting natural streams and rivers (see fig. 4) are summarized in the following table with respect to the critical depth of flow in the constriction y_{2c}.

With respect to Y_{2c}

Flow type	Normal stage	Water surface		
		Section 1	Sections 2–3	Section 4
I	above	above	above	above.
IIA	above	above	below	above.
IIB	below	above	below	below.
III	below	below	below	below

Type I is subcritical flow; types IIA and IIB are subcritical flow at section 1 but both pass through critical stage within the constriction while type III is supercritical flow throughout. Types IIA and IIB differ only in the positions of normal stage and critical depth. The development of the expressions for backwater for flow types I and II will next be considered.

A.1 Type I flow (subcritical)

An expression for backwater has been formulated by applying the principle of conservation of energy between the point of maximum backwater upstream from the bridge, section I, and a point downstream from the bridge at which the normal stage has been reestablished, section 4 (fig. A–1A). The method, first suggested by Izzard and reported in reference 6, was developed on the basis that the channel in the vicinity of the bridge is essentially straight, the cross sectional area of the stream is reasonably uniform and the gradient of the bottom is constant between sections 1 and 4. Also the analysis for type I applies only to steady subcritical flow.

Equating the energy between sections 1 and 4 (fig. A–1A).

$$S_0 L_{1-4} + y_1 + \frac{\alpha_1 V_1^2}{2g} = y_4 + \frac{\alpha_4 V_4^2}{2g} + h_T \qquad (27)$$

where h_T is the total energy loss between sections 1 and 4.

As the testing procedure in the model consisted of first establishing a normal water surface throughout the main channel—parallel to the bottom—the resistance to flow per foot of length, previous to installation of the bridge constriction, just balanced the vertical drop due to slope. These quantities cancel and expression (27) can be written

$$y_1 - y_4 = \frac{\alpha_4 V_4^2}{2g} - \frac{\alpha_1 V_1^2}{2g} + h_b \qquad (28)$$

The additional loss, h_b, can be expressed as the product of a loss coefficient, K^*, and a velocity head or

$$h_b = K^* \frac{\alpha_2 V_{n2}^2}{2g} \qquad (29)$$

where V_{n2} is average velocity in the contracted section based on the flow area below normal water surface.

Replacing $y_1 - y_4$ with h^*_1, and h_b with $K^*\alpha_2 V^2_{n2}/2g$, equation (29) becomes

$$h^*_1 = K^* \frac{\alpha_2 V^2_{n2}}{2g} + \left[\frac{\alpha_4 V_4^2}{2g} - \frac{\alpha_1 V_1^2}{2g}\right] \qquad (30)$$

Since the analysis is based on the assumption that the cross sectional areas at sections 1 and 4 are essentially the same, α_4 can be replaced by α_1. Also from the equation of continuity $A_1V_1 = A_4V_4 = A_{n2}V_{n2}$, velocities can be expressed as areas. So the expression for backwater becomes:

$$h_1^* = K^*\alpha_2 \frac{V^2_{n2}}{2g} + \alpha_1 \left[\left(\frac{A_{n2}}{A_4}\right)^2 - \left(\frac{A_{n2}}{A_1}\right)^2\right] \frac{V^2_{n2}}{2g} \qquad (4)$$

where the terms, applicable to prototype as well as

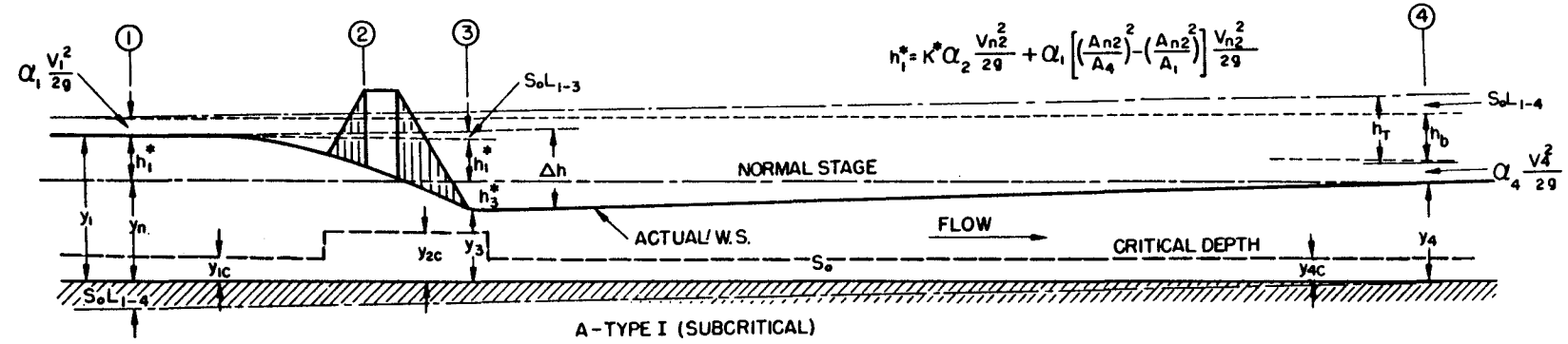

A-TYPE I (SUBCRITICAL)

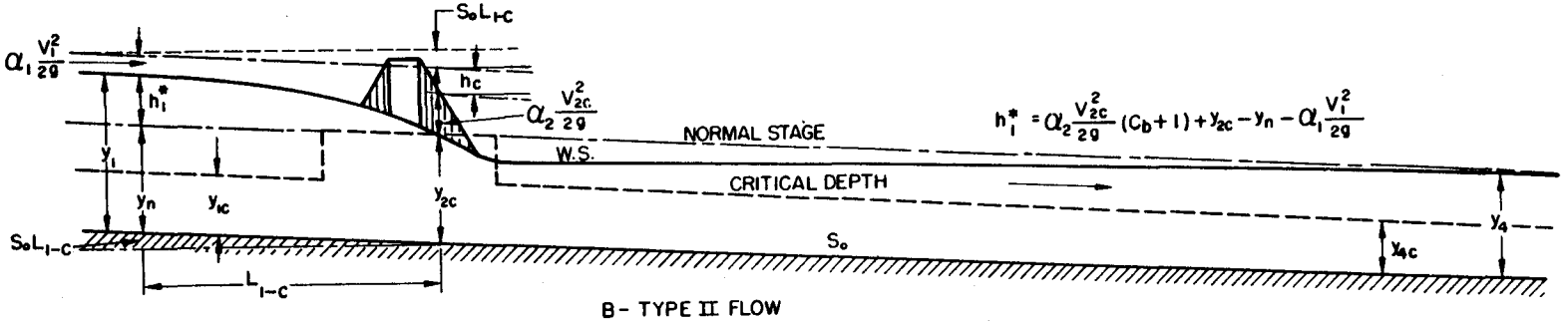

B- TYPE II FLOW
(PASSES THROUGH CRITICAL DEPTH)

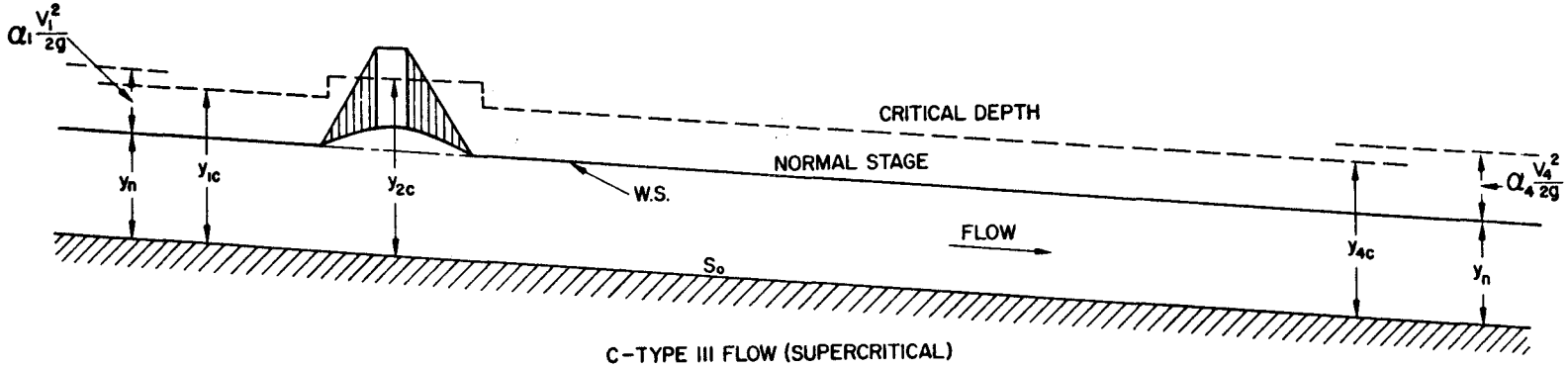

C-TYPE III FLOW (SUPERCRITICAL)

Figure A-1.—Flow types I, II, and III.

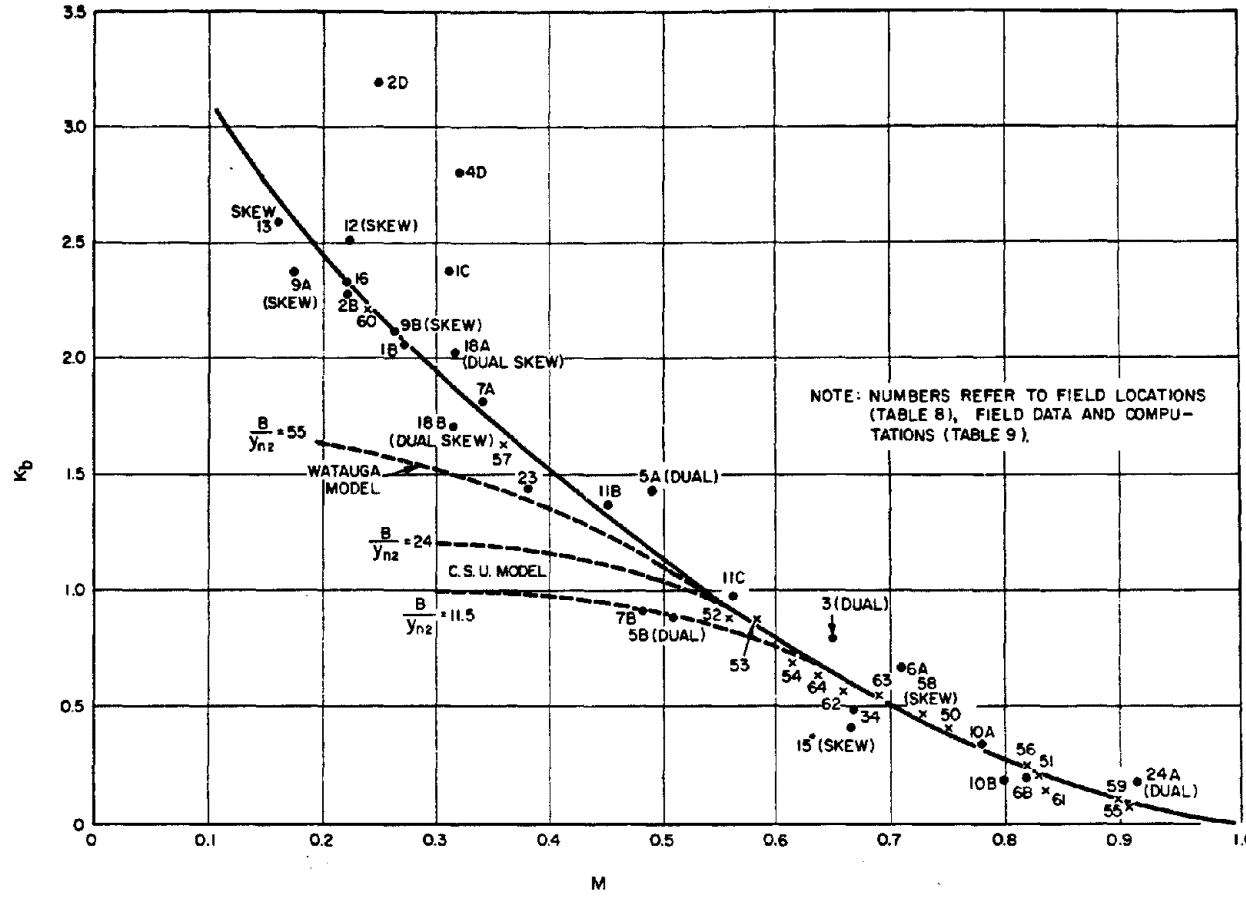

Figure A-2.—Backwater coefficient curve for type I flow.

model, are defined as follows:

h_1^* = total backwater (ft.)
K^* = total backwater head loss coefficient
α_1 = velocity head correction coefficient at sections 1 and 4
α_2 = velocity head correction coefficient at constriction
A_{n2} = gross water area in constriction measured below normal stage (sq. ft.)
V_{n2} = average velocity in constriction for flow at normal stage or Q/A_{n2} (f.p.s.)
A_4 = water area at section 4 (where normal stage has been re-established) (sq. ft.), and
A_1 = total water area at section 1, including backwater (sq. ft.)

If piers are present in the constriction, these are ignored in the determination of A_{n2}. The velocity V_{n2} does not represent an experimentally measured velocity but rather a reference velocity readily computed for both model and field structures. The expression

$$\alpha_1\left[\left(\frac{A_{n2}}{A_4}\right)^2-\left(\frac{A_{n2}}{A_1}\right)^2\right]\frac{V^2_{n2}}{2g} \tag{4b}$$

represents the difference in kinetic energy between sections 4 and 1, expressed in areas rather than velocities.

Should the backwater coefficient, K^*, be desired,

$$K^*=\frac{h_1^*}{\alpha_2 V^2_{n2}/2g}-\frac{\alpha_1}{\alpha_2}\left[\left(\frac{A_{n2}}{A_4}\right)^2-\left(\frac{A_{n2}}{A_1}\right)^2\right] \tag{31}$$

The energy stored in the backwater is entirely consumed between sections 1 and 4. It can be noted that in the development of expression (28) the normal channel resistance cancelled out. Thus h_b represents the additional energy required to balance out the remaining losses. The energy involved in h_b can be best explained by considering the losses from section to section:

(*a*) For a distance upstream from section 1, the

boundary resistance is less than normal due to a reduction of velocity in the backwater reach.

(*b*) Between sections 1 and 2 the energy loss is little different than normal since there is some reduction in velocity due to backwater, and convergence of the flow in this reach does not contribute materially to the excess energy loss.

(*c*) Between sections 2 and 3 the energy loss is greater than normal due to an increase in boundary resistance and also to internal shear which accompanies separation and lateral mixing between abutments. The magnitude of this loss varies with the degree of contraction, the ease with which the flow can enter the constriction, and with the velocity involved.

(*d*) The greater portion of the excess energy in h_b is lost between sections 3 and 4 and is chargeable principally to increased boundary resistance and lateral mixing. Ordinarily the constricted jet tends to expand horizontally at a rate of 5° to 6° per side until it reaches section 4 but the mixing and reexpansion pattern can be greatly influenced by physical factors such as whether the flood plain is clear or whether it is covered with a dense growth of brush and trees. The energy represented by h_b is dissipated first in viscous action, then in eddies and turbulence, and finally in heat.

Backwater coefficients obtained from the model studies are tabulated in the appendix of reference 18. Backwater coefficients from field measurements are recorded in tables B–1 and B–2 in appendix B.1 and the field points are shown plotted on figure A–2. The K_b represents the backwater coefficient chargeable to the contraction loss only while the symbol K^* is the total backwater coefficient representing the sum of all influencing factors.

A.2 Type II flow (water surface passes through critical depth).

Once critical depth is reached, the water surface upstream from the constriction is no longer influenced by conditions downstream. This is true even though the water surface may dip below critical depth, Y_{2c}, in the constriction and then return to subcritical flow as in type IIA (fig. A–1). Type IIB flow is similar except the water surface not only dips below Y_{2c} but also Y_{4c} downstream from the constriction. Both types of flow are subject to the same analysis since the criterion here is that the flow passes through critical depth. The backwater expression for flow types IIA and IIB is developed by equating the energy between section 1 and the point in the constriction at which the water surface passes through critical depth, Y_{2c}. Referring to figure A–1B,

$$S_0L_{1-c} + y_n + h_1^* + \alpha_1\frac{V_1^2}{2g} = Y_{2c} + \alpha_2\frac{V^2_{2c}}{2g} + h_c + S_0L_{1-c} \quad (32)$$

Canceling out normal boundary resistance against S_0L_{1-c} and substituting $C_b\alpha_2(V^2_{2c}/2g)$ for h_c,

$$y_n + h_1^* - Y_{2c} = \alpha_2\frac{V^2_{2c}}{2g} + C_b\alpha_2\frac{V^2_{2c}}{2g} - \frac{\alpha_1V_1^2}{2g}$$

Solving for backwater,

$$h_1^* = \frac{\alpha_2V^2_{2c}}{2g}(C_b + 1) + Y_{2c} - y_n - \frac{\alpha_1V_1^2}{2g}, \quad (26)$$

where

h_1^* = total bridge backwater (ft.)
y_n = normal flow depth (ft.) (model)
$\bar{Y}$ = normal flow depth or A_{n2}/b (ft.) (prototype)
Y_{2c} = critical depth in constriction or $(Q^2/b^2g)^{1/3}$ (ft.)
V_{2c} = critical velocity in constriction or $Q/Y_{2c}\cdot b$ (f.p.s.)
V_1 = velocity at section 1 or Q/A_1 (f.p.s.)
α_1, α_2 = velocity head correction coefficients at section 1 and in the constriction, respectively
C_b = backwater coefficient for type II flow (constriction loss only)

Should the backwater coefficient be desired,

$$C_b = \frac{h_1^* + y_n - Y_{2c}}{\alpha_2V^2_{2c}/2g} + \frac{\alpha_1}{\alpha_2}\left(\frac{V_1}{V_{2c}}\right)^2 - 1 \quad (25)$$

A number of the tests from the models fall into the type IIA and IIB category but the range is rather narrow. The data and computations for flow type II are included in table A–1, and the points for the backwater coefficient are plotted on figure A–3. The lower curve is for spillthrough and 45° wingwall abutments. The upper curve has no practical application as the constriction consisted of two vertical boards, one placed on each side of the test flume. The boards constricted the jet more severely than the abutment shapes which is reflected in the higher values of the coefficients. Additional model studies

Table A–1.—Critical Flow Through Bridge Constrictions (Type II and III Flow) Model Data and Computations.

Run No.	B ft.	b ft.	Q c.f.s.	$M = b/B$	Y_n ft.	h_1^* ft.	$Y_n+h_1^*$ ft.	Y_{1c} ft.	Y_{2c} ft.	Y_3 ft.	$A_1 = B(Y_n+h_1^*)$ ft.^{2}	$V_1 = Q/A_1$ f.p.s.	$A_{2c} = b \cdot Y_{2c}$ ft.^{2}	$V_{2c} = Q/A_{2c}$ f.p.s.	$V_{2c}^2/2g$ ft.	$Y_n+h_1^*-Y_{2c}$ ft.	$\frac{Y_n+h_1^*-Y_{2c}}{V_{2c}^2/2g}$	$\left(\frac{V_1}{V_3}\right)^2$	C_b	S_0	Abutment type	Flow type
(1)	(2)	(3)	(4)	(5)	(6)	(7)	(8)	(9)	(10)	(11)	(12)	(13)	(14)	(15)	(16)	(17)	(18)	(19)	(20)	(21)	(22)	(23)
357	7.90	2.00	2.50	0.253	0.333	0.282	0.615	0.146	0.364	0.282	4.859	0.555	0.728	3.434	0.182	0.251	1.379	0.022	0.401	0.0012	VB	B
267			2.91		.352	.335	.687	.162	.404	.295	5.427	.536	.808	3.601	.202	.283	1.401	.022	.423			B
266			3.95		.418	.417	.835	.198	.495	.341	6.597	.599	.990	3.990	.248	.340	1.371	.023	.394			B
456			5.00		.484	.476	.960	.231	.579	.409	7.584	.659	1.158	4.318	.264	.381	1.443	.023	.360			B
305						.484	.968	.231	.579	.377	7.647	.654				.389	1.473	.023	.396			B
229						.478	.962	.231	.579	.386	7.600	.658				.383	1.451	.023	.474			B
261						.481	.965	.231	.579	.391	7.624	.656				.386	1.462	.023	.485			B
602					.416	.527	.943	.231	.579	.280	7.450	.671				.304	1.379	.024	.403			B
262			5.75		.523	.573	1.096	.254	.636	.428	8.658	.664	1.272	4.520	.318	.460	1.447	.022	.469			B
858	2.98		2.50	.377	.333	.159	.492	.146	.280	.276	3.887	.643	.834	2.998	.140	.212	1.517	.046	.560			A
601	3.00		5.00	.380	.416	.318	.734	.232	.442	.319	5.799	.862	1.326	3.771	.221	.292	1.321	.052	.373	.0020		B
755					.484	.266	.750	.232	.442	.404	5.925	.844				.308	1.394	.050	.444	.0012		A
872						.274	.758	.232	.442	.414	5.988	.835				.316	1.430	.049	.479			A
304						.274	.758	.232	.442	.402	5.988	.835				.316	1.430	.049	.479			A
228						.273	.757	.232	.442	.407	5.980	.836				.315	1.425	.049	.474			A
1,288	2.81		3.00	.356	.360	.175	.535	.165	.329	.304	4.227	.710	.924	3.248	.164	.206	1.256	.048	.304		VW	A
1,302	2.83		5.00	.358	.484	.261	.745	.232	.461	.389	5.886	.849	1.305	3.831	.228	.284	1.246	.040	.286		VW	A
1,269	2.83		3.00	.358	.360	.184	.544	.165	.327	.311	4.298	.698	.925	3.243	.163	.217	1.331	.046	.377		90° WW	A
1,307	2.84		5.00	.359	.484	.265	.749	.232	.459	.405	5.917	.845	1.303	3.837	.229	.290	1.266	.048	.314			A
13	4.00	1.50	1.98	.375	.446	.146	.592	.197	.380	.381	2.360	.838	.570	3.474	.187	.212	1.135	.058	.193		45° WW	A
20			1.06		.232	.155	.387	.130	.250	.159	1.548	.685	.375	2.827	.124	.137	1.105	.058	.169	.0036		B
29			.66		.202	.086	.288	.094	.182	.179	1.152	.573	.273	2.418	.091	.106	1.165	.056	.221	.0024		A
19	2.00		1.06	.500	.232	.086	.318	.130	.206	.199	1.272	.833	.412	2.573	.103	.112	1.092	.105	.197	.0036		A
21			2.25		.382	.150	.532	.214	.340	.295	2.128	1.057	.680	3.309	.170	.192	1.087	.102	.189	.0024		A
30			1.57		.318	.098	.416	.169	.267	.252	1.664	.944	.534	2.940	.134	.148	1.104	.103	.207	.0024		A
823	7.90	2.416	2.50	.306	.333	.176	.509	.146	.322	.287	4.021	.622	.778	3.213	.160	.187	1.169	.037	.206	.0012		A
927		2.416	5.00	.306	.484	.305	.789	.232	.511	.287	6.233	.802	1.235	4.049	.255	.278	1.090	.039	.129			B
670		2.44	2.50	.309	.333	.181	.514	.146	.319	.286	4.061	.616	.778	3.213	.160	.195	1.219	.037	.250			A
281		2.45	5.00	.310	.484	.310	.794	.232	.506	.404	6.270	.800	1.240	4.032	.253	.288	1.140	.035	.175			B
557		2.46	5.00	.311	.484	.318	.802	.232	.505	.408	6.336	.789	1.242	4.026	.253	.297	1.174	.038	.217			B
558		2.46	5.00	.311	.484	.313	.797	.232	.505	.409	6.296	.794	1.242	4.026	.253	.292	1.154	.039	.193			B
109		2.50	5.30	.316	.497	.297	.794	.241	.519	.417	6.273	.845	1.298	4.083	.259	.275	1.062	.043	.105			B
1,355		2.85	3.00	.361	.360	.147	.507	.165	.325	.319	4.005	.749	.926	3.240	.163	.182	1.117	.053	.170			A
1,161R		2.91	3.00	.368	.360	.141	.501	.165	.321	.321	3.958	.758	.934	3.212	.160	.180	1.125	.056	.181			A
24	4.00	1.58	2.25	.395	.386	.227	.613	.214	.399	.314	2.452	.918	.630	3.571	.198	.214	1.081	.066	.147	.0024	ST	B
32		1.984	1.57	.496	.322	.103	.425	.169	.269	.266	1.700	.924	.534	2.940	.134	.156	1.164	.099	.263	.0024		A
23		2.08	2.25	.520	.386	.135	.521	.214	.332	.327	2.084	1.080	.691	3.256	.165	.189	1.145	.110	.255	.0012		A
16		2.35	1.07	.588	.233	.047	.280	.131	.186	.185	1.120	.955	.432	2.477	.096	.094	.979	.149	.128	.0036		A
445	7.90	2.32	2.50	.294	.333	.201	.534	.146	.331	.292	4.219	.593	.768	3.255	.165	.203	1.230	.033	.263	.0012		A
125		2.47	2.45	.313	.314	.190	.504	.144	.312	.253	3.982	.615	.771	3.178	.157	.192	1.223	.037	.268			A
123		2.496	2.68	.316	.331	.198	.529	.153	.329	.287	4.179	.614	.821	3.264	.165	.200	1.212	.039	.251			A
666		2.65	2.50	.335	.333	.152	.485	.146	.302	.296	3.832	.652	.800	3.125	.152	.183	1.204	.060	.264			A
589		2.795	5.00	.354	.416	.307	.723	.232	.464	.321	5.712	.875	1.297	3.855	.232	.259	1.116	.052	.168			B
1,061		2.877	5.00	.364	.484	.235	.719	.232	.455	.414	5.680	.880	1.309	3.820	.227	.264	1.163	.053	.216			A
563		2.917	5.00	.369	.484	.240	.724	.232	.451	.423	5.720	.874	1.316	3.799	.225	.273	1.213	.053	.266			A
107		2.945	5.30	.373	.497	.223	.720	.241	.466	.427	5.688	.932	1.372	3.863	.232	.254	1.095	.058	.153			A

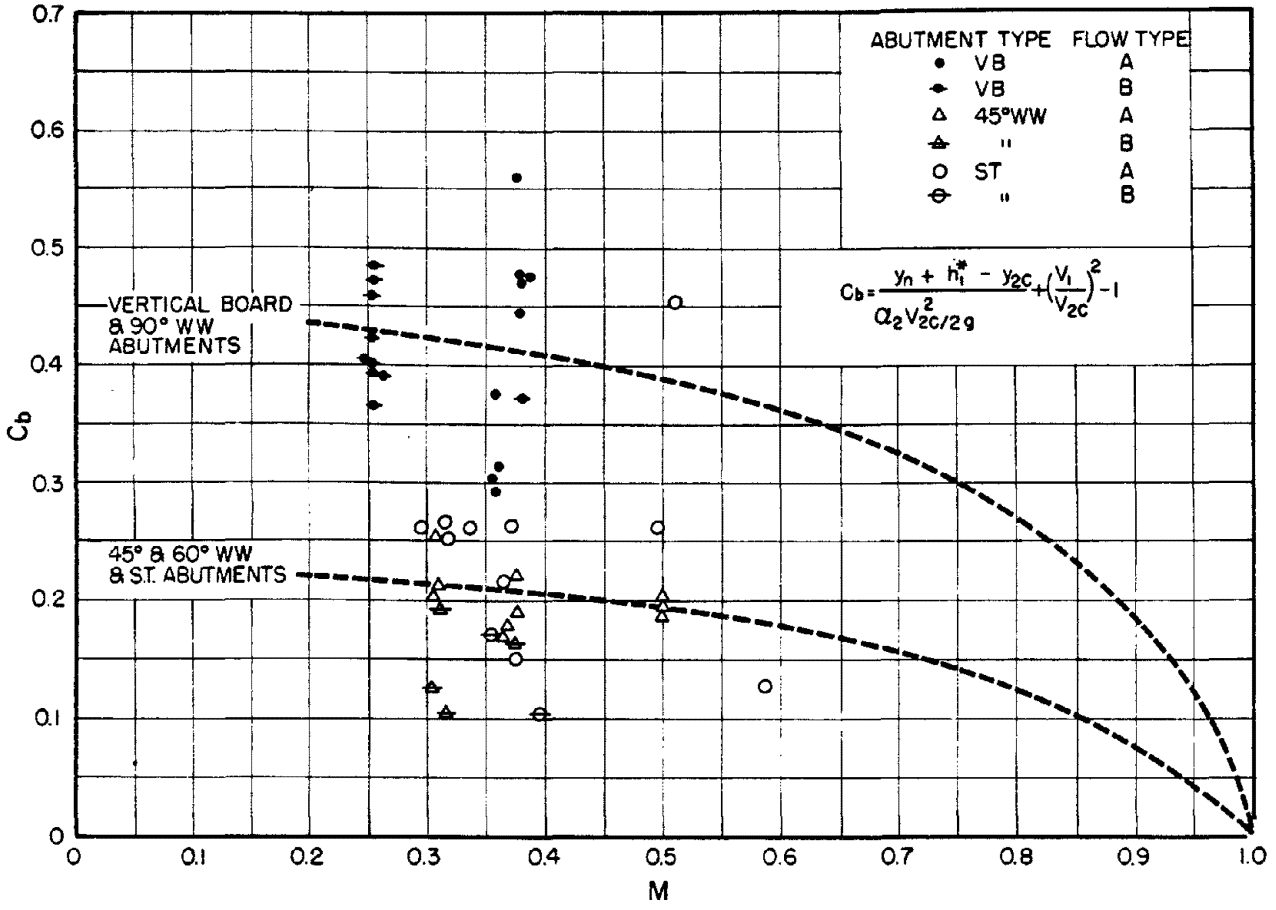

Figure A-3.—Backwater coefficient curve for type II flow.

are urgently needed to better define the type II backwater coefficient curve.

A.3 Type III flow (supercritical)

Theoretically there is no backwater produced by Type III flow. No detailed information is on hand for supercritical flow occurring both upstream and downstream from a bridge constriction. Should the design flood be normally traveling at supercritical velocities in the stream proper, it is questionable whether any constriction should be imposed on the cross section unless foundation conditions are excellent. Moreover, sufficient clearance should be provided to insure that the superstructure will never come in contact with the flow.

Appendix B.—BASIS OF REVISIONS

B.1 Backwater coefficient base curves. The backwater coefficient base curves for type I flow, as they appeared in the first edition, were based principally on model studies (*18*) with field measurements made on about a dozen short bridges with limited flood plains. This was the extent of the information available at the time and it was stated that the validity of the base curves might be questioned if used outside of the range mentioned.

Upon receipt of additional field measurements furnished by the U.S. Geological Survey in 1967, (*39*), it was found that a rather marked revision should be made in the backwater coefficient base curves. For the longer bridges and wider flood plains the model was entirely inadequate. For example, the maximum width to depth ratio obtained from the model was about 40, the largest width to depth ratio from the first field tests was 112, while the

Table B-1.—Summary of field measurements on bridge waterways.

[Data furnished by courtesy of U.S.G.S.]

No.	Location	Dates of measurements	Length spur dike, feet		Abutment type and slope	Remarks
			Left	Right		
1B	Bucatuna Creek, S.H. 18 near Quitman, Miss.	Apr. 6, 1964	26	24	1.5:1 ST	Analysis not applicable.
1C	---do---	Apr. 7, 1964	26	24	1.5:1 ST	Do.
2B	Long Creek, S.H. 18 near Quitman, Miss.	Apr. 6, 1964	23	23	1.5:1 ST	Do.
2D	---do---	Apr. 7, 1964	23	23	1.5:1 ST	Do.
3	Bowie Creek, I-59 near Hattiesburg, Miss.	Feb. 22, 1961 Feb. 23, 1961	132	9	4:1 ST	Dual bridges.
4D	East Tallahala Creek, S.H. 528 near Bay Springs, Miss.	Apr. 6, 1964	90	0	2:1 ST	Analysis not applicable.
5A	Tallahoma Creek, I-59 near Ellisville, Miss.	Feb. 23, 1961	15	108	3:1 ST	Dual bridges.
5B	---do---	Apr. 8, 1964	15	108	3:1 ST	Do.
6A	Tallahala Creek, S.H. 42 near Runnelstown, Miss.	Feb. 25, 1961	----	----	1.5:1 ST	
6B	---do---	Apr. 9 to 10, 1964	----	----	1.5:1 ST	
7A	Wolf River, S.H. 26 near Poplarville, Miss.	Feb. 18, 1961	----	----	2:1 ST	
7B	---do---	Mar. 2, 1964	49	0	2:1 ST	
9A	Bogue Chitto, U.S.H. 84 near Brookhaven, Miss.	Mar. 28, 1961	----	----	2:1 WW	30° skew.
9B	---do---	Mar. 2, 1964	----	----	2:1 WW	Do.
10A	West Hobolochitto Creek, S.H. 26 near Poplarville, Miss.	Nov. 4, 1961	----	----	2:1 ST	
10B	---do---	Mar. 2, 1964	127	0	2:1 ST	
11B	West Fork Tombigbee River, U.S.H. 45 near Nettletown, Miss.	Apr. 12, 1962	0	114	2:1 ST	
11C	---do---	Mar. 15, 1964	0	114	2:1 ST	
12	Yockanookany River, S.H. 35 near Kosciusko, Miss.	Dec. 18, 1964	----	----	2:1 ST	27° skew.
13	Black Creek, S.H. 589 near Purvis, Miss.	Apr. 28, 1962	96	0	3:1 ST	
15	Upper Little Creek, U.S.H. 98 near Columbia, Miss.	Apr. 28, 1962	----	----	1.5:1 ST	30° skew.
16	Luke Flupper Creek, S.H. 528 near Bay Springs, Miss.	Apr. 6, 1964	0	52	2:1 ST	
18A	Tallahala Creek, I-59 near Laurel, Miss.	Feb. 23, 1961	9	125	3:1 ST	(Dual bridges) 30° skew.
18B	---do---	Apr. 7, 1964	9	125	3:1 ST	Do.
20A	Big Black River, S.H. 16 near Canton, Miss.	Dec. 19, 1961	0	163	2:1 WW	Multiple opening.
22A	Big Black River, I-20 near Edwards, Miss.	Dec. 20, 1961	----	----	2:1 ST	Dual bridges.
23	Leaf River, U.S.H. 98 near McLain, Miss.	Feb. 26, 1961	----	----	2:1 ST	
24A	Leaf River, I-59 near Moselle, Miss.	Feb. 24, 1961	150	0	2:1 ST	Dual bridges—Multiple
24B	---do---	Feb. 24, 1961	0	70	2:1 ST	Do.
30A	Pascagoula River, S.H. 26 near Merrill, Miss.	Feb. 27, 1961	40	40	2:1 ST	Multiple opening
30B	---do---	Feb. 27, 1961	18	40	2:1 ST	Relief bridge.
33G	Pearl River, S.H. 43 near Canton, Miss.	Dec. 21, 1961	85	0	1.5:1 ST	Do.
34	White Sand Creek, County Highway, near Oakvale, Miss.	Mar. 29, 1961	----	----	1.5:1 ST	Scour recorded.
36	Susquehanna River, near Nanticoke, Pa.	Apr. 1, 1960	----	300	2:1 ST	45° skew.
37	Indus River at Tarbela Dam, District Hazara, West Pakistan.	Model	----	400	2:1 ST	
50	Bonnett Carre Sp. near New Orleans, La.	Feb. 28, 1937	----	----	2:1 ST	
51	Short Creek near Albertsville, Ala.	Nov. 28, 1948	----	----	1:1 ST	
52	Bond Creek, Dunham Basin, New York	Dec. 31, 1948	----	----	45° WW	
53	Auglaise River, Fort Jennings, Ohio	Feb. 15, 1950	----	----	45° WW	
54	Crooked Creek, Richmond, Mo.	July 6, 1951	----	----	1.5:1 ST	
55	W. Br. Delaware River, Hale Eddy, N.Y.	Mar. 22, 1948	----	----	90° WW	
56	Wild Rice Creek, Twin Valley, Minn.	May 9, 1950	----	----	45° WW	
57	Long Creek, Courtland, Miss.	May 28, 1954	----	----	2:1 ST	
58	Ottowa River, Allentown, Ohio	Feb. 14, 1950	----	----	90° WW	15° skew.
59	Illinois Bayou, Scottsville, Ark.	Jan. 24, 1949	----	----	2:1 ST	
60	S. Chickamauga Creek, Chickamauga, Tenn.	Mar. 29, 1948	----	----	3:1 ST	30° skew.
61	Kayaderosseros Creek, West Milton, N.Y.	Dec. 31, 1948	----	----	45° WW	
62	---do---	Apr. 6, 1952	----	----	38° WW	8° skew.
63	---do---	Apr. 2, 1952	----	----	38° WW	8° skew.
64	Schroon River, Riverbank, N.Y.	Apr. 18, 1952	----	----	30° WW	

Table B–2.—Summary of field measurements and computations on bridge backwater.

[Field measurements furnished by U.S.G.S.]

No.	Measured Q c.f.s.	M	b ft.	S_e ft./ft.	Measured Δh ft	$\overline{Y}$ ft.	$\frac{\Delta h}{\overline{Y}}$	L^* ft.	$\frac{L^*}{b}$	A_{n1} ft.^{2}	V_{n1} f.p.s.	α_1	α_2	K_b	$\frac{b}{\overline{Y}}$	$\frac{B}{\overline{Y}}$	Remarks
(1)	(2)	(3)	(4)	(5)	(6)	(7)	(8)	(9)	(10)	(11)	(12)	(13)	(14)	(15)	(16)	(17)	
1B	14,600	0.27	490	0.000776	2.44	4.95	0.490	490	1.00	2,427	6.02	2.29	1.44	2.07	99	763	
1C	9,330	.31	488	.000776	1.82	4.32	.420	440	.90	2,120	4.40	2.8	.....	2.39	113	770	
2B	8,950	.22	347	.00130	2.22	4.37	.510	347	1.00	1,492	6.00	1.36	1.11	2.27	81	710	
2D	4,170	.25	345	.00130	1.18	3.90	.300	276	.80	1,316	3.10	1.61	1.26	3.20	88	614	
3	36,400	.65	1,044	.000704	1.06	12.75	.083	625	.60	13,315	2.73	2.28	1.80	0.78	82	195	Dual.
4D	18,800	.32	486	.000755	1.62	9.85	.160	390	.80	4,844	3.89	1.42	1.26	2.80	49	114	
5A	13,500	.49	519	.000672	.52	12.10	.043	186	.36	6,294	2.15	2.51	1.57	1.43	43	154	Dual.
5B	11,500	.51	519	.000672	.33	11.90	.028	130	.25	6,165	1.85	2.58	1.57	0.84	43	154	Do.
6A	31,100	.71	1,191	.000653	.73	11.55	.063	550	.46	13,763	2.26	3.31	2.08	.67	103	177	
6B	22,800	.82	1,182	.000653	.42	9.70	.044	378	.32	11,450	1.99	3.08	2.58	.19	122	202	
7A	8,540	.34	241	.00134	.97	10.30	.094	140	.58	2,494	3.42	3.52	.....	1.83	24	118	
7B	3,160	.48	236	.00134	.32	7.45	.043	64	.27	1,755	1.80	3.29	2.12	.89	32	104	
9A	7,650	.17	172	.000947	1.68	7.63	.220	174	.88	1,310	5.85	1.24	.....	2.38	23	107	30° skew.
9B	2,910	.26	172	.000947	.61	6.70	.091	117	.59	1,150	2.53	1.34	1.98	2.14	26	92	30° skew.
10A	7,220	.78	417	.00122	.34	10.15	.034	125	.30	4,247	1.70	4.32	.....	.33	41	64	
10B	5,470	.80	408	.00124	.18	9.37	.019	61	.15	3,822	1.43	4.21	1.47	.18	44	61	
11B	62,470	.45	1,245	.000409	1.86	9.86	.190	1,020	.82	12,294	5.08	1.76	1.56	1.37	126	324	
11C	31,960	.56	1,240	.000409	1.54	7.00	.220	1,970	.78	8,718	3.67	2.05	2.47	.99	177	395	
12	15,300	.22	468	.000212	.97	8.63	.113	350	.65	4,650	3.80	2.38	.....	2.53	54	235	27° skew.
13	5,430	.16	385	.00100	.41	7.29	.056	134	.35	2,807	1.93	1.81	1.42	2.60	53	394	
15	3,880	.65	313	.00130	.36	7.28	.050	145	.40	2,280	1.70	2.05	2.06	.40	43	92	30° skew.
16	4,840	.22	162	.00156	2.76	4.50	.614	175	1.08	729	6.65	2.16	1.27	2.32	36	393	
18A	18,000	.32	584	.000679	1.98	10.40	.190	584	.....	4,230	4.20	2.77	1.44	2.03	.....	.....	Dual, 45° skew.
18B	21,300	.32	584	.000679	2.21	10.40	.205	583	.....	4,450	4.80	2.56	1.59	1.71	.....	.....	Do.
22A	32,557	.61	610	.00142	.38	.....	.....	.....	.....	.....	.....	.....	.....	.....	.....	.....	Dual bridge.
23	126,000	.38	2,132	.000379	1.86	16.55	.112	1,490	.70	35,321	3.56	1.67	3.28	1.44	129	585	
24A	31,210	.91	630	.000823	.89	18.80	.047	315	.50	11,849	2.64	1.40	1.35	.20	335		Dual bridge.
34	15,900	.67	192	.00133	1.09	14.40	.076	106	.55	2,777	5.74	2.38	.....	.47	13	24	Scour.
50	205,000	.75	5,900	.00035	2.00	13.40	.149	4,700	.80	79,600	2.58	.....	.....	.40	440	670	
51	12,000	.83	72	.00176	1.95	16.10	.120	54	.75	1,173	10.25	1.27	1.20	.18	4	7	
52	1,370	.56	20	.00108	2.02	7.25	.280	20	1.00	145	9.40	1.32	.....	.89	3	6	
53	8,970	.58	216	.00056	.43	13.80	.031	69	.32	2,873	3.12	1.77	1.32	.89	16	39	
54	17,400	.61	205	.00049	1.60	12.25	.124	150	.73	2,642	6.59	1.56	1.37	.70	16	30	
55	27,500	.91	220	.00058	.88	17.70	.050	90	.41	3,890	7.07	1.06	.....	.07	12	16	
56	3,400	.82	58	.000107	.55	9.05	.061	25	.43	525	6.48	1.11	1.44	.18	6	8	
57	34,400	.36	324	.000230	2.92	12.25	.238	294	.91	3,964	8.70	1.14	.....	1.62	26	91	
58	4,730	.73	94	.000375	.68	9.15	.075	98	.....	865	5.48	1.76	1.30	.48	10	18	15° skew.
59	70,000	.90	340	.00142	2.47	19.90	.124	282	.83	6,388	10.10	2.64	1.42	.06	17	26	
60	24,800	.24	390	.000108	1.13	14.25	.078	393	.....	5,000	4.98	1.18	1.60	2.17	24	92	30° skew.
61	4,340	.84	84	.00100	.70	7.25	.096	49	0.58	607	7.15	1.38	.....	.13	12	17	
62	2,620	.66	44	.00060	1.17	7.83	.150	33	.75	344	7.63	1.45	.....	.57	6	10	8° skew.
63	1,450	.69	44	.00060	.63	6.10	.113	29	.65	265	5.46	1.20	.....	.55	7	11	Do.
64	5,240	.64	83	.000656	1.60	7.05	.227	71	.90	584	9.00	1.42	.....	.62	12	20	

field tests from the streams in Mississippi brought this ratio to over 700. The field tests verified the position of the former model base curves for values of M from 1.0 to 0.55 (fig. A–2). For smaller values of the contraction ratio, the model curve flattens while the field data shows a rising trend. The flattening out of the model curves indicates that critical conditions were being approached at M = 0.55. Although the value of M for the field structures ranged below 0.20, all were well within the subcritical range. Thus, the right half of the base curve, from the model studies, remains unchanged while the left half of the curve was reconstructed from field results. All points shown on figure A–2 are from field data.

Most of the points are from bridges placed normal to the flow but it can be noted that some of the points are from skewed crossings and others are from dual bridges on the Interstate System. The numbers refer to bridge location and date of flood which can be identified by referring to table B–1. A summary of the field data available to date, together with pertinent computed information, is included in table B–2. The design curves now shown on figure 6 no longer differentiate between wingwall and spillthrough abutments except for severe types used on short bridges.

B.2 Distance to maximum backwater curves. To obtain consistency in the plotting of field data, it was advisable to draw a new set of curves to define "Distance to Maximum Backwater." Figure 11 of the 1960 edition has been replaced by figure 13 in this publication. The former was based entirely on model data which was unrewarding, while figure 13 was constructed from field data. Figure 13 is included for a second time as figure B–1 to show the points from which the curves were drawn. The numbers again identify the bridge location which may be identified from table B–1. The procedure amounted to a cut and try process along with the computations. Fortunately, there was sufficient information to define a satisfactory set of curves. (See cols. 7 through 10 of table B–2.) The principal reason for changing the parameter of the

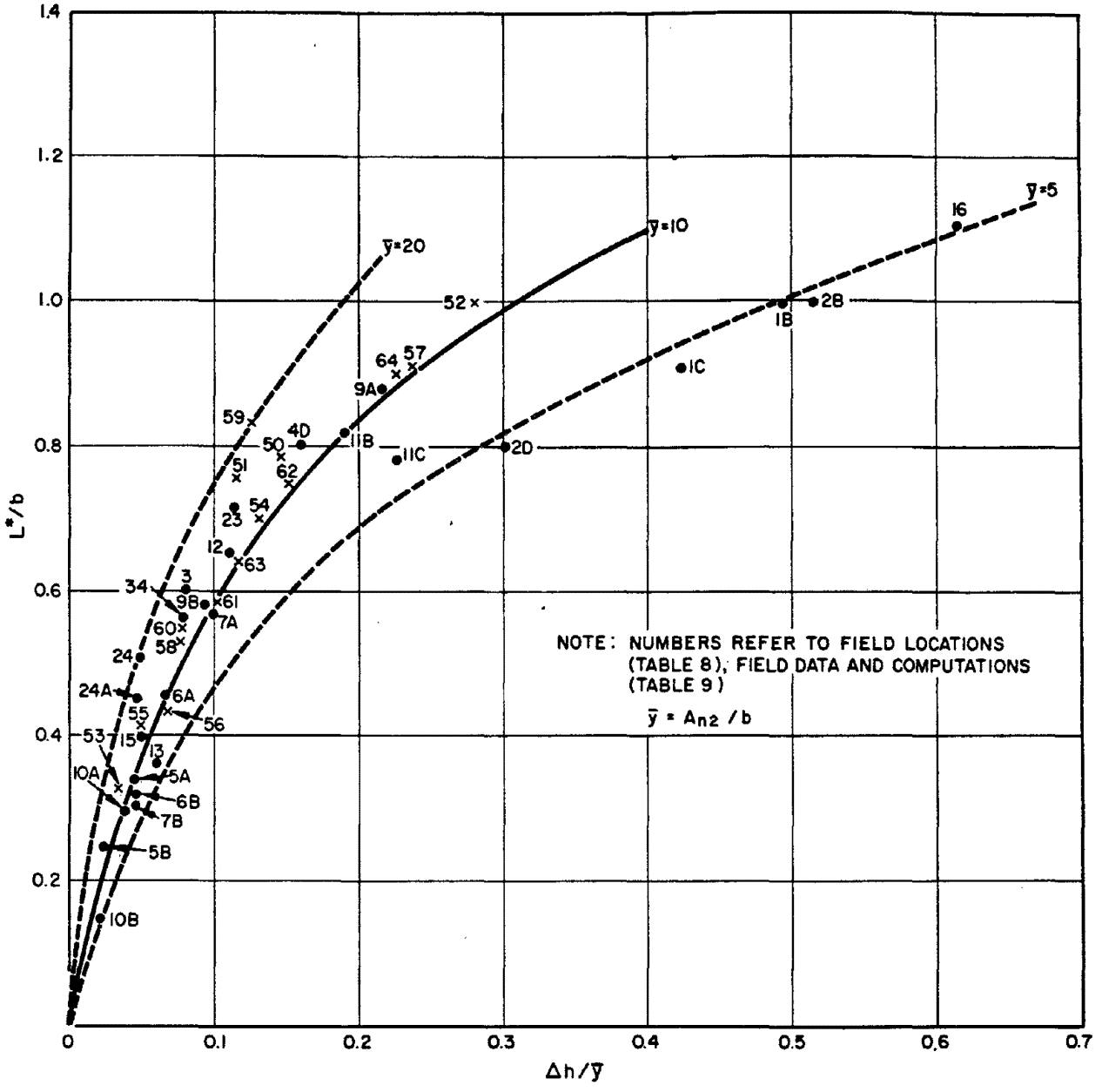

Figure B–1.—Distance to maximum backwater curves showing field data.

abscissa in figures 13 and B–1 to $\Delta h/\bar{y}$ was to facilitate the processing of the field data which is the exact reverse of the procedure for computing backwater.

B.3 Velocity head correction factor, α_2. Another concession made in order to get better correlation of field data was the introduction of a new factor in the computations, a correction factor for the velocity head in the constriction, α_2. The value of α_2 was computed from current meter measurements and soundings taken by the U.S. Geological Survey from the downstream side of the same bridges during high water. The water area under the bridge is divided into subsections in which the velocity is measured by current meter and the area is determined by soundings. The method of computation is described in section 1.11. Values of α_2 determined in this manner are recorded in column 14 of table B–2 and the points are plotted on figure B–2. The numbers again refer to the bridge location (table B–1). In each case α_1 at section 1 was plotted on the right. Then α_2 for each bridge and discharge

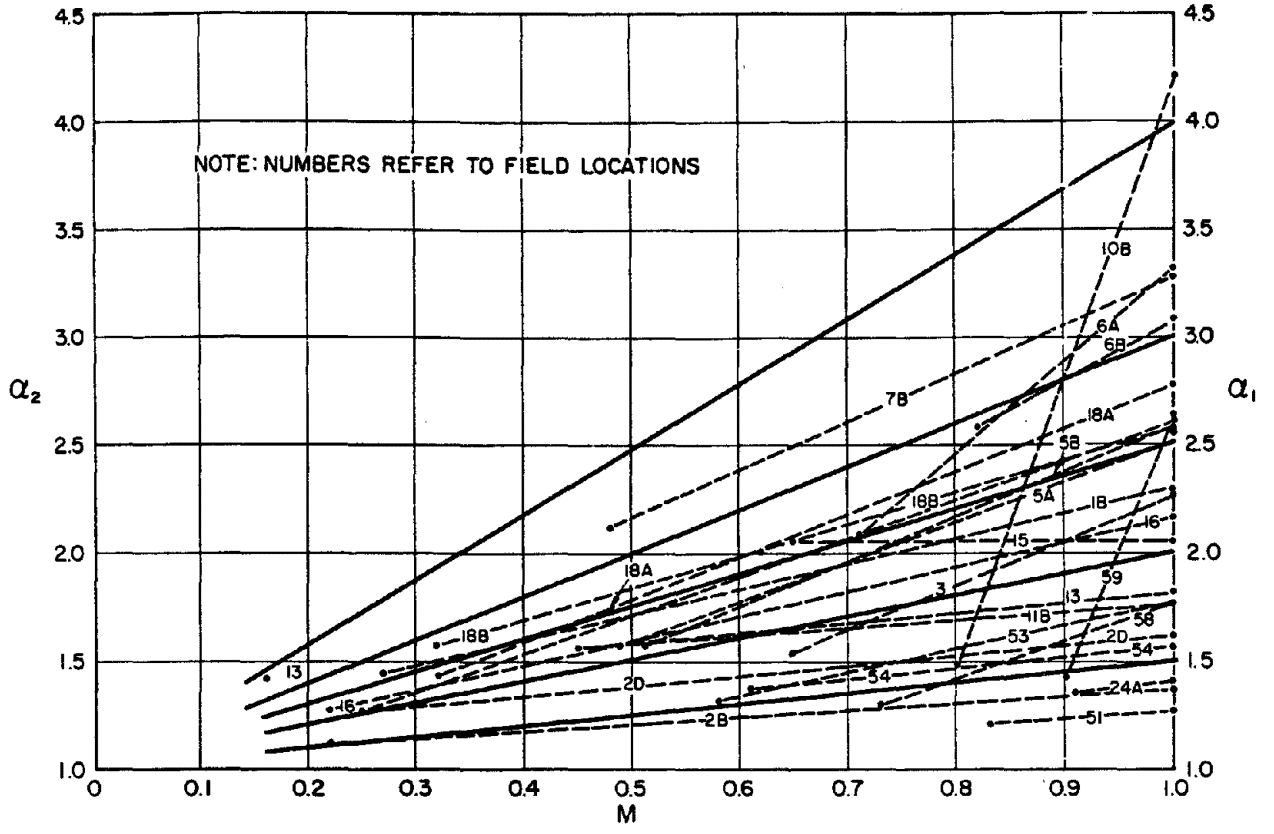

Figure B–2.—Curve for determining velocity head coefficient, α_2, showing field data.

was plotted with respect to the contraction ratio, M, and a line was drawn between them. Actually α_2 bears no fixed relation to α_1 but figure B–2 does show a trend. It can be said that α_1 is usually less than α_2 but there were exceptions. Obtaining α_2 from an existing bridge is one thing; to predict the value for a proposed bridge is another. It was for the latter reason that figure B–2 was prepared. It is strictly a chart for estimating purposes.

B.4 Dual bridges. Since the charts for dual bridges in this publication differ from those in the first edition an explanation is in order. The original curves were established entirely from model results. Since that time, measurements have shown that proportionately larger losses occur in the field than the model studies indicated. In the case of the differential level multiplication factor, figure 15, the field results dictate a marked shift upward for the single curve compared to its position in the original edition, even though the field information on dual bridges is still very limited. The model and field data for differential level are shown plotted on figure B–3. It can be observed that the contraction ratio, M, plays a minor role in the differential level multiplication factor. The field points are numbered and can be identified by referring to table B–1.

The points from which the revised backwater multiplication factor curve was drawn are shown on figure B–4. These are all model data since it was not possible to definitely differentiate backwater from Δh measurements taken in the field. The influence of the contraction ratio, M, formerly overemphasized, does not appear to be of much importance in the multiplication factor either, as figure B–4 indicates, so M has been dropped and the original family of curves have been replaced by the single modified curve shown on figure 14. The model data and computations from which figures 14 and 15 were prepared are recorded in table B–3.

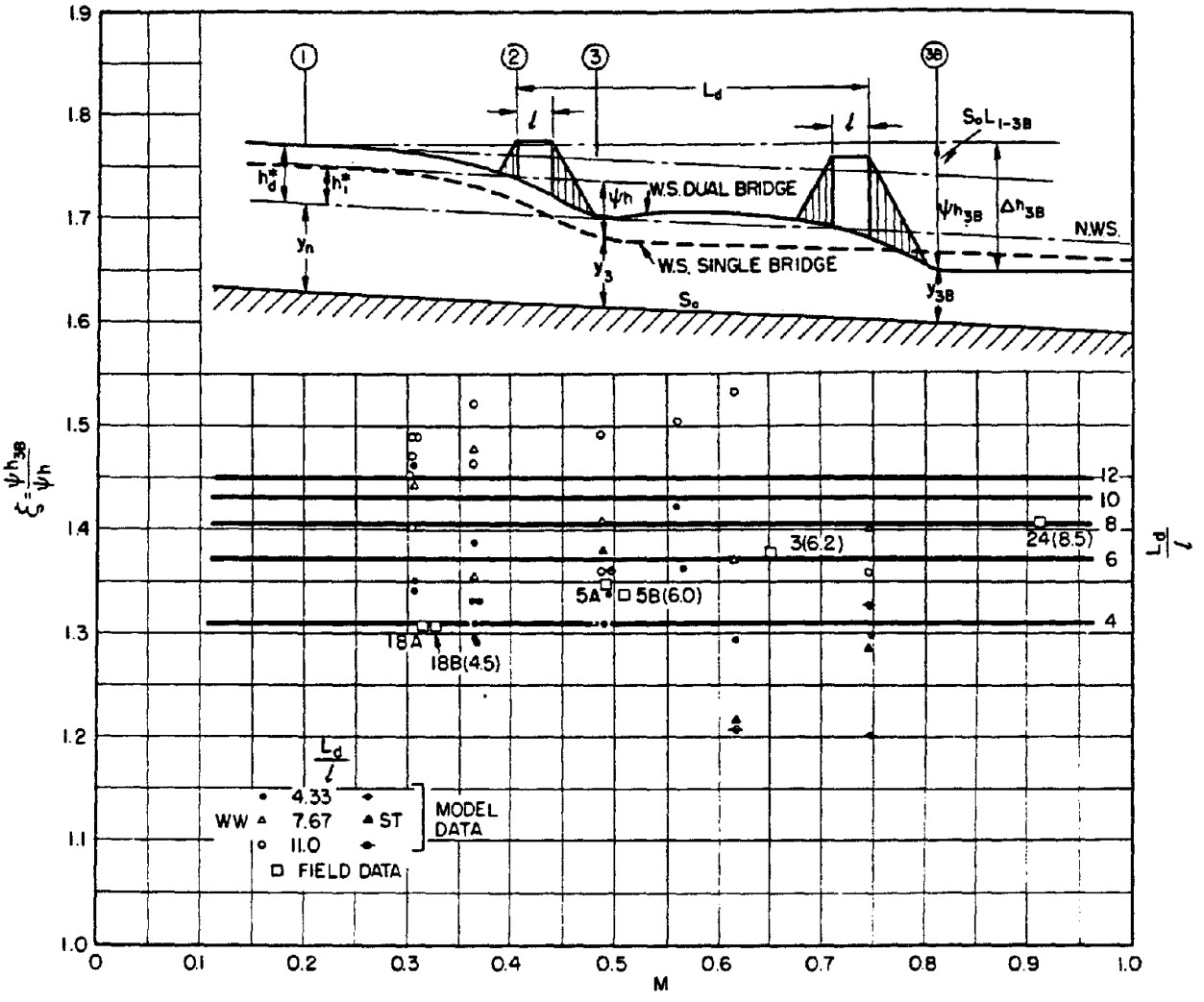

Figure B-3.—Differential level multiplication factor for dual parallel bridges.

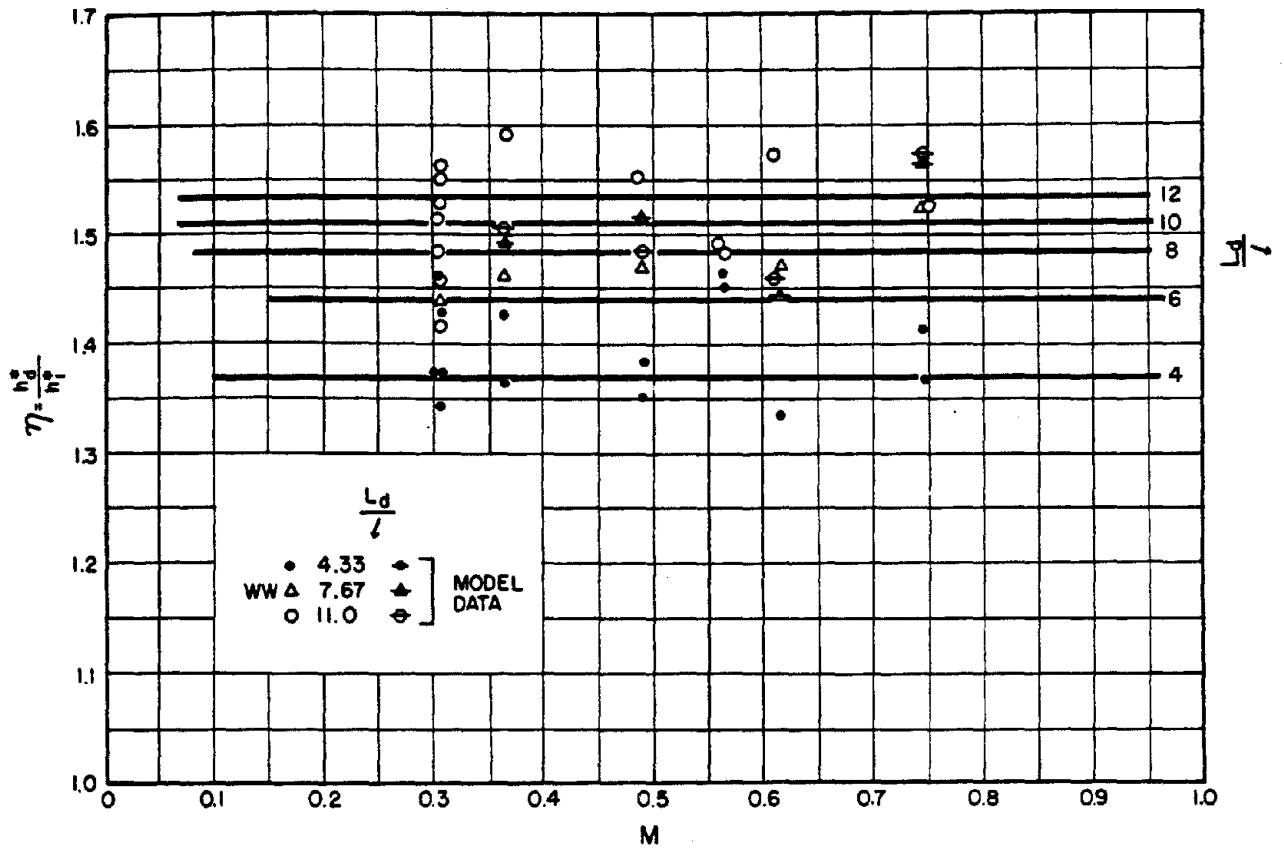

Figure B–4.—Backwater multiplication factor for dual parallel bridges.

Table B-3.—Model computations on dual bridges.

$B = 7.9'$ $S_0 = 0.0012$ $n = 0.024$ $1 = 1.0'$

Run No.	b ft.	Q c.f.s.	Y_n ft.	h_d^* ft.	$M = b/B$	$\frac{L_d}{1}$	$A_{n^2} = h_n^* b$ ft.	$V_{n^2} = Q/A_{n^2}$ f.p.s.	$\frac{V^2_{n^2}}{2g}$ ft.	K_b	$h_1^* = K_b \frac{V_{2n}^2}{2g}$ ft.	$\frac{h_d^*}{h_1^*}$	h_D ft.	$h_{sB}^* = h_n - h_D$ ft.	$h_d^* + h_{sB}^*$ ft.	$\frac{h_1^*}{h_1^* + h_s}$	$h_1^* + h_s^*$ ft.	$\frac{h_d^* + h_{sB}^*}{h_1^* + h_s^*}$	Abutment type
(1)	(2)	(3)	(4)	(5)	(6)	(7)	(8)	(9)	(10)	(11)	(12)	(13)	(14)	(15)	(16)	(17)	(18)	(19)	(20)
809	4.46	2.50	0.333	0.051	0.565	4.33	1.485	1.684	0.042	0.82	0.035	1.452	0.308	0.025	0.076	0.63	0.055	1.369	WW
816R	4.42			.055	.559	11.00	1.472	1.698	.045	.82	.037	1.486							45°
833	2.42			.195	.306	4.33	0.806	3.102	.149	.95	.142	1.373	.298	.035	.230	.83	.171	1.345	
834	2.42			.208							.142	1.465	.290	.043	.251	.83	.171	1.468	
839R	2.42			.203							.142	1.430	.285	.048	.251	.83	.171	1.468	
840	2.42			.217		11.00					.142	1.528	.295	.038	.255	.83	.171	1.491	
842R	2.42			.222							.142	1.563	.284	.049	.271	.83	.171	1.585	
847	2.42			.220							.142	1.549	.298	.035	.255	.83	.171	1.491	
960	2.42			.211							.142	1.486	.295	.038	.249	.83	.171	1.456	
967	2.42			.215							.142	1.514							
1,329	2.85	3.00	.370	0.170	.361	4.33	1.055	2.844	.125	.95	.119	1.429	.342	.028	.198	.79	.151	1.311	
30	3.87			.081	.490		1.432	2.095	.068	.88	.060	1.350	.337	.033	.114	.69	.086	1.311	
31	4.87			.039	.616		1.802	1.665	.043	.68	.029	1.336	.345	.075	.084	.59	.495	1.293	
32	5.90			.016	.747		2.183	1.374	.029	.40	.012	1.308	.353	.017	.033	.46	.254	1.299	
33	2.85			.174	.361	7.67	1.055	2.844	.125	.95	.119	1.462	.339	.031	.205	.79	.151	1.358	
34	3.85			.089	.487		1.425	2.105	.069	.88	.060	1.471	.337	.033	.122	.70	.086	1.412	
35	4.87			.043	.616		1.802	1.665	.043	.68	.029	1.473	.345	.025	.068	.59	.049	1.373	
36	5.87			.018	.743		2.172	1.381	.029	.40	.012	1.525	.352	.018	.036	.46	.026	1.401	
37	2.85			.190	.361	11.00	1.055	2.844	.125	.95	.119	1.593	.330	.040	.230	.79	.151	1.523	
38	3.85			.094	.487		1.425	2.105	.069	.88	.060	1.554	.337	.033	.127	.71	.085	1.491	
39	4.87			.046	.616		1.802	1.665	.043	.68	.029	1.575	.343	.027	.076	.58	.049	1.535	
1,340	5.87			.018	.743		2.172	1.381	.029	.40	.012	1.525	.353	.017	.036	.46	.026	1.360	
895R	4.42	5.00	.484	.089	.559	4.33	2.139	2.338	.081	.75	.061	1.464	.438	.046	.135	.64	.095	1.421	
902	2.42			.342	.306		1.171	4.270	.283	.90	.255	1.342	.394	.090	.412	.83	.307	1.342	
903	2.42			.367	.306	7.67	1.171	4.270	.283	.90	.254	1.440	.410	.074	.441	.83	.307	1.446	
908	2.42			.351	.306	4.33	1.171	4.270	.283	.90	.255	1.378	.391	.093	.444	.83	.307	1.446	
909	2.42			.361	.306	11.00	1.171	4.270	.283	.90	.255	1.417	.411	.073	.434	.83	.307	1.473	
915	2.42			.372	.306		1.171	4.270	.283	.90	.255	1.460	.406	.078	.430	.83	.307	1.401	
916RR	4.42			.095	.559		2.139	2.338	.085	.75	.064	1.491	.429	.055	.150	.64	.099	1.508	
1,317	2.866	5.00	.484	.265	.363		1.387	3.605	.202	.87	.175	1.509	.424	.060	.325	.79	.222	1.464	ST
18	3.866			.140	.489		1.871	2.672	.111	.85	.094	1.486	.440	.044	.184	.70	.135	1.363	
19	4.886			.070	.618		2.365	2.114	.069	.69	.048	1.460	.456	.028	.098	.59	.081	1.210	
20	5.886			.030	.745		2.849	1.755	.048	.40	.019	1.571	.459	.025	.055	.46	.041	1.330	
21	2.846			.266	.360	7.67	1.377	3.631	.205	.87	.178	1.494	.417	.067	.333	.79	.225	1.480	
22R	3.866			.142	.489		1.871	2.672	.111	.85	.094	1.507	.440	.044	.186	.70	.135	1.378	
23	4.856			.069	.615		2.350	2.128	.070	.68	.048	1.443	.664	.020	.097	.60	.080	1.217	
24	5.876			.030	.744		2.844	1.758	.048	.40	.019	1.567	.460	.024	.054	.46	.042	1.290	
25	2.876			.246	.364	4.33	1.392	3.592	.200	.90	.180	1.364	.413	.071	.317	.79	.228	1.390	
26R	3.886			.129	.492		1.880	2.660	.110	.85	.093	1.381	.432	.052	.181	.69	.135	1.341	
28	5.886			.027	.745		2.849	1.755	.048	.40	.019	1.414	.461	.023	.050	.46	.041	1.205	

Appendix C.—DEVELOPMENT OF CHART FOR DETERMINING LENGTH OF SPUR DIKES

The information available at this time on spur dikes are plotted on figure C–1. The field data (*39*) and the limited model data (*19*) and (*25*) from which the points were plotted, are summarized in table C–1. The information leaves much to be desired. Spur dikes in existance appear to have been proportioned by individual judgment rather than by any definite method; some are too long while others are extremely short when compared to the lengths given by figure C–1. The actual and computed lengths can be compared most readily by comparing the values of L_s in columns 18 and 19 of table C–1.

Model testing was not only limited in range by the discharge ratio, Q_f/Q_{100}, but the reproduction of flow patterns, scour patterns, scour depths, and embankment stability was not necessarily characteristic of the prototype structures. The model showed great variation in acceptable lengths of spur dikes so, rather than plot all the model data, a representative line was drawn through the lot. Values for four points read from the representative line are plotted as circles on figure C–1 and these are also tabulated at the bottom of table C–1. Since it was not advisable to construct a dimensionless design chart at this time, the model results were converted to prototype values by the Froude Law (scale 25:1). This ratio was determined by scaling up the model flow depth of 0.40 foot to 10 feet which was the average depth of flow encountered in the field tests.

It is apparent that the design curves (fig. 30), which are based principally on the information in table C–1, will most likely be subject to later adjustment as additional field data are obtained and more experience is gained. This is the first attempt at standardization of spur dike design for bridges.

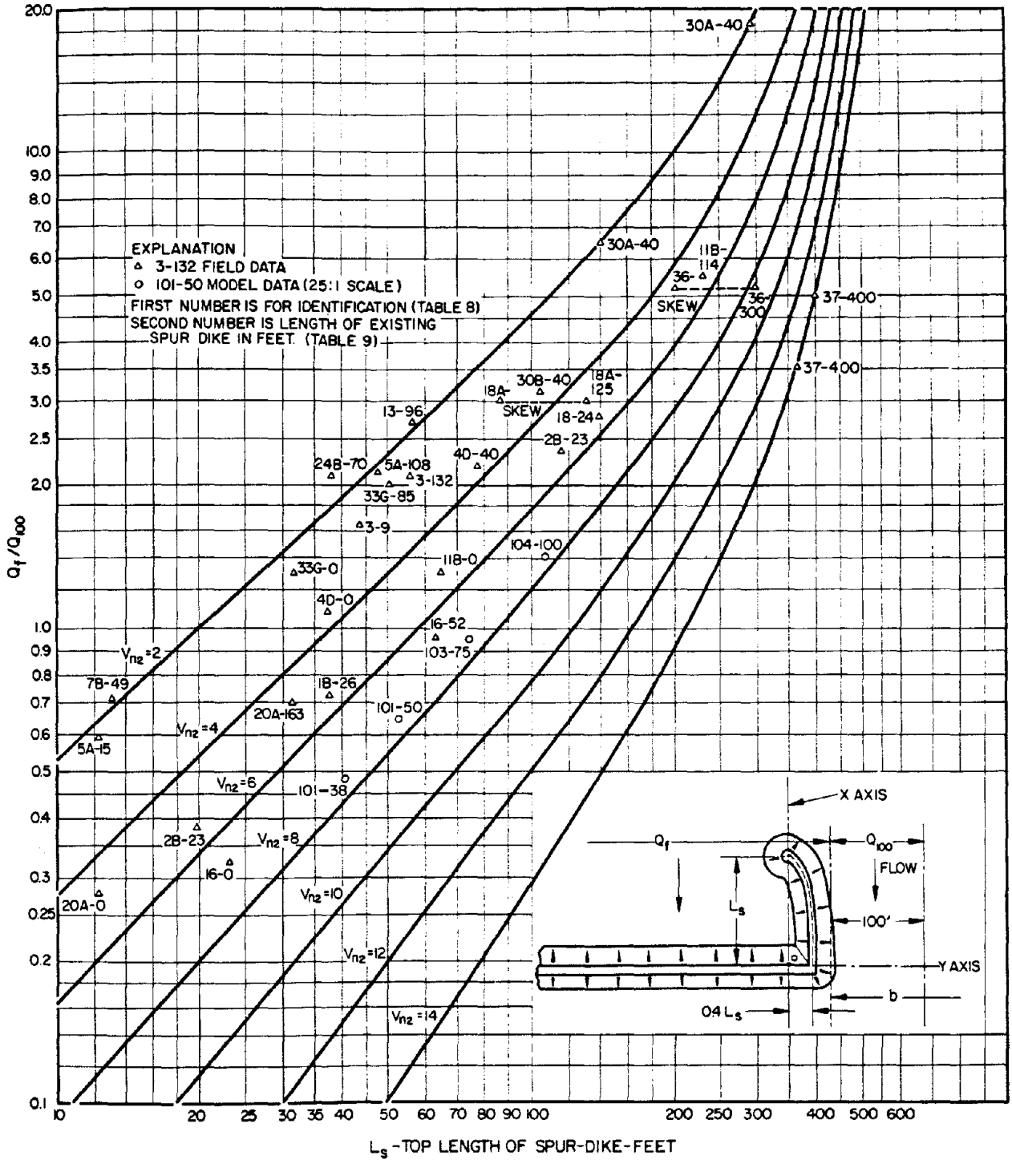

Figure C-1.—Length of spur dikes.

Table C–1.—Summary of field data and computations on spur dikes.

Field data furnished by U.S.G.S.

No.	Q c.f.s.	$K_1 \times 10^3$	$K_a \times 10^3$	$K_c \times 10^3$	$K_b \times 10^3$	Q_a c.f.s.	Q_c c.f.s.	Q_b c.f.s.	$e = 1 - \frac{K_a}{K_c}$	$\frac{Q_{100} = Q/b \times 100}{\text{c.f.s.}}$	b ft.	A_{n^2} ft.^{2}	$\bar{y} = A_{n^2}/b$ ft.	Q_a/Q_{100}	Q_c/Q_{100}	$V_{n^2} = Q/A_{n^2}$ ft./sec.	L_s existing ft.	L_s from figure 30 ft.	Remarks
(1)	(2)	(3)	(4)	(5)	(6)	(7)	(8)	(9)	(10)	(11)	(12)	(13)	(14)	(15)	(16)	(17)	(18)	(19)	(20)
1B	14,600	1,300	190	756	354	2,150	8,480	3,970	0.748	3,000	486	2,709	5.55	0.718	2.83	5.40	26	38	
2B	8,950	617	67.5	413.5	136	979	5,998	1,973	.837	2,580	347	1,671	4.82	.380	2.33	5.35	24	140	
																	23	20	
																	23	120	
3	36,400	3,606	570	706	2,330	5,753	7,127	23,520	.196	3,480	1,044	13,315	12.75	1.66	2.08	2.73	9	44	Dual bridge.
																	132	56	
4D	18,800	1,033	230	468	335	4,180	8,518	6,096	.505	3,880	486	4,966	10.20	1.08	2.20	3.80	0	38	
																	90	78	
5A	13,500	1,836	210	730	896	1,544	5,368	6,588	.712	2,610	519	6,427	12.40	.59	2.05	2.10	15	12	Dual bridge.
																	106	48	
7B	3,160	515	160	109	246	982	669	1,509	.322	1,340	236	1,756	7.45	.73	0.50	1.80	49	13	
																	0	0	
10B	5,470	296	34	26	236	629	480	4,361	.229	1,340	408	3,822	9.38	.47	0.36	1.43	127	0	
																	0	0	
11B	62,470	4,325	459	1,900	1,966	6,630	27,443	28,397	.759	5,000	1,245	12,294	9.90	1.32	5.50	5.08	0	65	
																	114	230	
13	5,430	1,590	212	1,117	261	724	3,815	891	.810	1,410	385	2,808	7.30	.51	2.71	1.93	0	0	
																	96	56	
16	4,840	467	91	274	102	943	2,840	1,057	.667	2,990	162	727	4.30	.32	0.95	6.67	0	23	
																	52	64	
18A	18,000	1,479	41	765	673	499	9,310	8,191	.946	3,090	584	6,067	10.40	.16	3.01	2.97	9	0	Dual bridge.
																	125	88+44	45° skew.
20A	3,763	159	39	99	21	923	2,343	497	.605	3,330	113	804	7.16	.28	0.70	4.69	0	12	Relief bridge.
																	163	32	
24A	31,210	3,440	100	200	3,140	907	1,815	28,488	.500	4,950	630	11,644	10.50	.18	0.37	2.65	0	0	Dual bridge.
																	150	0	
24B	10,302	1,370	90	620	660	677	4,662	4,963	.855	2,240	462	6,819	14.80	.30	2.08	1.52	0	0	
																	70	38	
30A	158,000	24,107	2,850	8,307	12,950	18,679	54,445	84,876	.657	2,870	5,512	79,400	14.40	6.52	18.95	1.99	40	140	
																	40	290	
30B	16,800	1,100	47	698	355	718	10,600	5,422	.933	3,380	497	4,852	9.80	.21	3.15	3.46	18	0	Relief bridge.
																	40	105	
33G	6,136	1,600	860	560	180	3,298	2,148	690	.349	1,655	370	2,404	6.50	2.00	1.30	2.55	85	50	Relief bridge.
																	0	32	
36	200,000					35,800	0	164,200	1.00	6,900	2,900	43,500	15.0	5.20	0	4.60	300	200+100	45° skew.
																	0	0	
37	750,000					113,500	80,000	556,500	.295	22,700	3,300	53,600	16.2	5.00	3.53	14.0	400	400	
																	400	360	
Typical model data converted to 25:1 scale																			
101	15,000					3,600	0	11,400	1.00	7,500	200	2,000	10.0	.48	0	7.50	38		
102	15,000					4,800	0	10,200	1.00	7,500	200	2,000	10.0	.64	0	7.50	50		
103	15,000					7,120	0	7,880	1.00	7,500	200	2,000	10.0	.95	0	7.50	75		
104	15,000					9,730	0	5,270	1.00	7,500	200	2,000	10.0	1.30	0	7.50	100		

U.S. GOVERNMENT PRINTING OFFICE: 1981-341-428/1321